

THE PATHOGENESIS OF AIDS-RELATED AND
NON-AIDS-RELATED KS: A MATHEMATICAL PERSPECTIVE

by

Obias M. Chimbola
Reg No. 16100075

Department of Mathematics and Statistical Sciences Botswana International
University of Science and Technology

Email: obias.chimbola@studentmail.biust.ac.bw
Tel: (+267)72692101

A Thesis Submitted to the College of Science in Fulfilment of the Requirements
for the Award of the Degree of Doctor of Philosophy in Pure and Applied
Mathematics of BIUST

Supervisors:

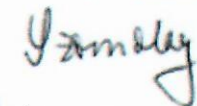
Prof. Edward M. Lungu
Department of Mathematics
and Statistical Sciences
College of Science, BIUST

Dr. Barbara Szomolay
Division of Infection
and immunity,
Cardiff University

Email: lungue@biust.ac.bw

Email: SzomolayB@cardiff.ac.uk

Signature.....

Signature.....

Date.....16/4/2021

Date.....16/4/2021

April 2021

Declaration and Copyright

I, **Obias M. Chimbola**, with student ID 16100075, hereby declare that this thesis has been composed by myself and that it has never been submitted for a degree at this or any other university or institution of higher learning. I confirm that the work contained in this thesis is my own original research work under the supervision of Prof. Edward M. Lungu and Dr. Barbara Szomolay. Any work done by others has been acknowledged and referenced accordingly.

Signature.....

Date.....16/04/2021

This thesis is copyright material protected under the Berne Convention, the Copyright Act of 1999 and other international and national enactments, in that behalf, on intellectual property. It must not be reproduced by any means, in full or in part, except in short extracts in fair dealing; for researcher private study, critical scholarly review or discourse with an acknowledgement, without the written permission of the office of the Provost on behalf of both the author and the BIUST.

Acknowledgement

In any large undertaking there are a number of people on whose shoulders we stand. This is certainly the case for me in this thesis, and the particular shoulders on which I stand are those of my supervisor Professor Edward M. Lungu and my co-supervisor Dr. Barbara Szomolay, Dr. John Njiagarah, and all my fellow Ph.D students at BIUST. I owe an immense debt of gratitude to my mentors Prof. Lungu and Dr. Szomolay for their unwavering support and direction during the entire period of my research. Colleagues who have worked with me and inspired me to learn about new areas and new directions abound. Especially fresh in my mind all the constructive criticisms that I received from my personal friends Dr. Obonye Doctor, Getahun Wegu Bekele from Botswana and Ethiopia, respectively. We spent most of the times discussing mathematical problems together. The research presented here would not have been possible without the very consistent support, both technical and financial of SIMONS FOUNDATION for financing my stay in Botswana and tuition for my studies at BIUST. In this regard, I wish to extend my profound gratitude to the managers of the project that is hosted by BIUST. These are no other than Prof.

Lungu and Prof. Zegeye Hailu. On a personal note, I would like to thank my wife; Selita Mwale, for the active role she played to ensure that our four kids were happy and received the necessary support in my absence. A special thank you is hereby extended for my beautiful children Ethel, Emmanuel, Eunice and Obias (Jr) for enduring my absence from them. I love you guys. May the almighty God continue to help you to grow in faith. Before I say my concluding remarks, I wish to sincerely thank the management of Mulungushi University for granting me study leave for three years and also for extending the leave as the world got engulfed in the COVID-19 pandemic. In spite of the financial challenges that my university might have continued to face as a result of the pandemic, management remained steadfast in ensuring my family received the necessary support. Last but not the least, I wish to thank my mother and late father for the courage of their convictions, selfless devotion, and commitment to excellence. To sum it up I owe my success to the almighty Father for allowing His will to be done. I shall continue to praise Him till my last breath. Amen

Dedication

I dedicate this project to my strength provider Lord Jesus Christ, myself and Chim-bola's family.

Abstract

Kaposi's sarcoma is a common AIDS-defining cancer that has continued to afflict patients living with HIV-1, especially, individuals who are currently not on HAART or whose HIV-1 status is not known. Even individuals who have had a prior HHV-8 infection and are on HAART are at an increased risk of developing KS whenever drug failure occurs and when one develops drug resistance to the drugs being administered. Like other herpesvirus, KS associated herpesvirus (KSHV), also known as human herpesvirus-8 (HHV-8) is a lifelong infection in a host. The non-AIDS related KS is less life threatening than the HIV related KS.

In this study, we first develop a mathematical model for the development of Classic KS that involves the interaction of infected B cells, infected progenitor cells, KS cells, HHV-8 virions and the innate immune response. The innate immune signalling molecules generated in response to viral infection lead to the production of a broad range of antiviral proteins and cytokines that generate the initial fight back against the infection. From this model we shall show that KS therapy alone is capable of reducing the HHV-8 load and consequently the tumor burden is diminished.

The innate response above is followed by an adaptive immune response which is a more robust response involving the killer T cells. The adaptive immunity is the second arm of the immune response that is elicited following the failure of the innate immunity to clear an infection. We have also incorporated three controls to explore the roles of HAART and anti-KS therapy in reducing the burden of AIDS-KS infection. From the model we show that if HAART is administered at optimal levels, both HIV-1 and HHV-8 can be reduced to undetectable levels.

In the second model, we have developed a mathematical model for non-AIDS-related KS (NAKS) that encompasses uninfected B and progenitor cells, HHV-8 specific effector cells, immune response that is tailored toward viral suppression, latently and lytically infected B cells, infected progenitor cells, Kaposi's sarcoma cells and HHV-8. The motivation of this study comes from the realization that little attention has been paid towards finding treatment options to inhibit reactivation of lytic replication of HHV-8 and other therapies to reduce infection of B cells by HHV-8. It is therefore imperative that efficacious drugs are developed to ease the affliction of NAKS patients. Unlike AIDS-related KS, NAKS variant normally results in an indolent tumor that individuals can live with throughout their lives. However, sometimes the cancer cells can spread to other internal organs in the host where metastasis can be life threatening. Due to increasing cases being recorded in sub-Saharan Africa, there is an urgency to develop new drugs and to recommend ways to increase the efficacies of some already existing drugs for this cancer. This study has recommended the range

of efficacies that we believe can adequately clear the KS infection, provided adherence protocols are maintained to avoid the emergence of drug resistance.

The predictions of these mathematical model have the potential to offer more effective therapeutic interventions in the treatment of NAKS or AIDS-related KS (AKS).

List of Publications

1. Chimbola O.M., Lungu E, and Szomolay B(2021). Effect of Innate and Adaptive Immune Mechanisms on Treatment Regimens in an AIDS-related Kaposi's Sarcoma Model. *Journal of Biological Dynamics* .
2. Chimbola,O.M.(2021)Mathematical Analysis of a model with HIV-1 mutation in the midst of a Cellular Immune Response. *International Journal of Science and Research*.
3. Chimbola, O.M. (2020) Mathematical Model of Classical Kaposi Sarcoma. *Applied Mathematics*, 11, 579-600. <https://doi.org/10.4236/am.2020.117040>.
4. Chimbola, O.M. (2020) Mathematical Model of HIV-1 Dynamics with T Cell Activation. *Journal of Applied Mathematics and Physics*, 8,13281345. <https://doi.org/10.4236/jamp.2020.8710>.
5. Chimbola, O.M. (2020) Book Chapter. F.No. SDI/BP/6172D/2925. Book Publisher International.
6. Chimbola O.M., Lungu E, and Szomolay B. Optimal Control Application to a Ka-

posi's Sarcoma Treatment Model. *International Journal of of Biomathematics* (**Minor revisions**).

7. K.A. Jane White, Ben Levy, Hannah Correia, **O.M.Chimbola**, et al. A Mathematical Model of Contact Tracing During the 2014-2016 West African Ebola Outbreak.

Theoretical and Mathematical Ecology.

8. K.A. Jane White, Ben Levy, Hannah Correia, O.M.Chimbola, et al. Modelling the effect of HIV/AIDS Stigma on HIV infection dynamics in Kenya. *Bulletin of*

Mathematical Biology (**Minor revisions**).

9. Chomba, C. , Obias, C. and Nyirenda, V. (2014) Game Ranching: A Sustainable Land Use Option and Economic Incentive for Biodiversity Conservation in Zambia.

Open Journal of Ecology, 4, 571-581. doi: 10.4236/oje.2014.49047.

10. Chansa Chomba, Douglas Kunda, Obias Chimbola, and Boyd Kaliki, Incidences and Fatalities of Road Traffic Accidents in Zambia for the period 2008-2013: A Prelude to Sustainable Road Transport Sector Development for Socio-Economic Development. *Journal of Sustainable Development in Africa* (Volume 19, No.1, 2017).

Contents

1	Introduction	1
1.1	Background of the study	1
1.2	Statement of the problem	2
1.3	A Dissection of Research Problems	5
1.4	Objectives	6
2	Literature Review	7
2.1	Vital statistics concerning AIDS-KS and non-AIDS-KS	7
2.2	Basis of Mathematical Modelling of KS	14
3	Preliminary Definitions and Concepts	17
3.1	Some Defintions	18
3.2	Existence and Uniqueness Theorem	19

3.3	The next generation operator approach for computing the basic reproduction number, \mathcal{R}_0	19
3.4	A technique for establishing global stability of the disease-free equilibrium when $\mathcal{R}_0 < 1$	21
3.5	Routh-Hurwitz Criteria	22
3.6	Optimal Control Problem	23
4	AIDS-related Kaposi's sarcoma Pathogenesis	27
4.1	Introduction	27
4.2	Model 1: KS model with innate mechanism	34
4.2.1	Model Formulation and Description	34
4.2.2	Analysis of the Model	38
4.2.3	Steady States and the Basic Reproduction Number	40
4.2.4	Local Stability of the Virus Free Equilibrium, ε^0	42
4.2.5	Existence of the Endemic Infection Equilibrium, ε^*	44
4.2.6	Numerical Simulations of the Model with Innate Mechanism	46
4.2.7	Sensitivity and Uncertainty Analysis	46
4.3	MODEL 2: AIDS-KS Model with Adaptive Mechanism	49
4.3.1	Model Formulation and Description	49

<i>CONTENTS</i>	xiii
4.3.2 Analysis of the Model	54
4.3.3 Numerical Simulations of the Model with Adaptive Mechanism	65
4.3.4 Sensitivity and Uncertainty Analysis	68
4.4 Optimal Control Applied to the Model with Adaptive Mechanism . .	70
4.4.1 Existence of Optimal Control	73
5 Non-AIDS-related Kaposi's Sarcoma: Role of Lytic Replication	81
5.1 Introduction	81
5.2 Model Development and Analysis	82
5.2.1 Model formulation	82
5.2.2 Analysis of the uncontrolled model where $u_1(t) = u_2(t) = 0$. .	91
5.2.3 Equilibria and the basic reproduction number, \mathcal{R}_0	93
5.2.4 Global stability of the infection free equilibrium (IFE) point, E_0	96
5.3 Numerical Simulations and Sensitivity Analysis	97
5.4 Model with Optimal Control	98
5.4.1 Existence and characterization of optimal control solution . .	99
5.5 Numerical Simulations and Sensitivity Analysis	103
5.6 Summary of Results	106
6 Discussion, Future Work and Recommendation	119

6.1 Discussion	119
6.2 Future Work	124
6.3 Recommendation	124
7 Appendix	125

List of Figures

2.1	Model for the pathogenesis of AIDS-KS. Adapted from [31]	16
4.1	Schematic diagram of the model with innate mechanism, describing interactions for Classic KS.	36
4.2	Dynamics of the individual components of the model with innate mechanism for different values of the efficacy threshold θ_{x_5} . The HHV-8 infection clears for $\theta_{x_5} < \theta_{x_5}^*$ even if $\mathcal{R}_0 > 1$	48
4.3	PRCCs for parameters of the innate model and $\log(\mathcal{R}_0)$ as a function of the most sensitive parameter, K_2	49
4.4	Schematic diagram for AIDS-KS model with adaptive immunity.	53
4.5	Dynamics of the individual components of the model with adaptive mechanism for $\mathcal{R}_0 = 1.7902$	65
4.6	Comparison of the long term dynamics of the uninfected CD4 T cell and B cells with regards to HIV-1 and HHV-8 load.	66

4.7	(a) Same as Figure 4.6(a) but for the first 300 days. Figure 4.6(b) The long term dynamics of infected B cells and KS cells with regards to HHV-8 load.	66
4.8	PRCCs for parameters of the adaptive model and $\log(\mathcal{R}_0)$ as a function of the two most sensitive parameters, N_{10} and β_2	67
4.9	Optimal controls in the first 20 days.	77
4.10	Population dynamics of infected cells and viruses during 300 days for varying values of the infected CD4 T cell-specific HAART efficacy u_1	78
4.11	Population dynamics of infected cells and viruses during 300 days for a new combination of optimal controls.	80
5.1	Schematic diagram of the non-AIDS KS model with immune response	86
5.2	\mathcal{R}_0 and PRCCs	108
5.3	Population Dynamics with $\mathcal{R}_0 = 0.9181$	109
5.4	Population Dynamics with $\mathcal{R}_0 = 1.2242$	110

5.5 Population dynamics for the uncontrolled and controlled systems. In this figure we have used: $\rho = 0.90$. We have set $u_1 = 0, 0.50, 0.80$ and $u_2 = 0, 0.53, 0.87$. The initial values in our simulation are $B(0) = 1.968 \times 10^5, P(0) = 8.994 \times 10^4, B_{i_L}(0) = 678.9, B_{i_a}(0) = 1418, P_i(0) = 2144, V_8(0) = 4.483 \times 10^5, E_8 = 759.3, K(0) = 629.9$. The rest of the parameters are as indicated in Table 3. 112

5.6 Population Dynamics for the uncontrolled and controlled systems. In this figure we have used: $\rho = 0.10$. We have set $u_1 = 0, 0.50, 0.80$ and $u_2 = 0, 0.53, 0.87$. The initial values in our simulation are $B(0) = 1.968 \times 10^5, P(0) = 8.994 \times 10^4, B_{i_L}(0) = 678.9, B_{i_a}(0) = 1418, P_i(0) = 2144, V_8(0) = 4.483 \times 10^5, E_8 = 759.3, K(0) = 629.9$. The rest of the parameters are as indicated in Table 3. 114

5.7 Population Dynamics for the uncontrolled and controlled systems. In this figure we have used: $\rho = 0.10$. We have set $u_1 = 0, 0.50, 0.80$ and $u_2 = 0, 0.50, 0.90$. The initial values in our simulation are $B(0) = 1.968 \times 10^5, P(0) = 8.994 \times 10^4, B_{i_L}(0) = 678.9, B_{i_a}(0) = 1418, P_i(0) = 2144, V_8(0) = 4.483 \times 10^5, E_8 = 759.3, K(0) = 629.9$. The rest of the parameters are as indicated in Table 3. 116

5.8 Population Dynamics for the uncontrolled and controlled systems. In this figure we have used: $\rho = 0.90$. We have set $u_1 = 0, 0.50, 0.80$ and $u_2 = 0, 0.50, 0.90$. The initial values in our simulation are $B(0) = 1.968 \times 10^5, P(0) = 8.994 \times 10^4, B_{i_L}(0) = 678.9, B_{i_a}(0) = 1418, P_i(0) = 2144, V_8(0) = 4.483 \times 10^5, E_8 = 759.3, K(0) = 629.9$. The rest of the parameters are as indicated in Table 3. 118

List of Tables

4.1	Parameters of the model with innate mechanism and their definitions.	38
4.2	Initial values of the model with adaptive mechanism and their definitions.	54
4.3	Parameters of the model with adaptive mechanism and their definitions.	56
4.4	Parameter values of the model with adaptive mechanism.	58
5.1	Initial values for the model state variables	87
5.2	Model parameters and their definitions	89
5.3	Model parameters and their ranges	90
7.4	Estimation of parameters.	133
7.1	Range of parameters for sensitivity analysis for the innate model. . .	140
7.2	Range of parameters for sensitivity analysis for the adaptive model. .	141

Chapter 1

Introduction

1.1 Background of the study

Kaposi's sarcoma (KS) is a multifocal malignancy mainly affecting elderly Mediterranean men, individuals in sub-Saharan Africa with impaired immune systems, either due to human immunodeficiency virus-1 (HIV-1) infection or immunosuppressive drugs after undergoing organ transplantation or weakening immunity due to old age. Human herpesvirus 8 (HHV-8) or Kaposi's sarcoma-associated herpesvirus (KSHV), is the etiological agent of KS [15], a neoplasm of endothelial origin that occurs in four distinct epidemiologic forms [17]: classic or Mediterranean KS, epidemic or AIDS-related KS (AIDS-KS), endemic or African KS, and iatrogenic or organ transplant-associated KS. Although the incidence of AIDS-KS has declined due to increased access to highly active antiretroviral therapy (HAART)[90], the disease

burden remains significantly high in sub-Saharan Africa and continues to be a source of morbidity and mortality in areas where co-infection of HIV-1 and HHV-8/KSHV is high [46]. With a high possibility of HIV-1 sufferers developing drug resistance, due largely to non adherence to HAART treatment protocols, there is fear that this could eventually trigger an increase in the number of cases of AIDS-related KS as a result of deteriorating immunocompetence among HIV-1 sufferers co-infected with HHV-8 [31]. The success of ART in treating HIV-1-associated KS has also been countered by the occasional occurrence of an immune reconstitution inflammatory syndrome, a condition characterized by severe, temporary enhancement of KS lesions due to an increase in inflammation and immunologic recovery after ART [27].

The discovery of HHV-8 and its contribution to KS development opened the potential for prophylaxis and treatment of the infection and cancer with antiviral drugs, and prevention of them with a vaccine. Strategies to achieve these ends require an intimate knowledge into the pathogenesis and immune surveillance of HHV-8 infection [54].

1.2 Statement of the problem

At the end of the 20th century, more than 21 million individuals worldwide had succumbed to AIDS, over 34 million had HIV infection, and over 95% of HIV infected persons resided in developing countries. Nine countries in Southern Africa, with 2%

of the world's population, accounted for one third of all HIV-infected persons [52].

In some countries of sub-Saharan Africa, the seroprevalence of HHV-8 suggests that more attention should be paid to this infection. For example, in Zambia, HHV-8 prevalence is estimated to be 37.5%, in Botswana the prevalence ranges between 54.7% – 90% depending on the test used [23, 79]. These prevalence levels are comparable if not higher than HIV-1 prevalence [22], yet little attention has been paid to containing this infection.

In 2018, KS was estimated to be the second most common cancer in Malawi, accounting for 20.5% of all the cancer cases diagnosed. In Uganda about 13% of all the cancer cases diagnosed were associated with KS. In Zimbabwe about 9% of all the cancer cases diagnosed regardless of one's HIV status [34], were associated with HHV-8 infection.

Kaposi's sarcoma occurrence in AIDS patients not receiving highly active antiretroviral therapy (HAART) is estimated to be 20000 times more likely than in the general population [40]. A number of studies [54, 63] have provided evidence to show that the incidence of AIDS-related KS has declined drastically since HAART became more accessible to HIV patients. Numerous studies, for example Krown S.E. [56], have documented the benefits of HAART measured by regression of KS tumor upon commencement of HAART and drug-mediated HIV-1 viral suppression and profound immune reconstitution.

In the quest to finding the solution to the burden imposed by HHV-8 infection on

KS patients in sub-Saharan Africa and the world, there is an urgent need to develop mathematical models that elucidate the in host dynamics of HHV-8 and how the infection progresses to KS in immunosuppressed patients especially those co-infected with the human immunodeficiency virus-1 (HIV-1).

This study seeks to develop mathematical models incorporating infected B cells, infected progenitor cells, KS cells, HHV-8 virions and the immune response with a view to determining the efficacy threshold of the immune response that can impede a potential classic KS from developing into a clinical KS. We consider two types of the immune response, the initial innate response and if this fails to clear the infection, to consider the more robust adaptive response.

The adaptive immune response is categorized into humoral and cell-mediated immunity. Humoral immunity is concerned with extracellular pathogens and comprise the antibody production by B cells which later mark the infected cells for destruction. In contrast, the cell-mediated immunity involves the cytotoxic T lymphocytes (CTLs) and the activated natural killer (NK) cells.

The current study will focus on the cell-mediated immunity driven by $C8^+$ T cells, which upon antigenic stimulation activates into specific effector T cells normally referred to as cytotoxic T lymphocytes (CTLs). The CTL response is triggered after naive $C8^+$ T cells are primed following recognition of foreign peptides bound on major histocompatibility complex class I (MHC I) molecules presented by the antigen presenting cells, e.g dendritic cells together with a co-stimulatory signal.

In the event that the innate immune response fails to halt the development of the infection, we seek to extend the model to include the co-infection of HHV-8 with HHV-1 and explore the level of the adaptive immune response that can clear the infection. We shall consider the interactions of $CD4^+$ T cells and HIV-1, and how this relationship enhances the relationship between B cells and HHV-8, and the role of viral specific $CD8^+$ T cells. We also consider the progression of infected progenitor cells into KS cells. An optimal control approach is adopted with a view to determining the drug efficacy level of HAART alone or a combination of HAART and KS chemotherapy capable of clearing the infection.

1.3 A Dissection of Research Problems

The brief introduction above has led us to address the following:

1. We want to formulate a within-host model for non-AIDS Kaposi's Sarcoma (NAKS) that mimics the dynamics of NAKS and investigate various therapies that can clear the infection.
2. We want to formulate a model of AIDS-KS and investigate two immunological responses, the innate and adaptive responses. Specifically, we want to investigate the conditions under which the adaptive response can control the viral escape.
3. We want to determine the conditions under which HAART alone can control the infection and the drug efficacy levels under which combined HAART and chemother-

apy can reduce or stop the AIDS-KS infection.

4. We want to formulate a within-host model for a non-AIDS related KS that accounts for B cells latently and lytically infected with HHV-8 as well as the innate and adaptive arm of the immune system. We will then employ an optimal control strategy to obtain treatment efficacies for therapeutic approaches aimed at blocking viral entry and impeding the reactivation of lytic replication.

1.4 Objectives

Our objectives in this thesis are:

1. To construct an in host model for NAKS that mimics the dynamics of NAKS and explore various therapies that are potent in clearing the infection.
2. To develop a model of AIDS-KS and explore two immunological responses, the innate and adaptive stages. We want to investigate conditions under which the adaptive response controls the viral escape in the absence of treatment.
3. To develop and analyse an optimal control model of AIDS-KS that includes HAART and chemotherapy as controls.
4. To formulate an in-host model of NAKS that includes blocking of B cell infection by HHV-8 and suppression of lytic reactivation of latently infected B cells.

Chapter 2

Literature Review

In this chapter, we review literature related to the dynamics of Kaposi's sarcoma and how Kaposi's sarcoma associated herpesvirus (KSHV) initiates the infection.

2.1 Vital statistics concerning AIDS-KS and non-AIDS-KS

Kaposi's sarcoma was first reported in 1872 by Moritz Kaposi, a Vienna-based Hungarian physician and dermatologist. He observed numerous cases of a multifocal pigmented sarcoma of the skin in elderly European men, who all died within 2 years of diagnosis [48]. The first variant of Kaposi's sarcoma identified by Moritz Kaposi was named classic KS or sporadic KS. From 1947, many reports documented cases of this tumor in Africa together with a lymphadenopathic form of KS in children.

This form of KS has now been called endemic or African KS [19]. KS, especially in sub-Saharan Africa, attracted attention from the 1980's when the AIDS pandemic was announced and an aggressive form of KS was reported among gay men [36]. This variant of KS is now called AIDS-related Kaposi's sarcoma (AIDS-KS) or epidemic KS.

The AIDS-KS, unlike the other variant (non-AIDS related KS), is associated with severe morbidity and mortality. This has prompted significant research efforts into its etiology which ultimately culminated into the discovery of Kaposi's sarcoma-associated herpesvirus (KSHV) or human herpesvirus-8 [15]. The risk for developing KS in the setting of HIV-1 has been reported to be amplified by 3,640-fold over the general population in the United States [24, 25, 38, 57, 76], however, this risk has drastically reduced due to immune reconstitution as a result of highly active antiretroviral therapy (HAART)[24, 41].

From the epidemiological point of view and as mentioned earlier, there are four variants of KS: Classical Kaposi's sarcoma (CKS) or sporadic, African (endemic), Iatrogenic or Transplant KS and acquired immune deficiency syndrome (AIDS)-related Kaposi's sarcoma (AIDS-KS). It is now known that the development of each form is dependent on prior infection with Kaposi's sarcoma-associated herpesvirus (KSHV) or the human herpesvirus-8 (HHV-8) [20]. However, for AIDS-KS and iatrogenic KS, HHV-8 infection only is insufficient for the development of KS, some form of immunodeficiency is required [20]. There are exceptional cases, for example, not ev-

ery AIDS patient develops KS despite profound immunodeficiency and only a few KSHV-infected transplant patients develop iatrogenic KS [20]. Moreover, classic and endemic KS patients are not necessarily immunosuppressed [49, 61]. Hence, the cofactors of endemic African KS are yet to be understood. Some of the causal factors implicated in its development are environmental, genetic, immunosenescence, sex and malnutrition [20].

In the context of the acquired immunodeficiency syndrome (AIDS), KS is the most common neoplasm and is one of the AIDS defining cancers (cancers that signal the initiation of AIDS), besides non-Hodgkin's disease and cervical cancer [35]. In HIV seropositive patients, KS lesions are widely spread in the skin and in most cases involve the visceral such as the lungs, gastrointestinal tract [44].

In contrast to the classic KS, iatrogenic KS is more aggressive with a widespread involvement of the visceral. Discontinuation of immunosuppressive treatment can sometimes lead to improvement in the immune response and can lead to tumor lesion regression [11].

KSHV/HHV-8 is a double stranded DNA virus with two transcriptional replication programmes namely, the latent and lytic phases [64, 85]. In the latent stage, only a handful of the viral genes are expressed [45, 88], for: maintenance of the viral genome, impediment of lytic reactivation and evasion of immune surveillance to protect the

latently infected cells from being recognised by the cellular-mediated immunity [8, 84]. Infection with HHV-8 is in many cases a life-long persistent infection in immunocompetent individuals. However, when there is disruption in latency triggered by factors such as environmental factors then latent infection can switch to the lytic phase [2]. When a virus enters a susceptible B cell it reproduces forms of the genome by using the cell genome and it eventually bursts to release the virions.

To the best of our knowledge, the studies by Nani, et al., [72] and Lungu, et al. [95] are some of the few published mathematical studies modeling HIV-KS dynamics. However, the development of within-host models of AIDS-KS incorporating and addressing HAART and chemotherapy efficacies are still open problems.

In 2011, Nani and Jin [72] developed a mathematical model for AIDS-associated Kaposi's sarcoma(AIDS-KS) incorporating highly active antiretroviral therapy (HAART) treatment. Nani and Jin [72] model is among the first few models incorporating and studying the impact of $CD8^+$ T cells on AIDS-KS during HAART treatment. The model included uninfected $CD4^+$ T cells, HIV-1 infected $CD4^+$ T cells, HIV-1 virions in blood plasma, HIV-1 specific $CD8^+$ T cells, concentration of drug molecules of the HAART treatment protocol and KS cells in the patient undergoing HAART treatment. In this model, the interaction between HHV-8 and the B cells was not explored in spite of the study being on Kaposi's sarcoma. According to Foreman [32] HHV-8

can persist in latently infected B cells in immunocompetent individuals. This scenario has the effect of maintaining the production of HHV-8 to low levels. However, in immunoincompetent individuals the latently infected B cells may be reactivated a scenario which can increase the production of HHV-8. According to Foreman [32] KS can result from a process of erroneous infection of activated progenitor endothelial cells by HHV-8 which ultimately transform into KS cells. In this model, the authors did not distinguish between the $CD8^+$ T cells that were responsible for killing infected $CD4^+$ T cells and infected B cells by specific cytotoxic T lymphocytes. In spite of these shortcomings this study concluded that HAART therapy had the potential to reduce the HIV viral load to undetectable levels and observed that ex-vivo infused IL-2 incubated specific $CD8^+$ T cells had the capacity to decrease the HHV-8 viral load and consequently to annihilate the tumor cells.

In 2013, Lungu et al.[60] formulated a deterministic mathematical model to quantify HAART treatment levels for patients co-infected with HIV-1 and HHV-8 in high prevalence settings. The study revealed that approximately 87% of the AIDS population could acquire protection against co-infection with HIV-1 and KS simply by providing treatment to 10% of the HIV population. The study further observed that since the majority of sub-Sahara African nations had already embraced HIV screening and counselling, such services could be extended to HHV-8 testing and KS disease counselling.

In 2014, Szomolay and Lungu [95] developed a mathematical model, at cellular level,

to study the dynamics of HIV-1-related KS pathogenesis. In that model which was based on the review by Foreman et al.[32], the authors [95] modeled KS progression as a dual process encompassing the primary infection of B cells, that reinforces HHV-8 replication and the secondary infection of endothelial progenitor cells, which reinforces the KS propagation. The study concluded that HAART administration to people co-infected with HIV-1 and HHV-8 viruses could significantly amplify the therapeutic response of low dose therapies. The study concluded that adherence levels above 85 percent were necessary for a substantial reduction in the risk of KS and HIV-1 for treatment periods of less than a year, but at least a 90 percent adherence level was recommended for longer treatment periods.

In another study, Nani and Jin [73] developed and analysed an within-host mathematical model for HIV-1-associated KS during HAART and adoptive cellular Immunotherapy (ACI). The same state variables as in [72] were investigated. However, the constant source for $CD8^+$ T cells included ex-vivo incubated lymphocytes besides the one that were replenished by the thymus. The study showed hypothetically that HAART had the potential to annihilate HIV-1 actively infected $CD4^+$ T cells and HIV-1 virions without necessarily clearing the KS cells. The study further concluded that ACI had the capacity to bring KS into remission for AIDS patients who were on HAART and that a combined therapy of ACI and HAART had the potential to reconstitute the $CD4^+$ T cell numbers to pre-HIV levels.

Herpesviruses, like human herpesvirus-8 (KSHV or HHV-8), are incredibly successful parasites - once the infection is established, the individual can become a virus carrier for life. The invasion success of HHV-8 is attributed to the virus' ability to enter host cells, establish latent infection and efficiently reactivate upon stimulation caused by immunodeficiency. Therapeutic interventions of any of these steps is vital to break the viral life cycle and is being targeted as effective strategies for treatment of herpesvirus-associated cancers. Compared to AIDS-related KS, no much attention has been paid to the non-AIDS related variant that has three main subtypes: classic KS, African endemic KS and iatrogenic KS. This is likely due to the fact that the HHV-8 sequences were identified by Chang et al. [15] during the same period the HIV/AIDS pandemic was peaking globally [51]. Moreover, compared to some HIV-related comorbidities such as tuberculosis and pneumonia, HIV/AIDS related KS yields fewer deaths.

As mentioned above, HHV-8 can establish a latent infection in immunocompetent patients [16, 32]. However, under certain conditions such as immunosuppression [53], latency can be disrupted and virions can be released from their reservoirs for dissemination [37]. HHV-8 reactivation is often induced by co-infection with other viruses, such as human immunodeficiency virus or human cytomegalovirus (HCMV). Although highly antiretroviral therapy (HAART) is the first-line therapy for AIDS-KS, currently there is no definitive cure for its non-AIDS related variant.

Non-AIDS related KS therapies include surgical excision, radiotherapy and chemother-

apy [3], depending on the size of the lesions. The Food and Drug Agency(FDA)-approved chemotherapeutics, such as liposomal doxorubicin or interferon- α are also available [83]. However, these therapies do not target the virus *per se* and their anti-tumor effect is only transient. In the past two decades several studies have investigated alternative antiviral therapies that have shown promise to block the HHV-8 entry into its target cell [97] or to inhibit lytic replication from latently infected host cells [16]. Chemical inhibitors used in virus entry studies have common side effects, although recombinant viruses in animal models have shown some promise [100]. A recent study has shown that tyrosine kinase inhibitors, already in clinical use for human malignancies is capable of inhibiting lytic reactivation and the development of HHV-8-infected tumors in mice [7]. These novel therapeutics for HHV-8 infection are known to cause less side effects than the traditional treatments [7, 16] and will most likely serve as potential therapeutic avenues due to their relative drug safety. Nevertheless, there is a need to explore the drug safety of these therapeutics in randomized clinical trials [74] and this is where *in silico* studies may help.

2.2 Basis of Mathematical Modelling of KS

The mathematical models in this thesis are based on the pioneering work of Foreman et al. [32]. In Foreman et al. [32], the proposed schematic diagram [Figure 2.1], begins with cytokines and growth factors produced by HIV-1 infected cells or other activated immune cells. These cytokines and growth factors stimulate the endothelial

progenitor cells (EPC), which are thought to be the precursors of the KS cells (spindle cells). The stimulation of EPC leads to the activation and proliferation of these precursor cells which ultimately transform them into pre-KS. The activation of EPC predisposes them to an erroneous infection by HHV-8 as more virions are produced as a result of reactivation of the latently infected B cells. KSHV normally establishes a latent infection in B cells and only allows a transient lytic replication in a way that spares the host cell. However, with HIV-1 infection, the increase in the cytokine production and HIV-1 Tat protein, the lytic reactivation of latently infected B cells is triggered. This scenario leads to the mass production of HHV-8 virions which ultimately begin to infect the already activated progenitor cells using the newly acquired receptors.

For more details we refer the reader to the schematic diagram below that we have adapted from [32].

Foreman Proposed Model of AIDS-KS

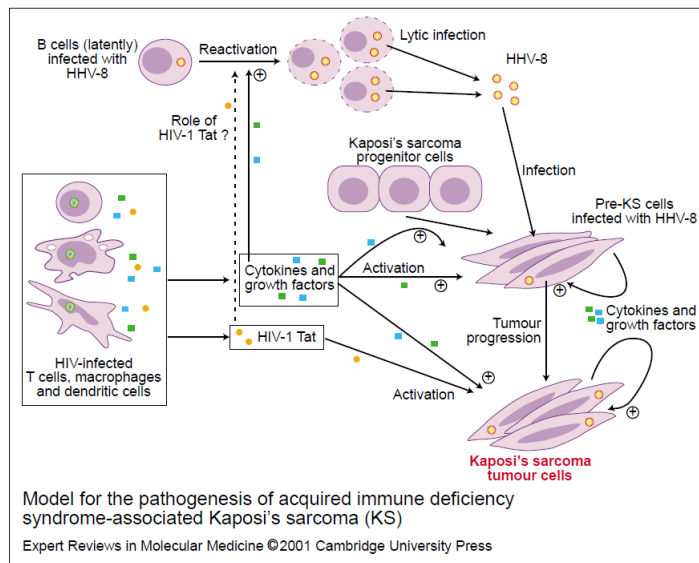


Figure 2.1: Model for the pathogenesis of AIDS-KS. Adapted from [31]

Chapter 3

Preliminary Definitions and Concepts

In this chapter we review some of the concepts used in this thesis. This review will make it easier to shorten some of the Lemmas and proofs developed in this thesis.

3.1 Some Defintions

Definition 3.1.1 [13] Consider a general system of the form $\mathbf{x}' = f(\mathbf{x}, t)$, where $\mathbf{x} \in \mathbb{R}^n$ is a vector of unknowns and

$$f(\mathbf{x}, t) = \begin{pmatrix} f_1(x_1, x_2, \dots, x_n, t) \\ f_2(x_1, x_2, \dots, x_n, t) \\ \vdots \\ f_n(x_1, x_2, \dots, x_n, t) \end{pmatrix}$$

is a vector-valued function $f : \mathbb{R}^{n+1} \rightarrow \mathbb{R}^n$. The system $\mathbf{x}' = f(\mathbf{x}, t)$, is said to be autonomous if f does not explicitly depend on t . That is, the system has the form $\mathbf{x}' = f(\mathbf{x})$.

Definition 3.1.2 [13] Suppose $f : \mathbb{R}^n \rightarrow \mathbb{R}^n$ is written in terms of its components and further suppose that the first partial derivatives of each component function exist.

That is, $\partial f_i / \partial x_j$ exists for $1 \leq i, j \leq n$. Then the Jacobian of f is the matrix

$$Jf(\mathbf{x}) = \begin{pmatrix} \frac{\partial f_1}{\partial x_1} & \frac{\partial f_1}{\partial x_2} & \cdots & \frac{\partial f_1}{\partial x_n} \\ \frac{\partial f_2}{\partial x_1} & \frac{\partial f_2}{\partial x_2} & \cdots & \frac{\partial f_2}{\partial x_n} \\ \vdots & \vdots & \ddots & \vdots \\ \frac{\partial f_n}{\partial x_1} & \frac{\partial f_n}{\partial x_2} & \cdots & \frac{\partial f_n}{\partial x_n} \end{pmatrix} \quad (3.1)$$

3.2 Existence and Uniqueness Theorem

Theorem 3.2.1 (Existence and Uniqueness of Solutions) [13] *Consider*

$$\dot{\mathbf{x}} = f(\mathbf{x}), \tag{3.2}$$

and $f : \mathbb{R}^n \rightarrow \mathbb{R}^n$, and $\mathbf{x}_0 \in \mathbb{R}^n$. Then, there is a $\delta > 0$, such that there is a unique solution $\mathbf{x}(t)$ to the differential equation with $\mathbf{x}(0) = \mathbf{x}_0$ for the interval $[0, \delta]$ with $t \in [0, \delta]$.

Definition 3.2.2 [13] *An equilibrium solution of $\dot{\mathbf{x}} = f(\mathbf{x})$ is any constant vector \mathbf{x}^* such that $f(\mathbf{x}^*) = \mathbf{0}$.*

Note that \mathbf{x}^* is also referred to as a steady state.

3.3 The next generation operator approach for computing the basic reproduction number, \mathcal{R}_0

The basic reproduction number, \mathcal{R}_0 , is often determined by considering the signs of the eigenvalues for the Jacobian matrix evaluated at the disease free equilibrium. Diekmann et al. 1990 [18] proposed a new method which they called the next generation operator approach. The determination of \mathcal{R}_0 is briefly presented below. The reader is referred to Diekmann et al.1990 [18] for details.

Consider a scenario where heterogeneity is discrete implying that the groups comprising the population have fixed characteristics.

Let $\mathbf{X} \in \mathbb{R}^r$, $\mathbf{Y} \in \mathbb{R}^s$, $\mathbf{Z} \in \mathbb{R}^n$, $r, s, n \geq 0$. Define the component of \mathbf{X} to be the number of susceptibles, recovered, and other classes of non-infected individuals. Let \mathbf{Y} represent the number of infected individuals who do not transmit the disease (various latent or non-infectious stages), and let \mathbf{Z} represent the number of infected individuals capable of transmitting the disease (e.g., infectious and non-quarantined individuals).

Define a function $h(\mathbf{X}, \mathbf{Y}, \mathbf{Z})$ such that $h(\mathbf{X}, \mathbf{0}, \mathbf{0}) = \mathbf{0}$.

Let an epidemiological model be represented in the form given below.

$$\begin{aligned}\frac{d\mathbf{X}}{dt} &= f(\mathbf{X}, \mathbf{Y}, \mathbf{Z}), \\ \frac{d\mathbf{Y}}{dt} &= g(\mathbf{X}, \mathbf{Y}, \mathbf{Z}), \\ \frac{d\mathbf{Z}}{dt} &= h(\mathbf{X}, \mathbf{Y}, \mathbf{Z}),\end{aligned}$$

Let $\mathbf{U}_0 = (\mathbf{X}^*, \mathbf{0}, \mathbf{0}) \in \mathbb{R}^{r+s+n}$ denote the disease-free equilibrium, that is,

$$f(\mathbf{X}^*, \mathbf{0}, \mathbf{0}) = g(\mathbf{X}^*, \mathbf{0}, \mathbf{0}) = h(\mathbf{X}^*, \mathbf{0}, \mathbf{0}) = 0. \quad (3.3)$$

Assuming that the equation $g(\mathbf{X}^*, \mathbf{Y}, \mathbf{Z}) = 0$ implicitly determines a function $\mathbf{Y} = \tilde{g}(\mathbf{X}^*, \mathbf{Y})$. Let $A = D_{\mathbf{Z}}h(\mathbf{X}^*, \tilde{g}(\mathbf{X}^*, \mathbf{0}), \mathbf{0})$ and further assume that A can be written in the form $A = M - D$, with $M \geq \mathbf{0}$ (that is, $m_{ij} \geq 0$) and $D > \mathbf{0}$, a diagonal matrix.

The basic reproductive number is defined as the spectral radius (dominant eigenvalue)

3.4. A TECHNIQUE FOR ESTABLISHING GLOBAL STABILITY OF THE DISEASE-FREE EQUILIBRIUM

of the matrix MD^{-1} , that is,

$$\mathcal{R}_0 = \rho(MD^{-1}).$$

3.4 A technique for establishing global stability of the disease-free equilibrium when $\mathcal{R}_0 < 1$.

The method outlined below is based on the works of Diekmann et al.[18].

Here we list two conditions that if met, guarantee the global asymptotic stability of the disease-free state. First, the given system must be written in the form:

$$\begin{aligned} \frac{d\mathbf{X}}{dt} &= F(\mathbf{X}, \mathbf{Z}), \\ \frac{d\mathbf{Z}}{dt} &= G(\mathbf{X}, \mathbf{Z}), G(\mathbf{X}, \mathbf{0}) = \mathbf{0}, \end{aligned} \tag{3.4}$$

where $\mathbf{X} \in \mathbb{R}^m$ denotes (its components) the number of uninfected individuals and $\mathbf{Z} \in \mathbb{R}^n$ denotes (its components) the number of infected individuals including latent, infectious, etc. $\mathbf{U}_0 = (\mathbf{X}^*, \mathbf{0})$ denotes the disease-free equilibrium of this system.

The conditions (H1) and (H2) below must be met to guarantee local asymptotic stability.

(H1) For $\frac{d\mathbf{X}}{dt} = F(\mathbf{X}, \mathbf{0})$, \mathbf{X}^* is globally asymptotically stable (g.a.s.),

(H2) $G(\mathbf{X}, \mathbf{Z}) = A\mathbf{Z} - \hat{G}(\mathbf{X}, \mathbf{Z})$, $\hat{G}(\mathbf{X}, \mathbf{Z}) \geq \mathbf{0}$ for $(\mathbf{X}, \mathbf{Z}) \in \Omega$, where $A = D_{\mathbf{Z}}G(\mathbf{X}^*, \mathbf{0})$

is an M-matrix (the off diagonal elements of A are nonnegative) and Ω is the region

where the model makes biological sense.

If system (3.4) satisfies the above two conditions then the following theorem hold:

Theorem. The fixed point $U_0 = (\mathbf{X}^*, \mathbf{0})$ is a globally asymptotically stable (g.a.s.) equilibrium of (3.4) provided that $\mathcal{R}_0 < 1$ and that assumptions (H1) and (H2) are satisfied.

3.5 Routh-Hurwitz Criteria

A method is devised for establishing stability of the steady states for large systems where direct computation of eigenvalues may not be easy. We follow closely the work presented in [67].

Let the following characteristic polynomial be taken from a Jacobian matrix.

$$\lambda^n + a_1\lambda^{n-1} + a_2\lambda^{n-2} + \dots + a_{j-1}\lambda^{n-j+1} + a_j\lambda^{n-j} + \dots + a_n = 0. \quad (3.5)$$

The Routh-Hurwitz criteria give the information about the signs of the real parts of eigenvalues and this is all that is needed to decide on the stability of an equilibrium point for a system of ordinary differential equations.

Let the entry in the l^{th} row and m^{th} column of the Hurwitz matrix, H_j , $j =$

1, 2, 3, ..., n , be denoted by h_{lm} . We define h_{lm} as

$$h_{lm} = \begin{cases} a_{2j-m} & \text{if } 0 < 2l - m \leq n \\ 1 & \text{if } 2l = m \\ 0 & \text{if } 2l < m \text{ or } 2l > n + m \end{cases} \quad (3.6)$$

All eigenvalues have negative real parts if and only if the determinants of H_j are positive, i.e.,

$$\det H_j > 0, \quad j = 1, 2, 3, \dots, n \quad (3.7)$$

We can also reformulate these conditions in more simpler terms for $n = 2, 3, 4, 5$.

$$n = 2 : \quad a_1 > 0, a_2 > 0,$$

$$n = 3 : \quad a_1 > 0, a_3 > 0, a_1 a_2 > a_3,$$

$$n = 4 : \quad a_1 > 0, a_3 > 0, a_4 > 0, a_1 a_2 a_3 > a_3^2 + a_1^2 a_4,$$

$$n = 5 : \quad a_i > 0 (i = 1, 2, 3, 4, 5), a_1 a_2 a_3 > a_3^2 + a_1^2 a_4, (a_1 a_4 - a_5)(a_1 a_2 a_3 - a_3^2 - a_1^2 a_4) > a_5 (a_1 a_2 - a_3)^2 + a_1 a_5^2.$$

3.6 Optimal Control Problem

We review some concepts pertaining to optimal control theory as presented in [1].

Consider a system

$$\begin{cases} \dot{\mathbf{x}} = \mathbf{f}(\mathbf{x}(t), \mathbf{u}(t), t), \\ \mathbf{x}(0) = \mathbf{x}_0, \end{cases} \quad (3.8)$$

The objective functional (cost functional), which is a measure of evaluating the system's performance, is given by:

$$J(\mathbf{u}) = h(\mathbf{x}(t_f)) + \int_0^{t_f} g(\mathbf{x}, \mathbf{u}, t) dt, \quad (3.9)$$

where $\mathbf{x}^T = (x_1, x_2, \dots, x_n) \in A \subset \mathbb{R}^n$ is the state vector, $\mathbf{u}^T = (u_1, u_2, \dots, u_m) \in U \subset \mathbb{R}^m$ is the control input vector (A and U designates the sets of admissible state trajectories and admissible controls, respectively), $\mathbf{f}^T = (f_1, f_2, \dots, f_n)$ is a continuously differentiable vector-valued function in each of its arguments, h is a differentiable scalar function, and g is a continuously differentiable function in each of its arguments.

The first term on the right side of (3.9) denotes a function value on the boundary called the payoff term and the second term indicates the performance of the system over the whole time interval, $[0, t_f]$. When a control input is added, the system follows some state trajectory, and the objective functional, $J(\mathbf{u})$, assigns a unique real number to the state trajectory. Hence, an optimal control may be defined as:

find an admissible control $\mathbf{u}^* \in U$ (and the associated admissible trajectory $\mathbf{x}^* \in A$) that minimizes the performance measure $J(\mathbf{u})$:

$$\min_{\mathbf{u}} J(\mathbf{u}), \quad (3.10)$$

subject to

$$\dot{\mathbf{x}} = \mathbf{f}(\mathbf{x}(t), \mathbf{u}(t), t), \quad (3.11)$$

$$\mathbf{x}(0) = \mathbf{x}_0, \quad (3.12)$$

$$\mathbf{u}(t) \in U, \text{ for all } t \in [0, t_f]. \quad (3.13)$$

The constraint in (3.11) can be transferred to the objective functional, $J(\mathbf{u})$, by introducing Lagrange multiplier $\boldsymbol{\lambda}^T(t) = (\lambda_1(t), \lambda_2(t), \dots, \lambda_n(t))$ (also called the co-state vector):

$$J(\mathbf{u}) = h(\mathbf{x}(t_f)) + \int_0^{t_f} \left(g(\mathbf{x}, \mathbf{u}, t) + \boldsymbol{\lambda}^T(t) (\mathbf{f}(\mathbf{x}, \mathbf{u}, t) - \dot{\mathbf{x}}) \right) dt$$

We now define the Hamiltonian function, H , as:

$$H(\mathbf{x}, \mathbf{u}, \boldsymbol{\lambda}, t) = g(\mathbf{x}, \mathbf{u}, t) + \boldsymbol{\lambda}^T(t) \mathbf{f}(\mathbf{x}, \mathbf{u}, t), \quad (3.14)$$

Pontryagin's minimum principle (PMP) specifies the necessary conditions for $\mathbf{u}(t)$ to be an optimal control, where the terminal time t_f and the terminal state $\mathbf{x}(t_f)$ are considered to be fixed and free (not restricted), respectively: let $\mathbf{u}^* : [0, t_f] \rightarrow U \subset \mathbb{R}^m$ be an optimal control, and let $\mathbf{x}^* : [0, t_f] \rightarrow A \subset \mathbb{R}^n$ (and $\boldsymbol{\lambda}^*$) be the corresponding optimal state (and co-state) trajectory. Then, the optimality set (i.e., \mathbf{u}^* , \mathbf{x}^* , and $\boldsymbol{\lambda}^*$) satisfies simultaneously the set of the following conditions.

(i) the state equation

$$\frac{d\mathbf{x}^*}{dt} = \frac{\partial H}{\partial \boldsymbol{\lambda}}(\mathbf{x}^*, \mathbf{u}^*, t), \quad \forall t \in [0, t_f], \quad (3.15)$$

with initial conditions on the state vector $\mathbf{x}^*(0) = \mathbf{x}_0$;

(ii) the co-state equation

$$\frac{d\boldsymbol{\lambda}^*}{dt} = -\frac{\partial H}{\partial \mathbf{x}}(\mathbf{x}^*, \mathbf{u}^*, \boldsymbol{\lambda}^*, t), \quad \forall t \in [0, t_f], \quad (3.16)$$

with terminal conditions on the co-state vector (transversality conditions):

$$\boldsymbol{\lambda}^*(t_f) = \frac{dh}{d\mathbf{x}}(\mathbf{x}^*(t_f)), \quad (3.17)$$

(iii) optimality condition (i.e. the optimal control \mathbf{u}^* minimizes the Hamiltonian function):

$$H(\mathbf{x}^*, \mathbf{u}^*, \boldsymbol{\lambda}^*, t) \leq H(\mathbf{x}^*, \mathbf{u}, \boldsymbol{\lambda}^*, t), \quad \forall t \in [0, t_f], \quad \forall \mathbf{u} \in U, . \quad (3.18)$$

Chapter 4

AIDS-related Kaposi's sarcoma

Pathogenesis

4.1 Introduction

Despite significant progress made in ending the HIV/AIDS epidemic, an estimated 38 million people were living with HIV at the end of 2018, resulting in about 2% of them dying. The African region remains to be the most affected, accounting for two third of the people living with HIV worldwide [98]. Although HIV-positive people who start antiretroviral therapy (HAART) have the same life expectancy as their HIV negative peers, they develop co-morbidities on average 16 years earlier than HIV negative people [75]. Kaposi's sarcoma (KS) is one of the most common malignancies causing co-morbidity in patients with human immunodeficiency virus-1 (HIV-1)

infection, especially at the later HIV stage (AIDS). Most of AIDS-related cancers are caused by oncogenic viruses such as Epstein Barr virus (EBV), Kaposi's sarcoma-associated herpesvirus (KSHV or HHV-8) and Human papillomavirus (HPV) [10].

There are four different forms of Kaposi's sarcoma: Classic or sporadic KS, African or Endemic KS, AIDS-associated or epidemic KS, and Transplant or Immunosuppression-associated or Iatrogenic KS [32]. The development of each of these forms is dependent on prior infection with HHV-8. However, HHV-8 infection alone is insufficient for the development of KS and some form of immunodeficiency is necessary for disease progression [95].

Most individuals infected with African KS and Classic KS but with strong immune responses have remained latently infected with HHV-8 throughout their lifetime [31, 32]. The co-factors involved in the development of Classic and Endemic KS are not fully understood although environmental and genetic factors such as age, sex, malnutrition, etc have been implicated [32]. Progression from HHV-8 infection to KS is a complex process. For instance, not every AIDS patient develops KS even in the face of profound immunosuppression, only a minority of HHV-8-infected transplant recipients develop iatrogenic KS, and that people with Classic or Endemic KS are not typically immunosuppressed [50, 62].

Whether HHV-8 infection develops into an asymptomatic or symptomatic KS, depends on the interplay between KSHV and the host immune system. When HHV-8 infection occurs, the immune system promotes an environment where cellular proliferation, cell migration, angiogenesis and cytokine/chemokine production are enhanced [32]. The immune response occurs in two stages: first by triggering the innate response and secondly, if the infection persists, the adaptive response [94]. A review by Foreman et al [32] has suggested how infection of progenitor cells by HHV-8 can initiate the development of all forms of KS. For individuals dually infected with both HIV-1 and HHV-8, the HHV-8 infection is enhanced by the HIV-1 growth factors which stimulate both uninfected and infected B cells to proliferate in response to T cell signals [32]. The T cell signals stimulate the latently infected B-cells. These cells that were dormant are now capable to proliferate and increase the population of HHV-8 producing cells.

HAART has proved to be effective in maintaining low viremia in HIV-1 infected individuals. In patients dually infected with HIV-1 and HHV-8, HAART has proved to be effective in clearing KS infections [9]. For many diseases such as malaria and many childhood diseases prevention is given priority over treatment. For example, individuals going to malaria Endemic areas are advised to take malaria prophylaxis drugs one week before departure. These drugs activate their immune system to fight and clear the infection before it develops into active disease. This approach can be

mimicked and applied to the case of AIDS-KS.

When a pathogen invades the body, the body triggers an innate, non-specific immune response to clear the infection. This response consists of cellular (immune cells) and chemical (e.g. cytokines) defenses to reduce the growth of the population of infected cells and to eliminate the pathogens. The innate immune response may be viewed as a way to suppress and control HHV-8 infection before the adaptive immune response characterised by the clonal expansion of lymphocytes is activated.

Using mathematical modelling, we show that a dynamic motif in Figure 1 comprising of interactions between infected B cells, infected progenitor cells, KS cells, HHV-8 virions and the innate immune response, is able to prevent a potentially Classic KS from developing into a clinical disease. This has twofold implications. First, key innate immune signaling molecules induced by viral infection lead to the production of a broad range of antiviral proteins and cytokines. Uncontrolled release of these cytokines can lead to cytokine storm, causing tissue damage or indirectly causing pathology even before the initiation of HAART [66]. Second, antibody test can detect HIV infection as early as 1-2 weeks after exposure and testing after 2 or 3 weeks is not very useful [43]. Hence, it is essential to understand at what level to deem the innate immune response or cytokine therapy to be safe.

If the infection progresses despite the innate response, the immune system mounts a more robust, longer lasting adaptive or acquired immune response. Hence, we construct a second model that mimics the body's adaptive immune response by including the interactions as in Figure 4 between HIV-1 virions, HIV-1- and HHV-8-specific effector cells, infected CD4 T cells, uninfected B and CD4 T cells. The initial condition of the extended model will be determined by the equilibrium states of the model with innate mechanism, whereby assuming an advanced stage of HIV-1 and HHV-8 co-infection. We will take an optimal control approach to determine the drug efficacy level of HAART alone or combined HAART and chemotherapy. This is motivated by the fact that HAART should be the first step therapy in optimal control of HIV infection for AIDS-KS. However, patients with high-risk KS rarely respond to HAART alone and hence, chemotherapy is recommended which requires balancing the immunosuppressive effects of chemotherapy with its potential benefit.

HHV-8/KSHV is primarily transmitted to human hosts via saliva. The replication of the virus, in the early stages of the infection, takes place in the epithelial cells of the oropharynx and subsequently targets B cells which are the primary reservoirs. The B cell infection normally results in latent infection in which only a handful of the viral genes are expressed principally for maintaining the viral DNA in an episomal form (the DNA is never integrated into the host cell genome but tethered to the host cell chromosome) and evading the host immune surveillance. Trafficking of the B

cells to the lymphoid tissues allows more infections of the B cells as viral lytic cycle is triggered. Latently infected B cells can disseminate to other parts of the body via blood. As more and more of these latently infected B cells are stimulated to activate, say due to inflammatory environment , created by the cytokines secreted from the HIV-1 infected cells, HHV-8 lytic replication cycle is triggered. This results in the release of more HHV-8 progeny virions in the host. This heightened viremia leads to the erroneous infection of activated endothelial progenitor cells (the precursors of the KS tumor cells). The infection of endothelial cells normally result in latency. However, these latently infected cells have very high proliferative potential and have the ability to transform into the spindle shaped cells. These cells have the ability to secrete more inflammatory cytokines in the microenvironment that promote their growth and enhance proliferation of these cells.

(a) HHV-8/KSHV is primarily transmitted to human hosts via saliva. The replication of the virus, in the early stages of the infection, takes place in the epithelial cells of the oropharynx and subsequently targets B cells which are the primary reservoirs. The B cell infection normally results in latent infection in which only a handful of the viral genes are expressed principally for maintaining the viral DNA in an episomal form (the DNA is never integrated into the host cell genome but tethered to the host cell chromosome) and evading the host immune surveillance. Trafficking of the B cells to the lymphoid tissues allows more infections of the B cells as viral lytic cycle is triggered. Latently infected B cells can disseminate to other parts of the body via

blood. As more and more of these latently infected B cells are stimulated to activate, say due to inflammatory environment, created by the cytokines secreted from the HIV-1 infected cells, HHV-8 lytic replication cycle is triggered. This results in the release of more HHV-8 progeny virions in the host. This heightened viremia leads to the erroneous infection of activated endothelial progenitor cells (the precursors of the KS tumor cells). The infection of endothelial cells normally result in latency. However, these latently infected cells have very high proliferative potential and have the ability to transform into the spindle shaped cells. These cells have the ability to secrete more inflammatory cytokines in the microenvironment that promote their growth and enhance proliferation of these cells.

There are several lines of evidence that indicate that KS oncogenesis is associated with the inability of the T-cell mediated immunity to control the KSHV infection. KSHV can establish life-long asymptomatic infection in immune-competent individuals. However, when T cell-immune control declines, for instance, through AIDS or treatment with immunosuppressive drugs, both the prevalence of KSHV infection and the incidence of KS in KSHV carriers dramatically increases. This is supported by the fact that the KS situation improves upon immune restoration due to HAART treatment or cessation of immunosuppressive treatment in the case of organ transplant KS. Due to the foregoing, we shall restrict our modelling to T-cell immune control and ignore the humoral arm of immunity.

To develop these models, we shall apply the Foreman et al [32] approach. According

to this hypothesis, AIDS-KS arises from the erroneous infection of progenitor cells by HHV-8 which is enhanced by action of HIV-1 infected host cells. These HIV-1 infected cells produce cytokines and growth factors that stimulate the progenitors of the KS cells which makes them susceptible to HHV-8 infection. In summary, we will show that early HHV-8-specific intervention is important as it can control the HHV-8 infection from developing into a progressive KS. We also determine efficacy levels for cART therapy at which HIV-1 and HHV-8 co-infection can be kept under control, thus providing valuable testable predictions for clinical researchers.

4.2 Model 1: KS model with innate mechanism

4.2.1 Model Formulation and Description

We present a model with innate mechanism that mimics HHV-8 infection dynamics leading to KS progression as suggested by Foreman et al, [32]. We simplify the model by considering the dynamics of infected states with source terms for infected progenitor cells dependent on HHV-8 levels and we have assumed a logistic growth for infected B cells. The model incorporates interactions between infected progenitor cells X_1 , KS cells X_2 , infected B cells X_3 , HHV-8 virions X_4 and the innate immune response X_5 . The equations are as follows:

$$\dot{X}_1(t) = K_1 \left(1 - \frac{X_5}{\theta_{x_5} + X_5}\right) X_4 \left(1 - \frac{X_4}{x_{4max}}\right) - \mu_{x_1} X_1. \quad (4.1)$$

Eq. (4.1) describes the dynamics of the infected progenitor cells, X_1 . The first term represents a source term which grows logistically with respect to the viral level, X_4 , and is moderated by the innate immune response X_5 . The effect of the innate immune response X_5 is moderated by the efficacy threshold for the innate immune response θ_{x_5} . We note that as θ_{x_5} approaches zero, the innate immune response has substantial effect on blocking the growth of infected progenitor cells. The second term represents the natural death of these cells.

$$\dot{X}_2(t) = \hat{\mu}_{x_1} X_1 - \mu_{x_2} X_2. \quad (4.2)$$

Eq. (4.2) represents the concentration of KS. The first term designates the growth of KS as the infected progenitor cells transform into cancerous cells. The second term is natural death of KS at a constant rate μ_{x_2} .

$$\dot{X}_3(t) = K_2 \left(1 - \frac{X_5}{\theta_{x_5} + X_5}\right) X_3 \left(1 - \frac{X_3}{x_{3max}}\right) - \mu_{x_3} X_3. \quad (4.3)$$

Eq. (4.3) describes the dynamics of the infected B cells. These are assumed to grow logistically but this growth is regulated by the efficacy threshold for the innate immune response and the last term is natural death of infected B cells at a constant rate μ_{x_3} .

$$\dot{X}_4(t) = N_{x_4} \mu_{x_3} X_3 - \mu_{x_4} X_4. \quad (4.4)$$

Eq. (4.4) represents the dynamics of HHV-8. The first term represents the production of these virus from the dying infected B cells, where N_{x_4} is the maximum carrying capacity of infected CD4 T cells. The last term represents the clearance of HHV-8 at a constant rate μ_{x_4} .

$$\dot{X}_5(t) = K_3 \frac{X_3}{\theta_{x_3} + X_3} - K_3 X_5 \tag{4.5}$$

Eq.(4.5) represents the innate immune response X_5 . The first term represents the stimulation of the innate immunity due to the presence of infected B cells, X_3 . It is assumed that X_5 is stimulated by the infected B cells, X_3 , in a saturable manner with the scaling constant, θ_{x_3} , and decays at a constant rate K_3 [6].

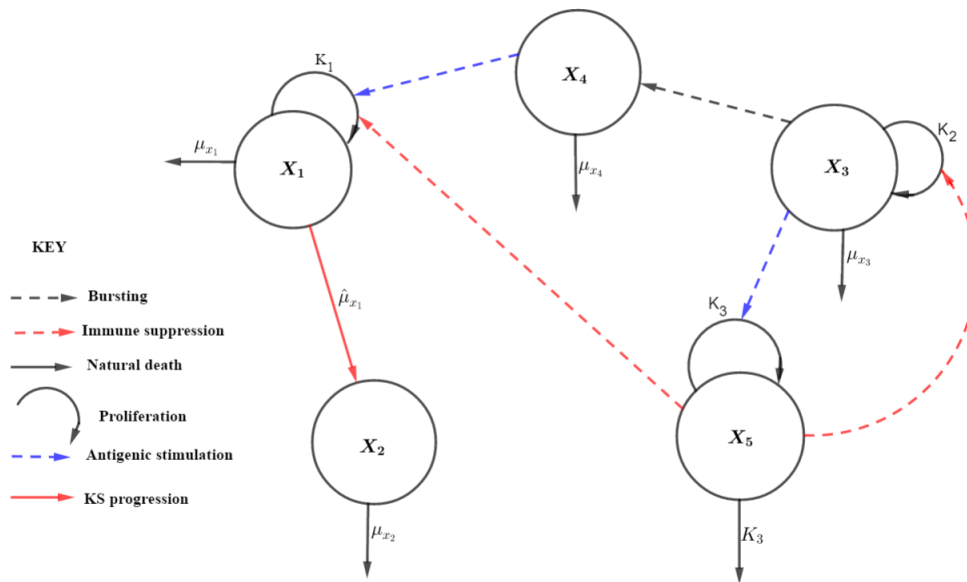


Figure 4.1: Schematic diagram of the model with innate mechanism, describing interactions for Classic KS.

Variable	Definition	Initial Value	Reference
X_1	Infected progenitor cells	0 cell mm ⁻³	[80]
X_2	KS cells	0 cell mm ⁻³	Estimated
X_3	Infected B cells	0 cell mm ⁻³	Estimated
X_4	HHV-8 viral load	0 cell mm ⁻³	Estimated
X_5	Innate immune response	10 ⁻²	Estimated
Parameter	Definition	Value	Reference
K_1	Infected progenitor cell proliferation rate	0.2 day ⁻¹	Estimated
K_2	Infected B cell proliferation rate	0.36 day ⁻¹	[95]
K_3	Innate immune response activation rate	0.01 day ⁻¹	[95]
θ_{x_3}	Innate immune response activation threshold	200 cell mm ⁻³	Estimated
θ_{x_5}	Efficacy threshold for innate immune response	0.08	Estimated
$x_{3_{max}}$	Infected B cell carrying capacity	400 cell mm ⁻³	[95]
$x_{4_{max}}$	HHV-8 carrying capacity	5×10^5 virions mm ⁻³	[95]
μ_{x_1}	Blanket death rate of infected progenitor cells	0.1 day ⁻¹	[95]
μ_{x_2}	Death rate of KS cells	0.03 day ⁻¹	[95]
$\hat{\mu}_{x_1}$	Progression rate of KS	0.09 day ⁻¹	[95]

μ_{x_3}	Death rate of infected B cells	0.33 day ⁻¹	[95]
μ_{x_4}	Clearance rate of HHV-8	0.57 day ⁻¹	[95]
N_{x_4}	Maximum carrying capacity of infected B cells	700	[95]

Table 4.1: Parameters of the model with innate mechanism and their definitions.

4.2.2 Analysis of the Model

Positivity and Boundedness of Solutions

We denote by \mathbb{R}_+^5 the set of points $X_t = (X_1(t), X_2(t), X_3(t), X_4(t), X_5(t))$ in \mathbb{R}^5 with positive coordinates and consider the system (4.1) – (4.5) with initial values

$$X^0 = (X_1^0, X_2^0, X_3^0, X_4^0, X_5^0) \in \mathbb{R}_+^5.$$

In this section we prove the following theorem

Theorem 4.2.1 *If $X_i^0 \geq 0$, then $X_i(t) \geq 0$ for all $t > 0$.*

Before we prove Theorem 4.2.1, we rearrange the system into a subsystem of infected progenitor and infected B cells, $W = (X_1(t), X_3(t))$, written in matrix form as

$$\dot{W} = M_w W + KF(q), \quad (4.6)$$

where

$$M_w = \begin{pmatrix} -\mu_{x_1} & 0 \\ 0 & -\mu_{x_3} \end{pmatrix}, \quad F(q) = h(X_5) \begin{pmatrix} f_4(X_4) \\ f_3(X_3) \end{pmatrix}, \quad \text{and } W = \begin{pmatrix} X_1 \\ X_3 \end{pmatrix}.$$

$$K = \begin{pmatrix} K_1 & 0 \\ 0 & K_2 \end{pmatrix}, \quad q = (X_3, X_4, X_5), \quad f_j(X_j) = X_j \left(1 - \frac{X_j}{x_{jmax}}\right), \quad j \in \{3, 4\}.$$
(4.7)

and a subsystem consisting of KS and HHV-8, $Y = (Y_2(t), Y_4(t)) = (X_2(t), X_4(t))$ written in matrix form as

$$\dot{Y} = M_y Y + \varepsilon W, \quad (4.8)$$

where

$$M_y = \begin{pmatrix} -\mu_{y_2} & 0 \\ 0 & -\mu_{y_4} \end{pmatrix}, \quad Y = \begin{pmatrix} Y_2 \\ Y_4 \end{pmatrix}, \quad \text{and } \varepsilon = \begin{pmatrix} \hat{\mu}_{x_1} & 0 \\ 0 & N_{x_4} \mu_{x_3} \end{pmatrix}.$$

The proof of Theorem 4.2.1 is done in three steps. First, we prove that the source terms in (4.6) are nonnegative, that is, $F(q) \geq 0$. Second, we will show that $X_i(t) \geq 0$, $i = 1, 3$, $t > 0$ and finally, we conclude that $Y_i(t) \geq 0$ for $t > 0$.

Proof 4.2.2 From equation (4.5) we can deduce that $X(t) \geq X(0) \exp(-K_3 t) \geq 0$.

Now, the source terms in (4.6) can be written as

$$F(q) = \left(1 - \frac{X_5}{\theta_{x_5} + X_5}\right) f_j(X_j), \quad \text{where } j \in \{3, 4\}.$$

Notice that $f_5(X_5) = 1 - \frac{X_5}{\theta_{x_5} + X_5} = \frac{\theta_{x_5}}{\theta_{x_5} + X_5} > 0$, for $\theta_{x_5} > 0$. The function $f_j(X_j)$ in (4.7) has zeros at $X_j = 0$ and $X_j = x_{j_{max}}$, has a peak at $X_j = \frac{x_{j_{max}}}{2}$ and is positive in the interval $0 < X_j < x_{j_{max}}$. Hence, $F(q) := f_5(X_5) f_j(X_j) \geq 0$.

The matrix M_w in (4.6) is a Mertzler matrix and since $F(q) \geq 0$, the solution of (4.7) is nonnegative for all $t > 0$. The matrix $\varepsilon \geq 0$ since $x_i \geq 0$ for $i = 1, 3$. The matrix M_y is a Mertzler matrix and hence, the solution of (4.8) is nonnegative for $t > 0$. We conclude that if $x_i^0 \geq 0$, $i = 1, 2, 3, 4, 5$, then the solution of the system (4.1) – (4.5) remains in \mathbb{R}_+^5 .

4.2.3 Steady States and the Basic Reproduction Number

The virus free equilibrium of the KS model with innate mechanism given by Equations (4.1) – (4.5) is $\varepsilon_0 = (X_1^0, X_2^0, X_3^0, X_4^0, X_5^0) = (0, 0, 0, 0, 0)$. In what follows, we will

calculate the basic reproduction number of the system (4.1) – (4.5) using the next generation operator method [14]. The basic reproduction number is determined by the number of newly infected B cells. Using this approach, we first assume that the model system (4.1) – (4.5) can be written in the form.

$$\begin{aligned}\frac{dX}{dt} &= f(\mathbf{X}, \mathbf{Y}, \mathbf{Z}), \\ \frac{dY}{dt} &= g(\mathbf{X}, \mathbf{Y}, \mathbf{Z}), \\ \frac{dZ}{dt} &= h(\mathbf{X}, \mathbf{Y}, \mathbf{Z}),\end{aligned}\tag{4.9}$$

where $\mathbf{X} \in \mathbb{R}$, $\mathbf{Y} \in \mathbb{R}$ and $\mathbf{Z} \in \mathbb{R}^3$, and $h(\mathbf{X}, \mathbf{0}, \mathbf{0}) = \mathbf{0}$. Assuming that the equation $g(\mathbf{X}^*, \mathbf{Y}, \mathbf{Z}) = \mathbf{0}$ implicitly determines a function $Y = \tilde{g}(\mathbf{X}^*, \mathbf{Z})$. We let $\mathbf{A} = D_Z h(\mathbf{X}^*, \tilde{g}(\mathbf{X}^*, \mathbf{0}), \mathbf{0})$ and further assume that \mathbf{A} can be written in the form $\mathbf{A} = \mathbf{M} - \mathbf{D}$, with $\mathbf{M} \geq \mathbf{0}$ (that is $m_{ij} \geq 0$) and $\mathbf{D} \geq \mathbf{0}$, a diagonal matrix.

In system (4.9), \mathbf{X} denotes the innate immune response, \mathbf{Y} represents the HHV-8 virions and the components of \mathbf{Z} represent the HHV-8-associated cells, i.e., $\mathbf{X} = X_5$, $\mathbf{Y} = X_4$, $\mathbf{Z} = (X_1, X_2, X_3)$. Let $\mathbf{U}_0 = (\mathbf{X}^*, \mathbf{0}, \mathbf{0})$ denote the virus free equilibrium, that is,

$$f(\mathbf{X}^*, \mathbf{0}, \mathbf{0}) = g(\mathbf{X}^*, \mathbf{0}, \mathbf{0}) = 0, \quad \text{and} \quad h(\mathbf{X}^*, \mathbf{0}, \mathbf{0}) = \mathbf{0}, \quad \text{with} \quad \mathbf{Y} = \tilde{g}(\mathbf{X}^*, \mathbf{Z}),$$

where

$$\tilde{g}(\mathbf{X}^*, \mathbf{Z}) = \frac{N_{x_4} \mu_{x_3} X_3}{\mu_{x_4}}.$$

We compute $\mathbf{A} = D_{\mathbf{Z}} h(\mathbf{X}^*, \tilde{\mathbf{g}}((\mathbf{X}^*, \mathbf{0}), \mathbf{0}))$ and get

$$\mathbf{M} = \begin{pmatrix} 0 & 0 & \frac{K_1 N_{x_4} \mu_{x_3}}{\mu_{x_4}} \\ \hat{\mu}_{x_1} & 0 & 0 \\ 0 & 0 & K_2 \end{pmatrix} \quad \text{and} \quad \mathbf{D}^{-1} = \begin{pmatrix} \frac{1}{\mu_{x_1}} & 0 & 0 \\ 0 & \frac{1}{\mu_{x_2}} & 0 \\ 0 & 0 & \frac{1}{\mu_{x_3}} \end{pmatrix}$$

The reproduction number is given by the next generation spectral radius $\rho(\mathbf{M}\mathbf{D}^{-1})$ to be

$$\mathcal{R}_0 = \frac{K_2}{\mu_{x_3}}.$$

4.2.4 Local Stability of the Virus Free Equilibrium, ε^0

Lemma 4.2.3 *The virus free equilibrium point ε^0 is locally asymptotically stable if $\mathcal{R}_0 < 1$.*

Proof 4.2.4 *We consider the Jacobian matrix of the system (4.1) – (4.5), evaluated at the virus free steady state denoted by $J(\varepsilon^0)$.*

$$J(\varepsilon^0) = \begin{pmatrix} -\mu_{x_1} & 0 & 0 & K_1 & 0 \\ \hat{\mu}_{x_1} & -\mu_{x_2} & 0 & 0 & 0 \\ 0 & 0 & K_2 - \mu_{x_3} & 0 & 0 \\ 0 & 0 & N_{x_4}\mu_{x_3} & -\mu_{x_4} & 0 \\ 0 & 0 & \frac{K_3}{\theta_{x_3}} & 0 & -K_3 \end{pmatrix}$$

The eigenvalues are

$$\lambda_1 = -K_3, \quad \lambda_2 = -\mu_{x_1}, \quad \lambda_3 = -\mu_{x_2}.$$

The other two eigenvalues are obtained from a 2×2 sub-matrix given by:

$$\mathbf{B} = \begin{pmatrix} K_2 - \mu_{x_3} & 0 \\ N_{x_4}\mu_{x_3} & -\mu_{x_4} \end{pmatrix}$$

For existence of negative eigenvalues of this sub - matrix, $Tr(\mathbf{B}) < 0$ and $Det(\mathbf{B}) > 0$.

We observe that

$$\begin{aligned} Tr(\mathbf{B}) &= \mu_{x_3}(\mathcal{R}_0 - 1) - \mu_{x_4} < 0, \quad \text{if } \mathcal{R}_0 < 1, \\ Det(\mathbf{B}) &= -\mu_{x_3}\mu_{x_4}(\mathcal{R}_0 - 1) > 0, \quad \text{if } \mathcal{R}_0 < 1. \end{aligned}$$

4.2.5 Existence of the Endemic Infection Equilibrium, ε^*

Setting the system (4.1)–(4.5) to zero and solving the resulting system simultaneously yields:

$$X_3 = 0 \text{ or } K_2 \left(1 - \frac{X_5}{\theta_{x_5} + X_5}\right) \left(1 - \frac{X_3}{x_{3max}}\right) - \mu_{x_3} = 0,$$

Suppose $X_3 \neq 0$. Then,

$$K_2 \left(1 - \frac{X_5}{\theta_{x_5} + X_5}\right) \left(1 - \frac{X_3}{x_{3max}}\right) - \mu_{x_3} = 0, \quad (4.10)$$

Using (4.5) to solve for X_5 and replacing in (4.10) yields

$$A_2 X_3^2 + A_1 X_3 + A_0 = 0,$$

where $A_2 = K_2 \theta_{x_5}$, $A_1 = \mu_{x_3} x_{3max} + K_2 \theta_{x_3} \theta_{x_5} + \mu_{x_3} \theta_{x_5} x_{3max} (1 - \mathcal{R}_0)$ and $A_0 = \mu_{x_3} \theta_{x_3} \theta_{x_5} x_{3max} (1 - \mathcal{R}_0)$. To establish the existence of a positive root for $g(X_3) = A_2 X_3^2 + A_1 X_3 + A_0$, say X_3^* , we argue as follows:

Note that $g(0) = \mu_{x_3} \theta_{x_3} \theta_{x_5} x_{3max} (1 - \mathcal{R}_0) < 0$ if $\mathcal{R}_0 > 1$ and by continuity of g , we have

$$\lim_{X_3 \rightarrow \infty} g(X_3) = +\infty.$$

This implies that there is a positive number, $X_3^* \in (0, +\infty)$ such that $g(X_3^*) = 0$.

Hence, we obtain the following coordinates for the endemic infection equilibrium, ε^* :

$$X_1^* = \frac{K_1 N_{x_4} \mu_{x_3} X_3^*}{\mu_{x_1} \mu_{x_4}} \left(\frac{\theta_{x_5} (\theta_{x_3} + X_3^*)}{\theta_{x_5} (\theta_{x_3} + X_3^*) + X_3^*} \right) \left(1 - \frac{N_{x_4} \mu_{x_3} X_3^*}{\mu_{x_4} x_{4max}} \right), \quad (4.11)$$

$$X_2^* = \frac{K_1 \hat{\mu}_{x_1} \mu_{x_3} N_{x_4} X_3^*}{\mu_{x_1} \mu_{x_2} \mu_{x_4}} \left(\frac{\theta_{x_5} (\theta_{x_3} + X_3^*)}{\theta_{x_5} (\theta_{x_3} + X_3^*) + X_3^*} \right) \left(1 - \frac{N_{x_4} \mu_{x_3} X_3^*}{\mu_{x_4} x_{4max}} \right) \quad (4.12)$$

$$X_4^* = \frac{\mu_{x_3} N_{x_4} X_3^*}{\mu_{x_4}}, \quad X_5^* = \frac{X_3^*}{\theta_{x_3} + X_3^*}. \quad (4.13)$$

Lemma 4.2.5 Consider the system (4.1) – (4.5). Then the following holds:

(i) If $\mathcal{R}_0 \leq 1$, then the virus free equilibrium, ε^0 , is the only equilibrium.

(ii) If $\mathcal{R}_0 > 1$, then there are two equilibria: the virus free equilibrium, ε^0 , and the virus present equilibrium, ε^* .

Proof 4.2.6 Suppose X_3^1, X_3^2 are two roots of the equation $g(X_3) = 0$, then

$$X_3^1 + X_3^2 = \frac{-\mu_{x_3} x_{3max} - K_2 \theta_{x_3} \theta_{x_5} - \mu_{x_3} \theta_{x_5} x_{3max} (1 - \mathcal{R}_0)}{K_2 \theta_{x_5}}, \quad X_3^1 X_3^2 = \frac{\mu_{x_3} \theta_{x_3} \theta_{x_5} x_{3max} (1 - \mathcal{R}_0)}{K_2 \theta_{x_5}}.$$

Since $A_1 \geq 0$ for $\mathcal{R}_0 \leq 1$, it follows that $X_3^1 + X_3^2 \leq 0$ and $X_3^1 X_3^2 \geq 0$ and so $X_3^1, X_3^2 \leq 0$. Hence, the system (4.1)–(4.5) has only one equilibrium point, ε^0 and this concludes (i). Now, suppose $\mathcal{R}_0 > 1$, then $-\mu_{x_3} \theta_{x_5} x_{3max} (1 - \mathcal{R}_0) > 0$ and $X_3^1 X_3^2 < 0$ indicating that $g(X_3) = 0$ has a unique positive root. This completes the proof of (ii).

4.2.6 Numerical Simulations of the Model with Innate Mechanism

The parameter values used in Figure 4.2 are given in Table 4.1. Numerical simulations in Figure 4.2 show the effect of parameter θ_{x_5} on the components of the model with innate mechanism. We found a critical value of the efficacy threshold for the innate immune response $\theta_{x_5}^* \approx 0.0205$, below which the HHV-8 infection clears even if $\mathcal{R}_0 > 1$. This has important implications for a potential anti-KS therapy, whereby the effect of pro-inflammatory cytokines such as IL-2, which stimulate type 1 immunity and were shown to have anti-KS potential [92, 93], can be associated with small θ_{x_5} .

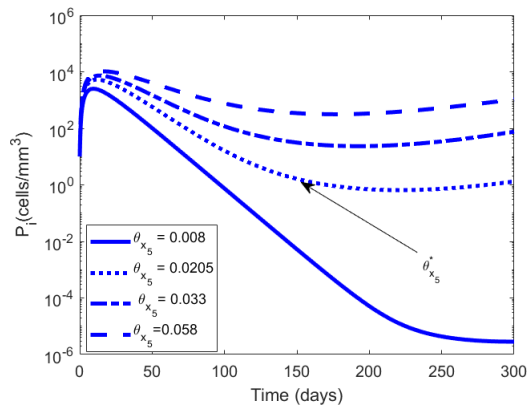
4.2.7 Sensitivity and Uncertainty Analysis

The choice of model parameters is never free from uncertainties. It is therefore necessary that a sensitivity analysis is conducted to explore simultaneously the whole parameter space rather than just using the nominal values. To achieve this we employ the Latin Hypercube sampling (LHS) scheme which is described in great detail in [70, 71].

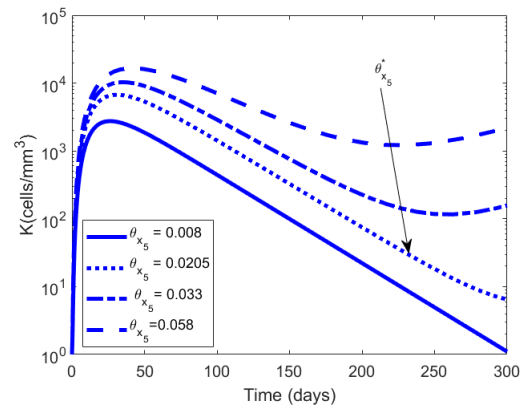
The results of the sensitivity analysis can help us identify which of the model parameters have a bearing on the infection process. Such parameters must be estimated with great precision. The sign of the PRCC identifies the specific qualitative rela-

relationship between the input parameter and the output variable. The positive value of the PRCC of a variable indicates that enhancement of the processes described by a variable makes the infection process worse. On the other hand, enhancing processes described by parameters with negative PRCCs would have a substantial effect on improving the prognosis.

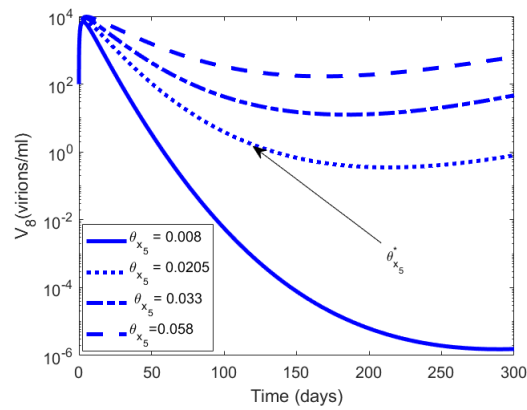
Figure 4.3 shows the sensitivity analysis of parameters from **Table 7.1** on \mathcal{R}_0 . In particular, the rate of infected B cell proliferation K_2 is strongly correlated with the reproduction number. This is in line with experimental observation that the immune activation may be also a factor in KS, driven by the initiation of HHV-8 infected cell proliferation by HIV-tat protein [65]. In what follows, we will study the more severe form of KS, AIDS-KS.



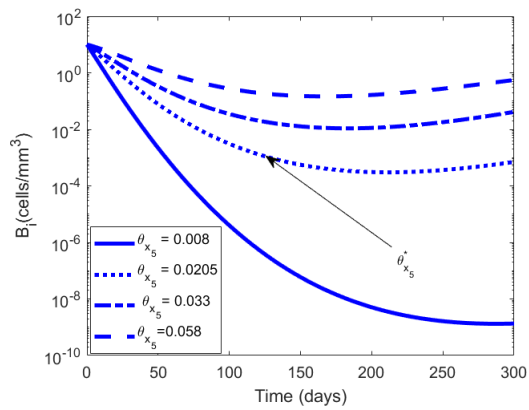
(a) Infected progenitor cells



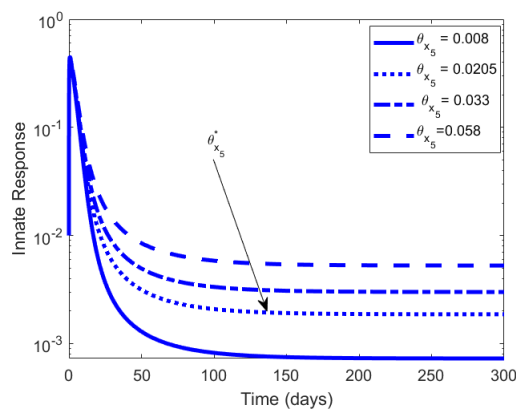
(b) KS cell dynamics



(c) HHV-8 dynamics



(d) Infected B cells dynamics

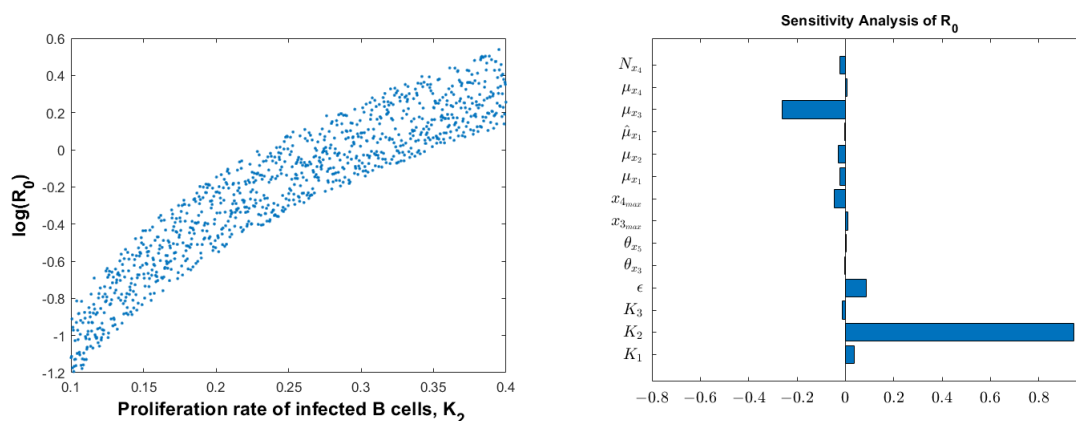


(e) Innate immune response

Figure 4.2: Dynamics of the individual components of the model with innate mech-

anism for different values of the efficacy threshold θ_{x_5} . The HHV-8 infection clears

for $\theta_{x_5} < \theta^*$ even if $\mathcal{R}_0 > 1$.

(a) Scatter plot for \mathcal{R}_0

(b) PRCCs for the model

Figure 4.3: PRCCs for parameters of the innate model and $\log(\mathcal{R}_0)$ as a function of the most sensitive parameter, K_2 .

4.3 MODEL 2: AIDS-KS Model with Adaptive Mechanism

4.3.1 Model Formulation and Description

In case of HIV-1 and HHV-8 co-infection, a more robust adaptive immune response is developed which includes virus-specific effector cells. When a cell is infected by a virus, it begins to display the viral proteins on its cell membrane. This cell is later recognized by the immune response as being nonself and can now be killed through the action of activated $CD8^+$ -T lymphocytes. The $CD8^+$ -T cells that are equipped with the cytotoxic role are referred to as the effector cells. Each pathogen can only be

dealt by a specific subset of T cells that were previously primed by antigens derived from that pathogen.

Their interaction with the infected and uninfected cell and virus populations is modelled below. For simplicity of notation, we denote

$$x_i := x_i(t), \text{ and } x_i^0 := x_i(0), \quad i = 1, 2, \dots, 10, \quad (4.14)$$

where x_1, x_2, x_3, x_4 in order denote the uninfected CD4 and B cell populations and the HHV-8 and HHV-1-specific effector cells, x_5, x_6, x_7, x_8 denote the infected CD4 T cell, B cell, progenitor cell populations and KS cells, and finally, x_9, x_{10} are the HIV-1 and HHV-8 virions.

We have formulated the adaptive immune response described by the following system of equations:

$$\dot{x}_1 = \Pi_1 \left(1 + \frac{\alpha_5 x_9}{x_9 + S_9} + \frac{\alpha_6 x_{10}}{x_{10} + S_{10}} \right) - \mu_1 x_1 - \beta_1 x_1 x_9. \quad (4.15)$$

Eq. (4.15) describes the dynamics of the susceptible CD4 T cells, x_1 . The first term in (4.15) represents the constant natural replacement of the CD4 T cells, x_1 , the second term represents proliferation of a proportion of circulating x_1 cells due to the presence of HIV-1 virions and the third term represents proliferation of a proportion of circulating x_1 cells due to the presence of HHV-8. The fourth term is the natural death of these cells at a constant rate, μ_1 , and the fifth term represents infection of

x_1 cells by HIV-1 at a constant infection rate β_1 .

$$\dot{x}_2 = \Pi_2 \left(1 + \frac{\alpha_5 x_9}{x_9 + S_9} + \frac{\alpha_6 x_{10}}{x_{10} + S_{10}} \right) - \mu_2 x_2 - \beta_2 x_2 x_{10}. \quad (4.16)$$

Eq. (4.16) describes the dynamics of the susceptible B cells, x_2 . The first term represents the constant natural replacement of the B cells, x_2 , the second term represents proliferation of a proportion of circulating x_2 cells due to the presence of HIV-1 virions and the third term represents proliferation of a proportion of circulating x_2 cells due to the presence of HHV-8. The fourth term is the natural death of these cells at a constant rate, μ_2 , and the fifth term represents infection of x_2 cells by HHV-8 at a constant infection rate β_2 .

$$\dot{x}_3 = \Pi_3 \left(1 + \frac{c_{10} x_{10}}{x_{10} + f_{10}} \right) - \mu_3 x_3. \quad (4.17)$$

Eq. (4.17) describes the dynamics of HHV-8 specific effector cells, x_3 . The first term represents constant replenishment of these cells from precursors. The second term represents the proliferation of a proportion of circulating x_3 cells due to the presence of the HHV-8 pathogen. The last term represents natural death of HHV-8 specific effector cells at the constant death rate, μ_3 .

$$\dot{x}_4 = \Pi_4 \left(1 + \frac{c_9 x_9}{x_9 + f_9} \right) - \mu_4 x_4. \quad (4.18)$$

Similar to above, Eq. (4.18) describes the dynamics of HIV-1 specific effector cells, x_4 .

$$\dot{x}_5 = \Pi_1 \left(\frac{\alpha_5 x_9}{x_9 + S_9} + \frac{\alpha_6 x_{10}}{x_{10} + S_{10}} \right) + \beta_1 x_1 x_9 - m_4 x_4 x_5 - \mu_5 x_5. \quad (4.19)$$

Eq. (4.19) represents a class of infected CD4 T cells, x_5 . The first term represents proliferation of a proportion of circulating x_5 cells due to the presence of HIV-1 virions and the second term represents proliferation of a proportion of circulating x_5 cells due to the presence of HHV-8 virions. The third term is the gain from infection of T cells by HIV-1. The fourth term is the lysing of infected CD4 T cells by HIV-1 specific effector cells and the last term represents natural death of these cells at a constant rate, μ_5 .

$$\dot{x}_6 = \Pi_2 \left(\frac{\alpha_5 x_9}{x_9 + S_9} + \frac{\alpha_6 x_{10}}{x_{10} + S_{10}} \right) + \beta_2 x_2 x_{10} - m_3 x_3 x_6 - \mu_6 x_6. \quad (4.20)$$

Similar to above, Eq. (4.20) represents a class of infected B cells, x_6 .

$$\dot{x}_7 = r_7 x_{10} \left(1 - \frac{x_{10}}{x_{10_{max}}} \right) - \mu_7 x_7 - d_3 x_3 x_7. \quad (4.21)$$

Eq. (4.21) represents the dynamics of infected progenitor cells. The first term accounts for the logistic growth rate of these cells that is assumed to depend on HHV-8. The second term is the progression of these cells to KS at a constant rate μ_7 [32]. The third term represents the killing of these cells by HHV-8 specific effector cells at a constant rate d_3 .

$$\dot{x}_8 = \mu_7 x_7 - \mu_8 x_8. \quad (4.22)$$

Eq. (4.22) represents the dynamics of KS. The first term represents the source from

infection of progenitor cells. The second term represents natural loss of KS cells.

$$\dot{x}_9 = N_9\mu_5x_5 - \mu_9x_9. \tag{4.23}$$

Eq. (4.23) represents the dynamics of HIV-1. The first term represents the production of virions from the bursting of the infected CD4 T cells. The parameter N_9 represents the maximum carrying capacity of infected CD4 T cells. The second term is the clearance rate of HIV-1.

$$\dot{x}_{10} = N_{10}\mu_6x_6 - \mu_{10}x_{10}. \tag{4.24}$$

Eq. (4.24) represents the rate of change of HHV-8. The first term represents the rate at which HHV-8 is produced from bursting of the infected B cells and the last term accounts for the clearance rate of HHV-8.

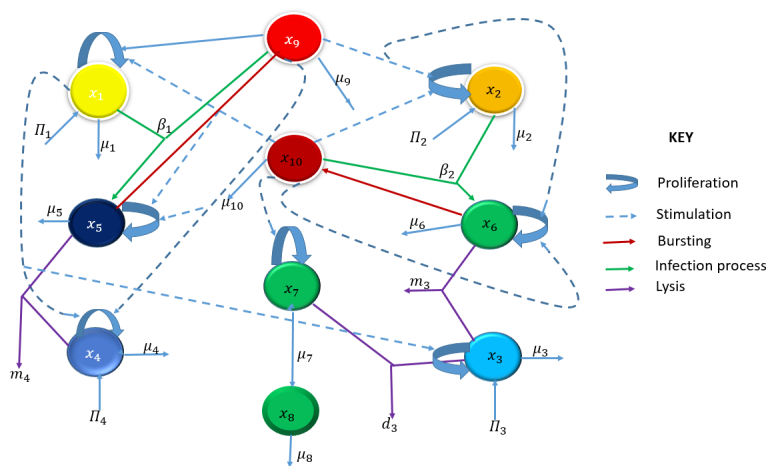


Figure 4.4: Schematic diagram for AIDS-KS model with adaptive immunity.

4.3.2 Analysis of the Model

Variable	Definitions	Initial Value	Reference
x_1	Uninfected CD4 T cells	10^5 cell ml ⁻¹	[80]
x_2	Uninfected B cells	10^4 cell ml ⁻¹	Estimated
x_3	HHV-8 effector cells	cell ml ⁻¹	Innate model
x_4	HIV-1 effector cells	10^4 cell ml ⁻¹	Estimated
x_5	Infected CD4 T cells	300 cell ml ⁻¹	Estimated
x_6	Infected B cells	32.4 cell ml ⁻¹	Innate model
x_7	Infected progenitor cells	61.3 cell ml ⁻¹	Innate model
x_8	KS cells	30.1 cell ml ⁻¹	Innate model
x_9	HHV-1 virions	100 virions ml ⁻¹	Estimated
x_{10}	HHV-8 virions	83.6 cell ml ⁻¹	Innate model

Table 4.2: Initial values of the model with adaptive mechanism and their definitions.

Parameter	Definitions
α_5	HIV-1-dependent enhancement of CD4 T cell proliferation
α_6	HHV-8-dependent enhancement of CD4 T cell proliferation
β_1	Infection rate of CD4 T cells by HIV-1

β_2	Infection rate of B cells by HHV-8
Π_1	Source of new CD4 T cells from the thymus
Π_2	Source of new B cells from the bone marrow
Π_3	Constant source of HHV-8 specific effector cells
Π_4	Constant source of HIV-1 specific effector cells
S_9	Half saturation for HIV-1-stimulated CD4 T cell proliferation
S_{10}	Half saturation for HHV-8-stimulated CD4 T cell proliferation
μ_1	Death rate of CD4 T cells
μ_2	Death rate of B cells
μ_3	HHV-8 specific effector cell death rate
μ_4	HIV-1 specific effector cell death rate
μ_5	Lytic death rate of infected CD4 T cells
μ_6	Death rate of free HHV-8 virus
μ_7	KS progression rate
μ_8	Natural death rate of KS cells
μ_9	Clearance rate of HIV-1 virions
μ_{10}	clearance rate of HHV-8 virions

N_9	Maximum carrying capacity of infected CD4 T cells
N_{10}	Maximum carrying capacity of infected B cells
m_3	Killing rate of HHV-8 infected B cells
m_4	Killing rate of HIV-1 infected CD4 T cell
c_9	Proliferation rate of HIV-1 specific CTLs
c_{10}	Proliferation rate of HHV-8 specific CTLs
d_3	Killing rate of infected progenitor cells
r_7	Maximum proliferation rate of infected progenitor cells
f_9	Half saturation for proliferation of HIV-1 specific CTLs
f_{10}	Half saturation for proliferation of HHV-8 specific CTLs
$x_{10_{max}}$	Maximum HHV-8 load

Table 4.3: Parameters of the model with adaptive mechanism and their definitions.

Parameter	Value	Reference
α_5	0.013	Estimated

α_6	0.045	Estimated
β_1	2.4×10^{-8} ml virion ⁻¹ day ⁻¹	[95]
β_2	1.5×10^{-7} ml virion ⁻¹ day ⁻¹	[95]
Π_1	10^4 cell ml ⁻¹ day ⁻¹	[95]
Π_2	48000 cell ml ⁻¹ day ⁻¹	[95]
Π_3	5×10^3 cell ml ⁻¹ day ⁻¹	Estimated
Π_4	2×10^4 cell ml ⁻¹ day ⁻¹	[95]
S_9	3×10^5 virions ml ⁻¹	Estimated
S_{10}	2×10^5 virions ml ⁻¹	Estimated
μ_1	0.01 day ⁻¹	[95]
μ_2	0.24 day ⁻¹	[95]
μ_3	0.1 day ⁻¹	[95]
μ_4	0.1 day ⁻¹	[95]
μ_5	0.24 day ⁻¹	[95]
μ_6	0.33 day ⁻¹	[95]
μ_7	0.1 day ⁻¹	[95]
μ_8	0.21 day ⁻¹	[95]

μ_9	3 day^{-1}	[95]
μ_{10}	0.57 day^{-1}	[95]
N_9	$1000 \text{ virions cell}^{-1}$	[95]
N_{10}	$700 \text{ virions cell}^{-1}$	[95]
m_3	$1.08 \times 10^{-4} \text{ ml cell}^{-1} \text{ day}^{-1}$	Estimated
m_4	$2 \times 10^{-7} \text{ ml cell}^{-1} \text{ day}^{-1}$	Estimated
c_9	0.03	[95]
c_{10}	0.047	[95]
d_3	$5 \times 10^{-4} \text{ ml cell}^{-1} \text{ day}^{-1}$	Estimated
r_7	$0.33 \text{ cells virion}^{-1} \text{ day}^{-1}$	[95]
f_9	$3 \times 10^5 \text{ virions ml}^{-1}$	Estimated
f_{10}	$2 \times 10^5 \text{ virions ml}^{-1}$	Estimated
$x_{10_{max}}$	$8 \times 10^9 \text{ virions ml}^{-1}$	Estimated

Table 4.4: Parameter values of the model with adaptive mechanism.

Positivity and Boundedness of Solutions

To prove the positivity and ensure that the model (4.15) – (4.24) is well-posed, we assume the following:

$$(A1) : \quad f(x_9, x_{10}) = \frac{x_9}{x_9 + S_9} + \frac{x_{10}}{x_{10} + S_{10}} \geq 0, \quad \forall (x_9, x_{10}) \in \mathbb{R}_+^2.$$

$$(A2) : \quad g(x) = rx \left(1 - \frac{x}{x_{max}}\right) \geq 0, \quad \text{for } 0 \leq x \leq \frac{x_{max}}{2}.$$

Lemma 4.3.1 *Consider the system (4.15) – (4.24) and assume that (A1) and (A2) hold.*

(a) *If $x_i(0) \geq 0$, $i = 1, 2, 3, \dots, 10$, then the solution $x_i \geq 0$, $\forall t > 0$.*

(b) *Moreover, $x_i(t) < \infty$, $i = 1, 2, \dots, 10$, $\forall t \geq 0$.*

First we will rearrange the system (4.15) – (4.24) into a subsystem of uninfected (S1) states (Eqns 4.15-4.18) and infected (S2) states (Eqns 4.19-4.24). It will be shown that if the noninfected states in (S1) are non-negative for all $t \geq 0$, then the infected states in (S2) are non-negative for all $t \geq 0$.

Proof 4.3.2 *(Proof of Lemma 4.3.1(a)) The subsystem of uninfected states (S1) can be written as a system of differential inequalities*

$$\frac{dx_i}{dt} \geq \left(A_i - \sum_{j=1}^{10} B_{ij}x_j \right) x_i + \hat{\Pi}_i \quad (4.25)$$

where $B_{ij} \geq 0$, $\hat{\Pi}_i = L_i(x_9, x_{10})$, for $i = 1, 2, 3, 4$. The last component is defined as $\hat{\Pi}(x_9, x_{10}) = (L_1, L_2, L_3, L_4)^T$,

$$\begin{aligned} L_1 &= \Pi_1 \left(1 + \frac{\alpha_5 x_9}{x_9 + S_9} + \frac{\alpha_6 x_{10}}{x_{10} + S_{10}} \right), & L_3 &= \Pi_3 \left(1 + \frac{c_{10} x_{10}}{x_{10} + f_{10}} \right) \\ L_2 &= \Pi_2 \left(1 + \frac{\alpha_5 x_9}{x_9 + S_9} + \frac{\alpha_6 x_{10}}{x_{10} + S_{10}} \right), & L_4 &= \Pi_4 \left(1 + \frac{c_9 x_9}{x_9 + f_9} \right). \end{aligned}$$

Clearly, $\hat{\Pi}(0, 0) > (0, 0, 0, 0)^T$ by virtue of (A1). Suppose the assertion $x_i(t) \geq 0$ for $i = 1, 2, 3, 4$ is not true. Then there exists a smallest number t_0 , such that

$$x_i(t) < 0 \text{ for } 1 \leq i \leq 4, \quad 0 \leq t \leq t_0$$

$$x_i(t_0) = 0 \text{ for at least one } i, \text{ say } i_0.$$

Then, x_{i_0} is a decreasing function and we would have

$$\frac{dx_{i_0}(t_0)}{dt} \leq 0.$$

However, from the differential inequality (4.25) for $x_{i_0}(t)$ we get

$$\frac{dx_{i_0}(t_0)}{dt} \geq \hat{\pi}_{i_0} > 0$$

which is a contradiction. Hence, if $x_i(0) \geq 0$, $i = 1, 2, 3, 4$ then, $x_i(t) \geq 0$ for all $t > 0, i = 1, 2, 3, 4$.

The subsystem of infected states (S_2) can be written in the matrix form $\dot{Y}(t) = MY$,

where $Y = \begin{pmatrix} x_5 & x_6 & x_7 & x_8 & x_9 & x_{10} \end{pmatrix}^T$, and

$$M = \begin{pmatrix} -M_{11} & 0 & 0 & 0 & M_{15} & M_{16} \\ 0 & -M_{22} & 0 & 0 & M_{25} & M_{26} \\ 0 & 0 & -M_{33} & 0 & 0 & M_{36} \\ 0 & 0 & \mu_7 & -\mu_8 & 0 & 0 \\ N_9\mu_5 & 0 & 0 & 0 & -\mu_9 & 0 \\ 0 & N_{10}\mu_6 & 0 & 0 & 0 & -\mu_6 \end{pmatrix}$$

with entries

$$\begin{aligned} M_{11} &= \mu_5 + m_4x_4, & M_{22} &= \mu_6 + m_3x_3, & M_{33} &= \mu_7 + d_3x_3, & M_{15} &= \frac{\alpha_5\Pi_1S_9}{(x_9 + S_9)^2} + \beta_1x_1, \\ M_{16} &= \frac{\alpha_6\Pi_1S_{10}}{(x_{10} + S_{10})^2}, & M_{25} &= \frac{\alpha_5\Pi_2S_9}{(x_9 + S_9)^2}, & M_{26} &= \frac{\alpha_6\Pi_2S_{10}}{(x_{10} + S_{10})^2} + \beta_2x_2, & M_{36} &= r_7\left(1 - \frac{2x_{10}}{x_{10max}}\right). \end{aligned}$$

By virtue of (A1) and (A2), M is a Metzler matrix. Hence, the infected states $x_i(t) \geq$

0 for all $t > 0$, $i = 5, 6, 7, 8, 9, 10$

The proof of Lemma 4.3.1(b) is given in **Lemma 4** in the Appendix.

Virus Free Equilibrium and the Basic Reproduction Number

The system (4.15) – (4.24) has a virus free equilibrium, ε^0 , given by

$$\varepsilon^0 = \left(\frac{\Pi_1}{\mu_1}, \frac{\Pi_2}{\mu_2}, \frac{\Pi_3}{\mu_3}, \frac{\Pi_4}{\mu_4}, 0, 0, 0, 0, 0, 0 \right).$$

Applying the next generation matrix-approach [96], the basic reproduction number for model (4.15) – (4.24) reads as follows:

$$\mathcal{R}_0 = \frac{1}{2} \left[\mathcal{R}_{V_1} + \mathcal{R}_{V_8} + \sqrt{(\mathcal{R}_{V_1} + \mathcal{R}_{V_8})^2 + 4\mathcal{R}_{V_1}\mathcal{R}_{V_8}(\Phi - 1)} \right], \quad (4.26)$$

where

$$\Phi = \frac{\mu_1\mu_2\alpha_5\alpha_6}{K_1K_2} = \frac{\mu_1\mu_2\alpha_5\alpha_6}{\mu_1\mu_2\alpha_5\alpha_6 + \mu_1\alpha_5\beta_2S_{10} + \mu_2\alpha_6\beta_1S_9 + \beta_1\beta_2S_9S_{10}}, \quad 0 \leq \Phi < 1,$$

and

$$\mathcal{R}_{V_1} = \frac{\mu_4\mu_5N_9\Pi_1(\alpha_5\mu_1 + \beta_1S_9)}{\mu_1\mu_9S_9(\mu_4\mu_5 + m_4\Pi_4)}, \quad \mathcal{R}_{V_8} = \frac{\mu_3\mu_6N_{10}\Pi_2(\alpha_6\mu_2 + \beta_2S_{10})}{\mu_2\mu_{10}S_{10}(\mu_3\mu_6 + m_3\Pi_3)}, \quad (4.27)$$

are the reproduction numbers attributed to HIV-1 and HHV-8 infections, respectively.

Note that the effect of virus-specific effector cells in (4.27) varies from weak to perfect as m_j changes. It readily follows that

$$\mathcal{R}_{V_1} < \frac{N_9\Pi_1(\alpha_5\mu_1 + \beta_1S_9)}{\mu_1\mu_9S_9} =: \mathcal{R}_1, \quad \mathcal{R}_{V_8} < \frac{N_{10}\Pi_2(\alpha_6\mu_2 + \beta_2S_{10})}{\mu_2\mu_{10}S_{10}} =: \mathcal{R}_8, \quad (4.28)$$

where $\mathcal{R}_1, \mathcal{R}_8$ are the reproduction numbers when the virus-specific effector cells are dysfunctional.

Given (4.26) – (4.27) we make the following observations:

Observation 4.3.3 *If $\alpha_5 = 0$ or $\alpha_6 = 0$, then $\Phi = 0$ and the model reproduction number is given by $\mathcal{R}_0 = \max\{\mathcal{R}_{V_1}, \mathcal{R}_{V_8}\}$*

Observation 4.3.4 *Decreasing/increasing α_5 or α_6 decreases/increases the reproduction number. Since α_5 and α_6 are the proliferation terms of the uninfected/infected B and T cell populations, an optimal control approach will be necessary that will balance the level of proliferation during a potential chemo- or immunotherapy.*

Observation 4.3.5 *When $\Phi = 1$, the reproduction number reduces to*

$$\mathcal{R}_0 = \frac{1}{2} \left[\mathcal{R}_{V_1} + \mathcal{R}_{V_8} + \sqrt{(\mathcal{R}_{V_1} + \mathcal{R}_{V_8})^2} \right] = \mathcal{R}_{V_1} + \mathcal{R}_{V_8} \quad (4.29)$$

It is possible in this case for the infection to persist if $\mathcal{R}_{V_1} + \mathcal{R}_{V_8} > 1$, even if $\mathcal{R}_{V_1} < 1$ and $\mathcal{R}_{V_8} < 1$.

Global Stability for the Virus Free Equilibrium, ε^0

Theorem 4.3.6 *Decompose the system (4.15) – (4.24) as in 7.0.1 in the Appendix.*

Then the steady state $U_0 = (X^, \mathbf{0})$ of the system (4.15)-(4.24) is globally asymptotically stable for $\alpha_5 = \alpha_6 = 0$ and $\mathcal{R}_0 < 1$.*

Proof 4.3.7 *Denote $X^* = \left(\frac{\Pi_1}{\mu_1}, \frac{\Pi_2}{\mu_2}, \frac{\Pi_3}{\mu_3}, \frac{\Pi_4}{\mu_4} \right)$. Then following (7.1), we set $X =$*

(x_1, x_2, x_3, x_4) and $Y = (x_5, x_6, x_7, x_8, x_9, x_{10})$ and define

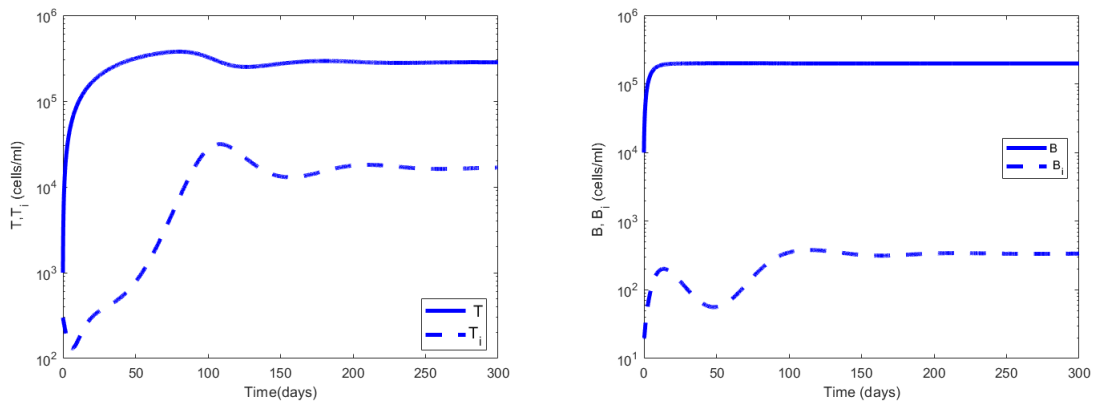
$$F(X, 0) = \begin{pmatrix} \Pi_1 - \mu_1 \\ \Pi_2 - \mu_2 \\ \Pi_3 - \mu_3 \\ \Pi_4 - \mu_4 \end{pmatrix}, \quad G(X, Y) = \begin{pmatrix} m_4(x_4^* - x_4^0)x_5 + \beta_1(x_1^0 - x_1^*)x_9 + \Pi_1 \sum_{j=5}^6 \delta_j x_{j+4} \\ m_4(x_3^* - x_3^0)x_6 + \beta_2(x_2^0 - x_2^*)x_{10} + \Pi_2 \sum_{j=5}^6 \delta_j x_{j+4} \\ d_3(x_3^* - x_3^0)x_7 + r_7 \frac{x_{10}^2}{x_{10max}} \\ 0 \\ 0 \\ 0 \end{pmatrix},$$

where

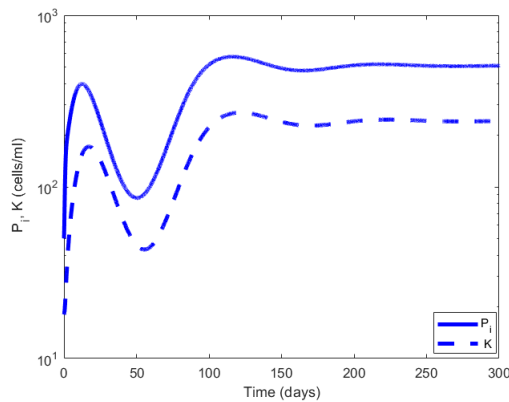
$$\delta_j = \alpha_j \left(\frac{1}{S_{j+4}} - \frac{1}{x_{j+4} + S_{j+4}} \right), \quad j = 5, 6.$$

The global stability of the system (4.15) – (4.24) at ε^0 requires that $\hat{G}(X, Y) \geq \mathbf{0}$ [14]. Moreover, $x_i^* > x_i^0$, for $i = 3, 4$ and $x_j^0 > x_j^*$, for $j = 1, 2$. Then X^* is a globally asymptotically stable solution of the system $\frac{dX}{dt} = F(X, 0)$ since $F(X, 0)$ is the limiting function of $\frac{dX}{dt} = F(X(t), Y(t))$, that is, $\lim_{t \rightarrow \infty} X(t) = X^*$. It follows that $\hat{G}(X, Y) \geq \mathbf{0}$ and so ε^0 is globally asymptotically stable.

4.3.3 Numerical Simulations of the Model with Adaptive Mechanism



(a) Uninfected CD4 T cells and infected CD4 T cells (b) Uninfected B cells and infected B cells



(c) Infected progenitor cells and KS cells

Figure 4.5: Dynamics of the individual components of the model with adaptive mechanism for $\mathcal{R}_0 = 1.7902$.

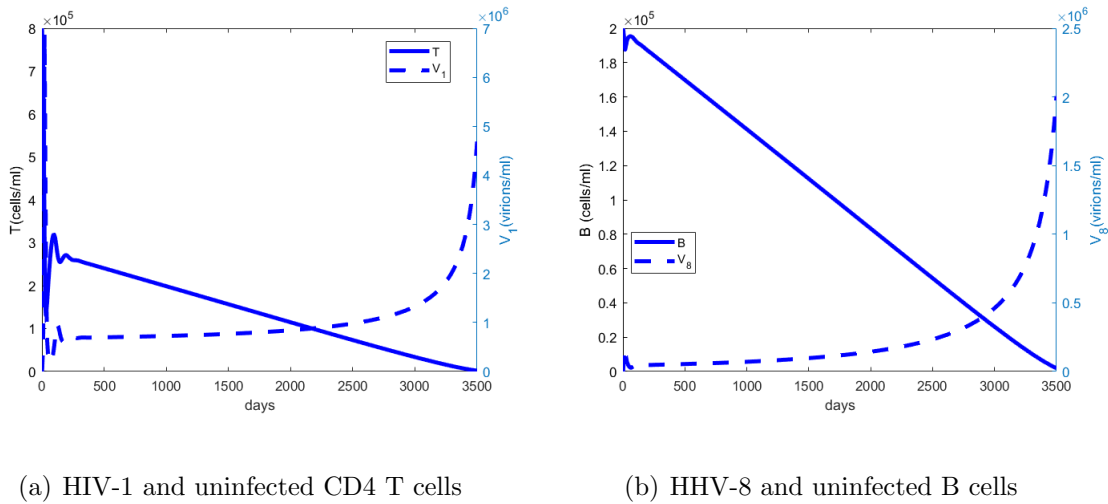


Figure 4.6: Comparison of the long term dynamics of the uninfected CD4 T cell and B cells with regards to HIV-1 and HHV-8 load.

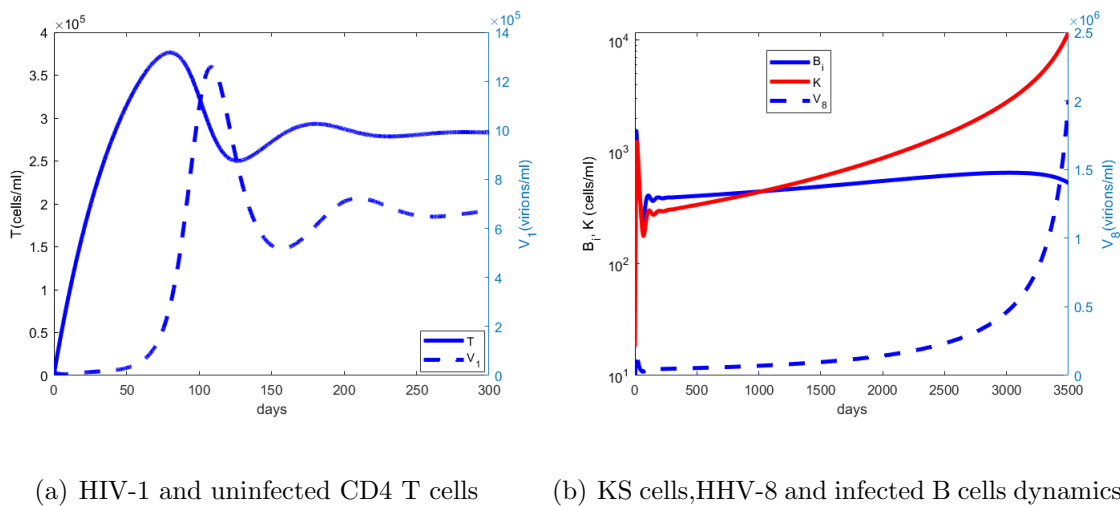
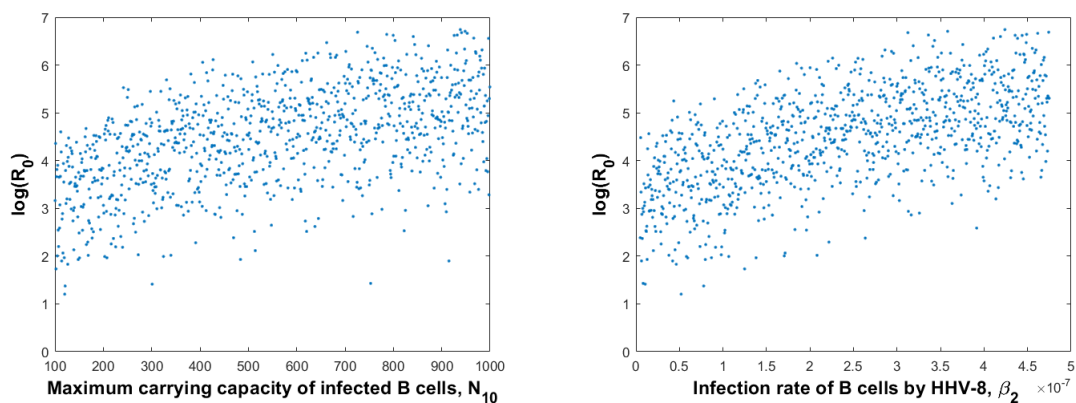
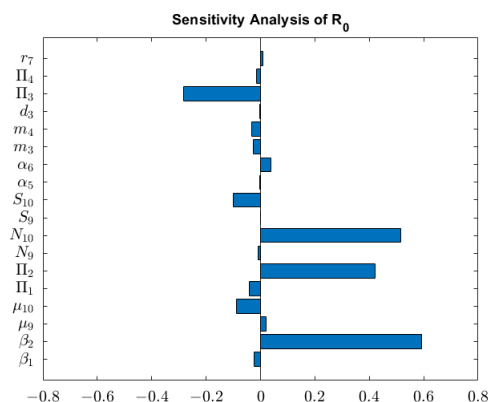


Figure 4.7: (a) Same as Figure 4.6(a) but for the first 300 days. Figure 4.6(b) The long term dynamics of infected B cells and KS cells with regards to HHV-8 load.

(a) Scatter plot for \mathcal{R}_0 (b) Scatter plot for \mathcal{R}_0 

(c) PRCCs for the model

Figure 4.8: PRCCs for parameters of the adaptive model and $\log(\mathcal{R}_0)$ as a function of the two most sensitive parameters, N_{10} and β_2 .

The parameter values used in Figures 4.5 – 4.7 are given in Table 4.4. Assuming an advanced HIV-1 and HHV-8 co-infection stage, the initial condition of the system (4.15)-(4.24) was chosen to be the equilibrium point of the system (4.1)-(4.5). Figure 4.5 shows the dynamics of the uninfected/infected B-cells and CD4 T cells,

infected progenitor cells and KS cells for a period of 300 days. The population of infected CD4 T cells reaches a peak at 100 days by then the population of infected B cells have already reached a steady state. These results, in line with experimental evidence, support the fact that KS may accelerate the clinical course of HIV-1 infection.

Figure 4.6 compares the long term dynamics of HIV-1 and HHV-8 populations with uninfected CD4 T and B cells. The uninfected CD4 T cell population starts rapidly declining after about 300 days and the HIV-1 population switches from a stable to an exponential growth after about 6 years. For the infected B cell population this switch occurs after about 8 years. The delay in the switching time from a stable to exponential growth between the HIV-1 and HHV-8 viral load indicates that HHV-8 supports the clinical course of KS. Figure 4.7 shows that the uninfected CD4 T cell population peaks at about 60 days, 40 days before the HIV-1 peak and that the KS cell population will have a steeper rise than the relatively stable infected B cell population. This suggests that at later stages of AIDS-KS, the reservoirs of HHV-8 will be predominantly the infected progenitor cells.

4.3.4 Sensitivity and Uncertainty Analysis

The choice of model parameters is never free from uncertainties. It is therefore necessary that a sensitivity analysis is conducted to explore simultaneously the whole

parameter space rather than just using the nominal values. To achieve this we employ the Latin Hypercube sampling (LHS) scheme which is described in great detail in [70, 71].

The results of the sensitivity analysis can help us identify which of the model parameters have a bearing on the infection process. Such parameters must be estimated with great precision. The sign of the PRCC identifies the specific qualitative relationship between the input parameter and the output variable. The positive value of the PRCC of a variable indicates that enhancement of the processes described by a variable makes the infection process worse. On the other hand, enhancing processes described by parameters with negative PRCCs would have a substantial effect on improving the prognosis.

Figure 4.8 shows the sensitivity analysis of parameters from Table 7.2 on \mathcal{R}_0 . The maximum carrying capacity of infected B cells is strongly positively correlated with \mathcal{R}_0 , whereas the HHV-8 clearance rate has the opposite effect. The logarithm of the reproduction number as a function of these two parameters is also shown. For small values of N_{10} , the increase is fast, implying that one can overestimate the severity of the infection. For large values of N_{10} , the increase is slow, implying that disease progression is stable and the conclusions are not adversely affected. The relationship between the $\log(\mathcal{R}_0)$ and the clearance rate of HHV-8 virions is almost linear, suggesting a moderate negative correlation with the progression of AIDS-KS.

4.4 Optimal Control Applied to the Model with Adaptive Mechanism

We now apply an optimal control approach to the system (4.15) – (4.24). In order to determine the optimal strategy for controlling AIDS-KS with cART, we introduce three time dependent controls: $u_1(t)$, $u_2(t)$ and $u_3(t)$. The control $u_1(t)$ is the efficacy of HAART for preventing the infection of CD4 T cells by HIV-1 and $u_2(t)$ is the efficacy of HAART in preventing the infection of B cells by HHV-8. The third control $u_3(t)$ represents the efficacy of an anti-KS therapy by enhancing the proliferation of CD4 T and B cells.

$$\dot{x}_1 = \Pi_1 + \frac{(\alpha_5(1 - u_3(t)))x_9}{x_9 + S_9}\Pi_1 + \frac{(\epsilon\alpha_5(1 - u_3(t)))x_{10}}{x_{10} + S_{10}}\Pi_1 - \mu_1x_1 - (1 - u_1(t))\beta_1x_1x_9. \quad (4.30)$$

Eq. (4.30) describes the dynamics of the uninfected CD4 T cells. The meanings of the various terms are given in Eq.(4.15). However, the proliferation constants, α_i , $i = 5, 6$ in (4.15) are now replaced by $(\alpha_5(1 - u_3))$ and $(\epsilon\alpha_5(1 - u_3))$, respectively. Note that α_6 is here assumed to be a multiple of α_5 which is purely done for technical reasons. The infection coefficient, β_1 , is replaced by $(1 - u_1(t))\beta_1$, where $u_1(t)$ is the efficacy of HAART in preventing the infection of healthy CD4 T cells and hence, $u_1(t)$ could represent treatment with either the fusion inhibitor or the reverse transcriptase

inhibitor.

$$\dot{x}_2 = \Pi_2 + \frac{(\alpha_5(1 - u_3(t)))5x_9}{x_9 + S_9}\Pi_2 + \frac{(\epsilon\alpha_5(1 - u_3(t)))x_{10}}{x_{10} + S_{10}}\Pi_2 - \mu_2x_2 - (1 - u_1(t))\beta_2x_2x_{10}. \quad (4.31)$$

Eq. (4.31) describes the dynamics of the susceptible B cells. The meanings of the various terms are given in Eq.(4.16). The second and third terms are explained in E (4.30). The first and fourth terms are explained in Eq (4.16). The infection coefficient, β_2 , is replaced by $(1 - u_1(t))\beta_2$, where $u_1(t)$ is the efficacy of HAART in preventing the infection of healthy B cells. It is well documented that AIDS-KS patients undergoing HAART treatment undergo remission and hence, we assume that HAART treatment reduces the infection rate of B cells by HHV-8.

$$\dot{x}_3 = \Pi_3 + \frac{c_{10}\Pi_3x_{10}}{x_{10} + f_{10}} - \mu_3x_3. \quad (4.32)$$

Eq. (4.32) describes the dynamics of HHV-8 specific effector cells, x_3 . The terms are as explained in Eq. (4.17).

$$\dot{x}_4 = \Pi_4 + \frac{c_9\Pi_4x_9}{x_9 + f_9} - \mu_4x_4. \quad (4.33)$$

Eq. (4.33) describes the dynamics of HIV-1 specific effector cells, x_4 .The terms are as explained in Eq. (4.18).

$$\dot{x}_5 = \frac{(\alpha_5(1 - u_3(t)))x_9}{x_9 + S_9}\Pi_1 + \frac{(\epsilon\alpha_5(1 - u_3(t)))x_{10}}{x_{10} + S_{10}}\Pi_1 + (1 - u_1(t))\beta_1x_1x_9 - m_4x_4x_5 - \mu_5x_5. \quad (4.34)$$

Eq. (4.34) represents a class of infected CD4 T cells, x_5 . The first two terms are as explained in (4.30) and (4.31) above. The third term is the gain from eqn. (4.30) and the other terms are as explained in Eq. (4.19).

$$\dot{x}_6 = \frac{(\alpha_5(1 - u_3(t)))x_9}{x_9 + S_9}\Pi_2 + \frac{(\epsilon\alpha_5(1 - u_3(t)))x_{10}}{x_{10} + S_{10}}\Pi_2 + (1 - u_1(t))\beta_2x_2x_{10} - m_3x_3x_6 - \mu_6x_6. \quad (4.35)$$

Eq. (4.35) represents a class of infected B cells, x_6 . The first two terms are as explained in (4.34) above. The third term is the gain from eqn. (4.31) and the other terms are as explained in Eq. (4.20).

$$\dot{x}_7 = (1 - u_1(t))r_7x_{10}\left(1 - \frac{x_{10}}{x_{10_{max}}}\right) - \mu_7x_7 - d_3x_3x_7. \quad (4.36)$$

Eq. (4.36) represents the dynamics of infected progenitor cells. In the first term the logistic growth rate r_7 is reduced by a factor $(1 - u_1(t))$ due to the action of HAART in blocking the infection of progenitor cells by HHV-8. The other terms are as explained before in Eq. (4.21).

$$\dot{x}_8 = \mu_7x_7 - \mu_8x_8. \quad (4.37)$$

Eq. (4.37) represents the dynamics of KS. The terms are already explained in Eq. (4.22).

$$\dot{x}_9 = N_9\mu_5(1 - u_2(t))x_5 - \mu_9x_9. \quad (4.38)$$

Eq. (4.38) represents the HIV-1 dynamics. The first term is decreased by a factor $1 - u_2(t)$ to reflect the action of HAART in blocking the production of infectious and mature HIV-1 virions. The other term is explained in Eq. (4.23).

$$\dot{x}_{10} = N_{10}\mu_6(1 - u_2(t))x_6 - \mu_{10}x_{10}. \quad (4.39)$$

Similar to Eq. (4.38), Eq. (4.39) represents the HHV-8 dynamics.

To this end, we consider the objective (or cost) functional

$$J(u_1, u_2, u_3) = \int_0^T [A_1x_5 + A_2x_6 + A_3x_7 + \frac{1}{2}B_1u_1^2 + \frac{1}{2}B_2u_2^2 + \frac{1}{2}B_3u_3^2] dt, \quad (4.40)$$

where the control functions $u_1(t), u_2(t)$ and $u_3(t)$ are bounded, Lebesgue integrable functions on $[0, T_f]$ and $A_i, B_i, i = 1, 2, 3$ are positive constants.

4.4.1 Existence of Optimal Control

Our control problem is formulated by minimising the functional J subject to the system (4.30) – (4.39). That is, we seek to find optimal controls u_1^*, u_2^* and u_3^* such that

$$J(u_1^*, u_2^*, u_3^*) = \min \left\{ J(u_1, u_2, u_3) \mid u_1, u_2, u_3 \in U \right\} \quad (4.41)$$

where

$$U = \left\{ (u_1, u_2, u_3) \text{ such that } u_1, u_2, u_3 \text{ are measurable with } 0 \leq u_i \leq 1, \text{ for } t \in [0, T_f] \right\}$$

is the control set.

The necessary conditions that an optimal solution must satisfy come from the Pontryagin et al [82] Maximum principle. This principle converts the system (4.30) – (4.39) with Eq. (4.40) into a problem of minimizing pointwise a Hamiltonian H , with respect to u_1, u_2 and u_3 . The Hamiltonian function of the optimal problem is given by:

$$\begin{aligned}
H(\mathbf{x}, \mathbf{u}, \lambda_{\mathbf{x}}, \mathbf{t}) = & A_1x_5 + A_2x_6 + A_3x_7 + \frac{1}{2}B_1u_1^2 + \frac{1}{2}B_2u_2^2 + \frac{1}{2}B_3u_3^2 \\
& + \lambda_{x_1} \left(\Pi_1 + \alpha_5(1 - u_3)\Pi_1 \left(\frac{x_9}{x_9 + S_9} + \frac{\epsilon x_{10}}{x_{10} + S_{10}} \right) - \mu_1x_1 - (1 - u_1)\beta_1x_1x_9 \right) \\
& + \lambda_{x_2} \left(\Pi_2 + \alpha_5(1 - u_3)\Pi_2 \left(\frac{x_9}{x_9 + S_9} + \frac{\epsilon x_{10}}{x_{10} + S_{10}} \right) - \mu_2x_2 - (1 - u_1)\beta_2x_2x_{10} \right) \\
& + \lambda_{x_3} \left(\Pi_3 + \frac{c_{10}\Pi_3x_{10}}{x_{10} + f_{10}} - \mu_3x_3 \right) + \lambda_{x_4} \left(\Pi_4 + \frac{c_9\Pi_4x_9}{x_9 + f_9} - \mu_4x_4 \right) \\
& + \lambda_{x_5} \left(\alpha_5(1 - u_3)\Pi_1 \left(\frac{x_9}{x_9 + S_9} + \frac{\epsilon x_{10}}{x_{10} + S_{10}} \right) + (1 - u_1)\beta_1x_1x_9 - m_4x_4x_5 - \mu_5x_5 \right) \\
& + \lambda_{x_6} \left(\alpha_5(1 - u_3)\Pi_2 \left(\frac{x_9}{x_9 + S_9} + \frac{\epsilon x_{10}}{x_{10} + S_{10}} \right) + (1 - u_1)\beta_2x_2x_{10} - m_3x_3x_6 - \mu_6x_6 \right) \\
& + \lambda_{x_7} \left((1 - u_1)r_7x_{10} \left(1 - \frac{x_{10}}{x_{10max}} \right) - \mu_7x_7 - d_3x_3x_7 \right) + \lambda_{x_8} \left(\mu_7x_7 - \mu_8x_8 \right) \\
& + \lambda_{x_9} \left(N_9\mu_5(1 - u_2)x_5 - \mu_9x_9 \right) + \lambda_{x_{10}} \left(N_{10}\mu_6(1 - u_2)x_6 - \mu_{10}x_{10} \right)
\end{aligned}$$

where, $\mathbf{x} = (x_1, x_2, \dots, x_{10})$, $\mathbf{u} = (u_1, u_2, u_3)$, $\lambda_{\mathbf{x}} = (\lambda_{x_1}, \lambda_{x_2}, \dots, \lambda_{x_{10}})$ and λ_{x_i} , $i = 1, 2, \dots, 10$ are the adjoint or co-state variable corresponding to the state variable x_i .

The system of equations is found by taking appropriate partial derivatives of the

Hamiltonian with respect to the associated state variable, x_i .

Theorem 4.4.1 *Given optimal controls u_1^*, u_2^*, u_3^* that minimize $J(u_1, u_2, u_3)$ over U , and the solutions x_1, x_2, \dots, x_{10} of the corresponding state system (4.30) – (4.39) with Eq. (4.40), then there exist adjoint variables λ_{x_i} satisfying*

$$\frac{\partial H}{\partial x_i} = -\frac{d\lambda_{x_i}}{dt}, \quad \lambda_{x_i}(T_f) = 0, \quad i = 1, 2, \dots, 10$$

and

$$u_i^* = \min \left\{ 1, \max \left(0, \hat{u}_i \right) \right\}, \quad i = 1, 2 \quad u_3^* = \min \left\{ 0.5, \max \left(0, \hat{u}_3 \right) \right\}$$

where u_i^* , $i = 1, 2, 3$ are given by

$$\begin{aligned} \hat{u}_1 &= \frac{x_1 \lambda_{x_1} + \beta_1 x_1 x_9 (\lambda_{x_5} - \lambda_{x_1}) + \beta_2 x_2 x_{10} (\lambda_{x_6} - \lambda_{x_2}) + r_7 x_{10} \left(1 - \frac{x_{10}}{x_{10max}} \right) \lambda_{x_7}}{B_1}, \\ \hat{u}_2 &= \frac{N_9 \mu_5 x_5 \lambda_{x_9} + N_{10} \mu_6 x_6 \lambda_{x_{10}}}{B_2}, \\ \hat{u}_3 &= \left(\frac{\alpha_5 x_9}{x_9 + S_9} + \frac{\epsilon \alpha_5 x_{10}}{x_{10} + S_{10}} \right) \frac{\left(\Pi_1 (\lambda_{x_1} + \lambda_{x_5}) + \Pi_2 (\lambda_{x_2} + \lambda_{x_6}) \right)}{B_3}. \end{aligned}$$

Proof 4.4.2 *Corollary 4.1 of Fleming and Rishel [30] gives the existence of an optimal control due to the convexity of the integrand of J with respect to u_1, u_2 and u_3 . In addition, it also guarantees a priori boundedness of the state solutions and the Lipschitz property of the state system with respect to the state variables. The differential equations governing the adjoint variables are obtained by differentiation of the Hamiltonian function, evaluated at the optimal control. Then the adjoint differential*

equations can be written as

$$\begin{aligned}
\frac{d\lambda_{x_1}}{dt} &= \mu_1\lambda_{x_1} - (1 - u_1)\beta_1x_9(\lambda_{x_5} - \lambda_{x_1}), \\
\frac{d\lambda_{x_2}}{dt} &= \mu_2\lambda_{x_2} - (1 - u_1)\beta_2x_{10}(\lambda_{x_6} - \lambda_{x_2}), \\
\frac{d\lambda_{x_3}}{dt} &= \mu_3\lambda_{x_3} + m_3x_6\lambda_{x_6} + d_3x_7\lambda_{x_7}, \\
\frac{d\lambda_{x_4}}{dt} &= \mu\lambda_{x_4} + m_4x_5\lambda_{x_5}, \\
\frac{d\lambda_{x_5}}{dt} &= -A_1 + (\mu_5 + m_4x_4)\lambda_{x_5} - N_9\mu_5(1 - u_2)\lambda_{x_9}, \\
\frac{d\lambda_{x_6}}{dt} &= -A_2 + (\mu_6 + m_3x_3)\lambda_{x_6} - N_{10}\mu_6(1 - u_2)\lambda_{x_{10}}, \\
\frac{d\lambda_{x_7}}{dt} &= -A_3 + (\mu_7 + d_3x_3)\lambda_{x_7} - \mu_7\lambda_{x_8}, \\
\frac{d\lambda_{x_8}}{dt} &= \mu_8\lambda_{x_8}, \\
\frac{d\lambda_{x_9}}{dt} &= -\frac{(1 - u_3)\alpha_5S_9}{(x_9 + S_9)^2} \left(\Pi_1(\lambda_{x_1} + \lambda_{x_5}) + \Pi_2(\lambda_{x_2} + \lambda_{x_6}) \right) \\
&\quad + (1 - u_1)\beta_1x_1(\lambda_{x_1} - \lambda_{x_5}) - \frac{c_9\Pi_4f_9}{(x_9 + f_9)^2}\lambda_{x_4} + \mu_9\lambda_{x_9}, \\
\frac{d\lambda_{x_{10}}}{dt} &= -\frac{(1 - u_3)\epsilon\alpha_5S_{10}}{(x_{10} + S_{10})^2} \left(\Pi_1(\lambda_{x_1} + \lambda_{x_5}) + \Pi_2(\lambda_{x_2} + \lambda_{x_6}) \right) \\
&\quad + (1 - u_1)\beta_2x_2(\lambda_{x_2} - \lambda_{x_6}) - \frac{c_{10}\Pi_3f_{10}}{(x_{10} + f_{10})^2}\lambda_{x_3} + \mu_{10}\lambda_{x_{10}} - \frac{(1 - u_1)r_7(x_{10_{max}} - 2x_{10})}{x_{10_{max}}}
\end{aligned}$$

In what follows, we differentiate the Hamiltonian H with respect to $u_i(t)$, $i = 1, 2, 3$

to obtain

$$u_i^* = \min \left\{ 1, \max \left(0, \hat{u}_1 \right) \right\}, \quad i = 1, 2. \quad u_3^* = \min \left\{ 0.5, \max \left(0, \hat{u}_3 \right) \right\}.$$

4.4. OPTIMAL CONTROL APPLIED TO THE MODEL WITH ADAPTIVE MECHANISM 77

By standard control arguments involving the bounds on the controls, we conclude

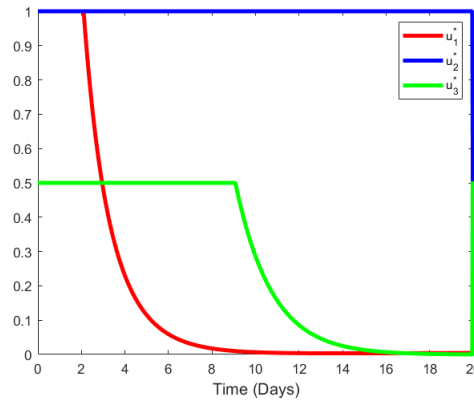
$$u_i^* = \begin{cases} \hat{u}_i, & \text{if } 0 < \hat{u}_i < 1; \\ 0, & \text{if } \hat{u}_i \leq 0; \\ 1, & \text{if } \hat{u}_i \geq 1. \end{cases}$$

which can be compactly written as

$$u_i^* = \min\{1, \max(0, \hat{u}_i)\}, \quad i = 1, 2 \quad \text{and} \quad u_3^* = \begin{cases} \hat{u}_3, & \text{if } 0 < \hat{u}_3 < 0.5; \\ 0, & \text{if } \hat{u}_3 \leq 0; \\ 1, & \text{if } \hat{u}_3 \geq 0.5. \end{cases}$$

Analogously, this can be written as

$$u_3^* = \min\{0.5, \max(0, \hat{u}_3)\}$$



(a) Control profiles of optimal controls, u_1^* , u_2^* , u_3^*

Figure 4.9: Optimal controls in the first 20 days.

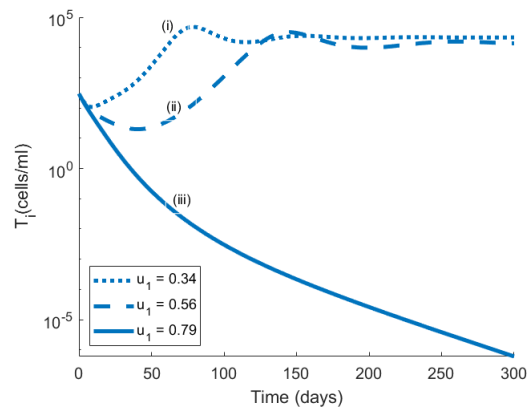
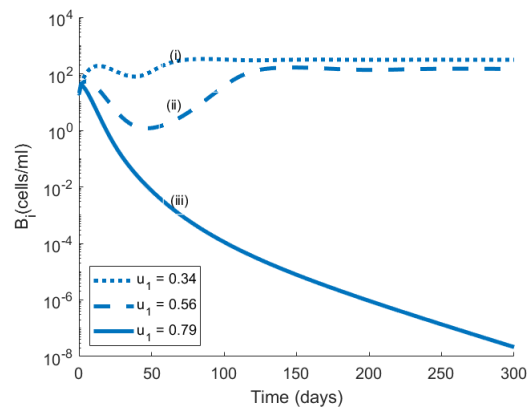
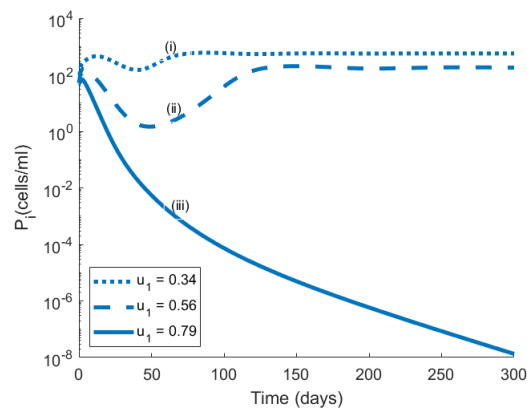
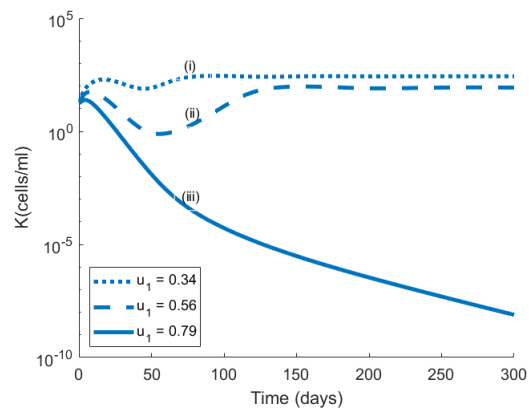
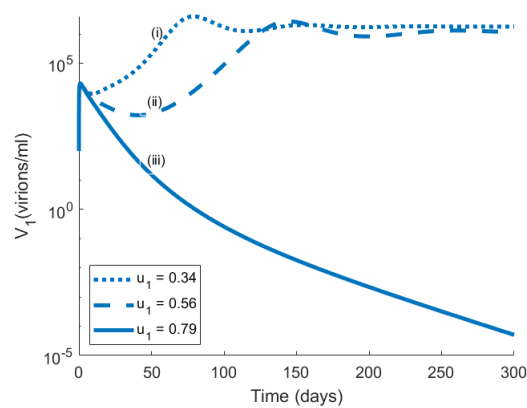
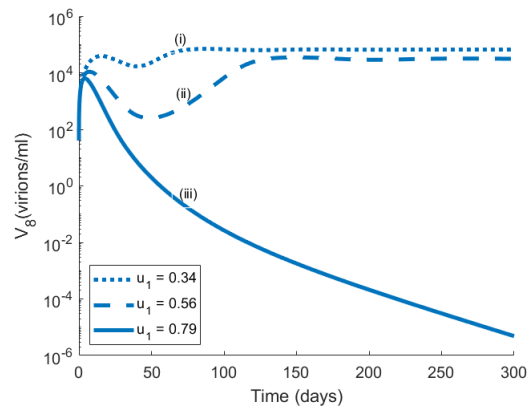
(a) Infected T cells with $u_2 = 0.48, u_3 = 0.25$ (b) Infected B cells with $u_2 = 0.48, u_3 = 0.25$ (c) Infected progenitor cells with $u_2 = 0.48, u_3 = 0.25$ (d) KS cells with $u_2 = 0.48, u_3 = 0.25$ (e) HIV-1 with $u_2 = 0.48, u_3 = 0.25$ (f) HHV-8 with $u_2 = 0.48, u_3 = 0.25$

Figure 4.10: Population dynamics of infected cells and viruses during 300 days for varying values of the infected CD4 T cell-specific HAART efficacy u_1 .

Figure 4.9 shows the profiles of the optimal variables u_1^* , u_2^* and u_3^* in the first 20 days. The initial values $u_i^*(20)$, $i = 1, 2, 3$ are used in an iterative procedure for periods much longer than 20 days. Figure 4.10 depicts the dynamics of the infected cell populations and viral loads for fixed values of u_2 and u_3 during 300 days for different values of the HAART efficacy parameter u_1 . For optimal efficacy $u_1^* \approx 0.79$, the HIV-1 and HHV-8 populations drop below the level of detection. This parameter combination, however, is not unique as illustrated in Figure 4.11. Figure 4.11 shows that reduced infected CD4 T cell-specific HAART efficacy (from $u_1^* \approx 0.79$ to $u_1^* \approx 0.67$) and increased infected B cell-specific HAART efficacy (from $u_2^* \approx 0.48$ to $u_2^* \approx 0.68$) in combination with reduced KS therapy-specific efficacy (from $u_3^* \approx 0.25$ to $u_3^* \approx 0.15$) is also able to control HIV-1 and HHV-8 co-infection.

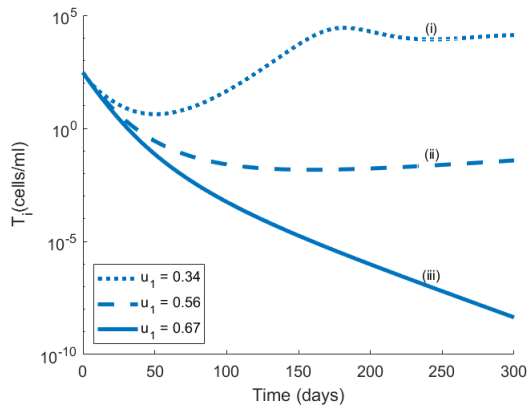
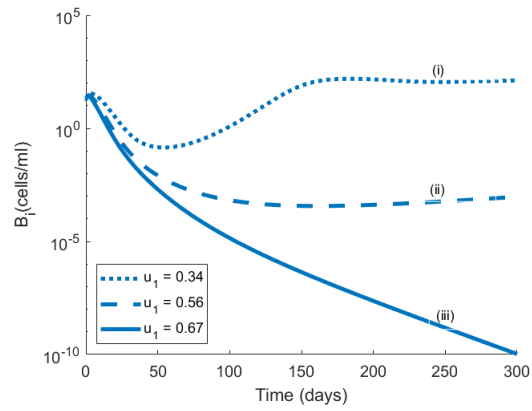
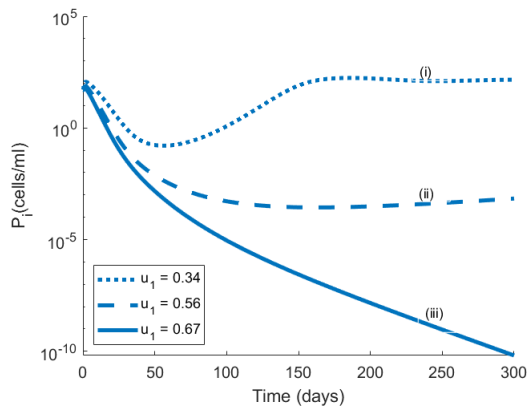
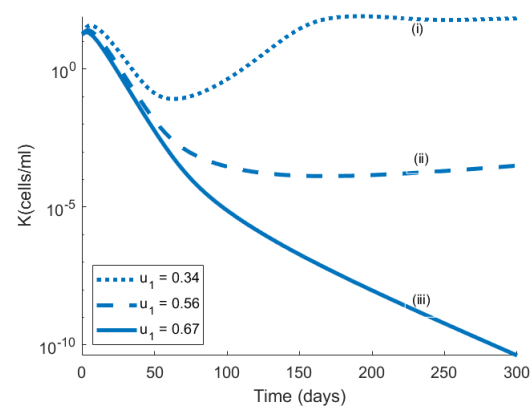
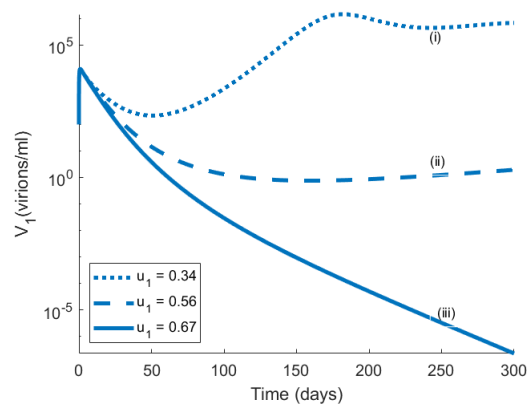
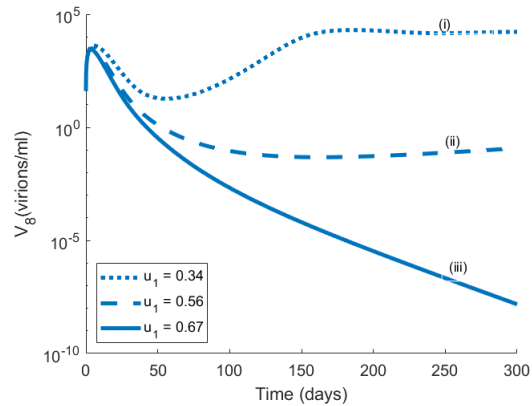
(a) Infected T cells with $u_2 = 0.68, u_3 = 0.15$ (b) Infected B cells with $u_2 = 0.68, u_3 = 0.15$ (c) Infected progenitor cells with $u_2 = 0.68, u_3 = 0.15$ (d) KS cells with $u_2 = 0.68, u_3 = 0.15$ (e) HIV-1 with $u_2 = 0.68, u_3 = 0.15$ (f) HHV-8 with $u_2 = 0.68, u_3 = 0.15$

Figure 4.11: Population dynamics of infected cells and viruses during 300 days for a new combination of optimal controls.

Chapter 5

Non-AIDS-related Kaposi's

Sarcoma: Role of Lytic Replication

5.1 Introduction

The human herpesvirus-8 (HHV-8) is a gammaherpesvirus first reported by Cheng and Moore [15]. HHV-8 causes Kaposi's sarcoma (KS) in humans, a form of skin cancer that can spread to internal organs [10]. There are four types of this cancer, namely classical KS (sporadic), African KS (endemic), AIDS-related KS (epidemic), and Transplant (Iatrogenic) KS [5].

In the past 10 years very few mathematical models of within-host dynamics considered KS and only in the context of HIV co-infection [72, 73, 95]. In this study we present a

mathematical model of non-AIDS related KS that takes into account the latently and lytically HHV-8-infected B-cells. Several studies demonstrated the importance of T-cell immunity in controlling HHV-8 reactivation [68] in different phases of the HHV-8 infection [86]. Hence, our model accounts for the effect of the innate and adaptive immune responses. We consider a drug therapy that accounts for (1) inhibiting viral entry and (2) blocking the production of actively infected B-cells due to transition from the latently infected class. The latter drug therapy corresponds to blocking lytic HHV-8 replication in the literature since the latent/lytic phase of the viral cycle is described by the latently/actively infected B-cells. We employ optimal control approaches to determine treatment efficacies for the two novel therapeutics and make *in silico* comparisons between them. Our results have the potential to better inform preclinical drug safety decisions for non-AIDS related KS (NAKS).

5.2 Model Development and Analysis

5.2.1 Model formulation

We construct an in host model that includes the following populations: Uninfected B cells, (x_1) , latently infected B cells, (x_5) , productively infected B cells, (x_6) , uninfected progenitor cells, (x_2) , infected progenitor cells, (x_7) , HHV-8 specific effector cells, (x_3) , innate immune response, (x_4) , Kaposi's sarcoma cells, (x_8) , and HHV-8 virions, (x_9) . The dynamics of these populations are depicted in the schematic dia-

gram represented by **Figure 5.1**.

In order to study the effects of antiviral drugs, we introduce two time dependent controls, $u_1(t)$ and $u_2(t)$, in our system to determine the optimal strategy for controlling NAKS. $u_1(t)$ is the effectiveness of the endocytic pathway inhibitors [33] that block the mechanism that HHV-8 virus uses in infecting the activated B cells and $u_2(t)$ is the effectiveness of celecoxib in blocking reactivation of latently infected B cells [16]. We present a mathematical model for the infection of progenitor and B cells by HHV-8. We explore the dynamics of infected cells with the objective of making recommendations regarding treatment that would prevent B cell activation and ultimately delay the development of the disease.

The dynamics of the various classes are described below:

$$\dot{x}_1 = \Pi_1 - (1 - u_1(t))\beta_1 x_1 x_9 - \mu_1 x_1. \quad (5.1)$$

Eq. (5.1) describes the dynamics of the target B cells, x_1 . The first term represents the constant source, Π_1 , of these cells from the bone marrow. The second term denotes the reduced infectivity of these cells at the rate $(1 - u_1(t))\beta_1 x_9$ due the HHV-8 and the last term is the death of these cells at a constant rate μ_1 .

$$\dot{x}_2 = \Pi_2 - \beta_2 x_2 x_9 - \mu_2 x_2. \quad (5.2)$$

Eqs. (5.2) represents the dynamics of the target progenitor cells. The first term is the constant source of these cells from the bone marrow. The second term represents

the erroneous infectivity of these precursors by HHV-8 at the rate $\beta_2 x_9$ [32] and the last term is the death of these cells at a constant rate μ_2 .

$$\dot{x}_3 = \Pi_3 + r_3 x_3 x_6 - \mu_3 x_3. \quad (5.3)$$

Eq.(5.3) represents the dynamics of the HHV-8 specific effector cells. The first term represents a constant source from the memory pool with the host and the second term depicts the proliferation of effector cells due to the presence of infection. The third term is the natural death at a constant rate, μ_3 .

$$\dot{x}_4 = \frac{r_4 x_6}{1 + m x_6} - \mu_4 x_4. \quad (5.4)$$

Eq. (5.4) represents the dynamics of immune response. The first term represents the production of the hormone that triggers the immune response. The production is induced by the actively infected B cells. The last term represents the decay of the immune response at a constant rate, μ_4 .

$$\dot{x}_5 = (1 - u_1(t))\rho\beta_1 x_1 x_9 - (1 - u_2(t))\gamma x_5 - \mu_5 x_5. \quad (5.5)$$

Eq. (5.5) represents the dynamics of latently infected B cells. The first term depicts a proportion of the infection of B cells that goes into latency. This term is further reduced by the activity of the control, $u_1(t)$. The second term represents removal of these cells due to activation. This removal is further heighten by the activity of the control, $u_2(t)$, and the last term is the natural death at a constant rate, μ_5 .

$$\dot{x}_6 = (1 - u_1(t))\left(1 - \rho\right)\beta_1 x_1 x_9 + (1 - u_2(t))\gamma x_5 - \alpha_6 x_3 x_6 - \mu_6 x_6. \quad (5.6)$$

Eq. (5.6) represents the dynamics of productively infected B cells. The first term depicts a proportion of original infections that become productive immediately following the infection by HHV-8. The second term is the gain due to activation of latently infected B cells. The third term is the killing of these cells by HHV-8 specific cells and the last term is the natural death at a constant rate, μ_6 .

$$\dot{x}_7 = \beta_2 x_2 x_9 - \alpha_7 x_3 x_7 - \mu_7 x_7. \quad (5.7)$$

Eq. (5.7) represents the dynamics of infected progenitor cells. The first term depicts the infections resulting from HHV-8 erroneous infection of progenitor cells and the second term is killing of these cells by HHV-8 specific effector cells. The last term represents the progression to KS at a constant rate, μ_7 .

$$\dot{x}_8 = \mu_7 x_7 - \alpha_8 x_3 x_8 - \mu_8 x_8. \quad (5.8)$$

Eq. (5.8) describes the dynamics of KS cells. The first term is generation of KS cells at a constant rate, μ_7 . The second term is the killing of these cells by HHV-8 specific cells and the last term is the loss due to apoptosis.

$$\dot{x}_9 = \frac{N_9 \mu_6}{1 + \theta_4 x_4} x_6 - \mu_9 x_9. \quad (5.9)$$

Eq. (5.9) describes the dynamics of HHV-8 virions. The first term is the production of these virions resulting from the lysis of productively infected B cells that is opposed by the immune response and the last term is the decay at a constant rate, μ_9 .

For a comprehensive list of parameters with their definitions the reader is referred to

Table 5.2.

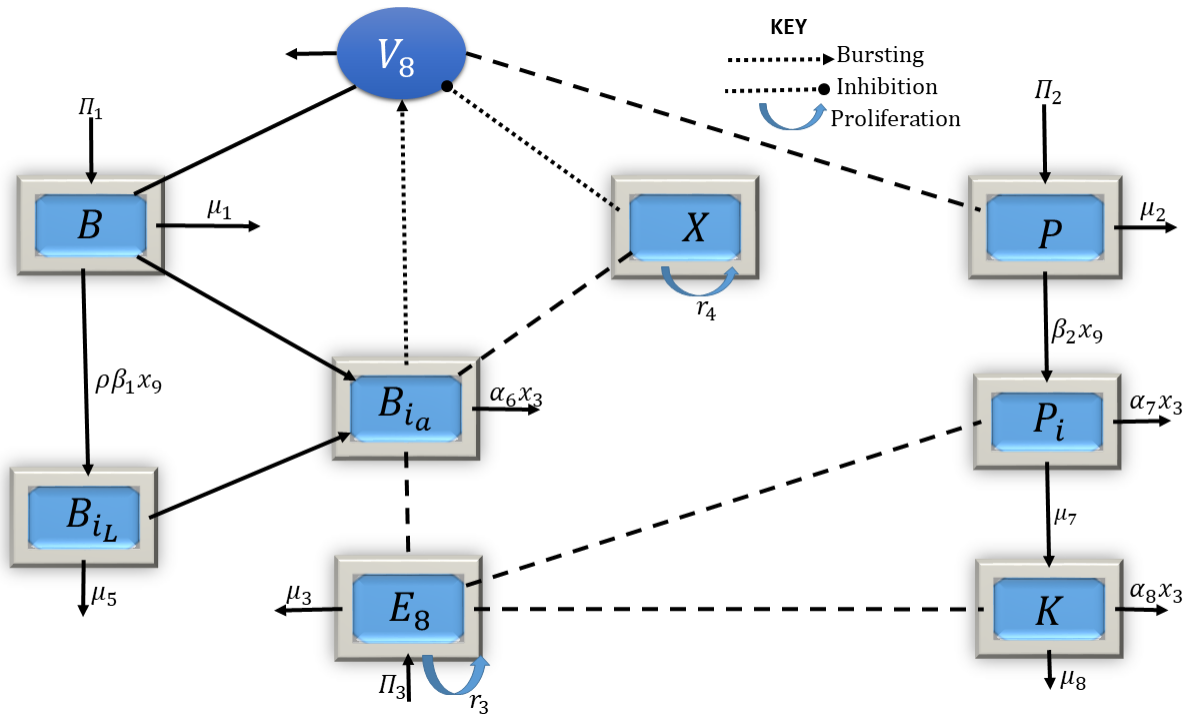


Figure 5.1: Schematic diagram of the non-AIDS KS model with immune response

Variable	Definitions	Value	Source
x_1^0	Initial target B cells	2×10^5 cells ml ⁻¹	[58, 59].
x_2^0	Initial target progenitor cells	10^5 cells ml ⁻¹	[58, 59].
x_3^0	Initial HHV-8 specific effector cells	500 cells ml ⁻¹	[58, 59].
x_4^0	Initial amount of immune response	0	Estimated.
x_5^0	Initial latently infected B cells	0	Estimated.
x_6^0	Initial productively infected B cells	0 cells ml ⁻¹	Estimated.
x_7^0	Initial infected progenitor cells	0 cells ml ⁻¹	Estimated.
x_8^0	Initial KS cells	0 cells ml ⁻¹	Estimated.
x_9^0	Initial HHV-8 viral load	1 virion ml ⁻¹	[58, 59].

Table 5.1: Initial values for the model state variables

Parameter	Definitions
Π_1	Source of new B cells from bone marrow
Π_2	Source of new progenitor cells from bone marrow
Π_3	Production rate of healthy CD8+ T cells from natural sources e.g thymus
μ_1	Death rate of B cells
μ_2	Death rate of healthy progenitor cells

μ_3	Death rate of HHV-8 specific effector cells
μ_4	Waning rate of immune response
μ_5	Death rate of latently infected B cells
μ_6	Death rate of productively infected B cells
μ_7	KS progression rate constant
μ_8	Death rate of KS due to apoptosis
μ_9	Decay rate constant of HHV-8
β_1	Infection rate of B cells by HHV-8
β_2	Infection rate of progenitor cells by HHV-8
r_3	Antigenic proliferation of HHV-8 specific CD8+ T cells
r_4	Production rate of immune response
m	Strength of immunosuppression
ρ	Proportion of infections that result in latently infected B cells
γ	Activation rate of latently infected B cells
θ_4	Efficacy threshold constant
α_6	Killing rate of productively infected B cells
α_7	Killing rate of infected progenitor cells

α_8	Killing rate of KS cells
N_9	Maximal carrying capacity of productively infected B cells

Table 5.2: Model parameters and their definitions

Parameter	Range/Value	Source
Π_1	[16800, 102600]48000 cell mL ⁻¹ day ⁻¹	[95]
Π_2	[859,2659]2000 cell mL ⁻¹ day ⁻¹	[95]
Π_3	[2,20]10 cell mL ⁻¹ day ⁻¹	[95]
μ_1	0.24 day ⁻¹	Estimated.
μ_2	[0.005,0.024] day ⁻¹	Estimated.
μ_3	0.01 day ⁻¹	[95].
μ_4	0.0001 day ⁻¹	Estimated.
μ_5	0.30 day ⁻¹	Estimated.
μ_6	0.33 day ⁻¹	[95]
μ_7	0.1 day ⁻¹	Estimated.
μ_8	5×10^{-6} day ⁻¹	Estimated.

μ_9	0.57 day^{-1}	[95]
β_1	$[4.75 \times 10^{-9}, 4.75 \times 10^{-7}] 2.4 \times 10^{-8} \text{ mL virus}^{-1} \text{ day}^{-1}$	[95]
β_2	$[4.75 \times 10^{-9}, 4.75 \times 10^{-7}] 2.4 \times 10^{-8} \text{ mL virus}^{-1} \text{ day}^{-1}$	[95]
r_3	$6 \times 10^{-7} \text{ mL cell}^{-1} \text{ day}^{-1}$	Estimated.
r_4	$0 - 10 \text{ day}^{-1}$	Estimated.
m	0.8	Estimated.
ρ	0.001 day^{-1}	Estimated.
γ	1.1 day^{-1}	Estimated.
θ_4	0.8	Estimated.
α_6	$[5.47 \times 10^{-5}, 1.09 \times 10^{-4}] \text{ mL cell}^{-1} \text{ day}^{-1}$	[95]
α_7	$5 \times 10^{-4} \text{ mL cell}^{-1} \text{ day}^{-1}$	[95]
α_8	$5 \times 10^{-4} \text{ mL cell}^{-1} \text{ day}^{-1}$	[95]
N_9	$[600, 1000] \text{ virions cell}^{-1}$	[95]

Table 5.3: Model parameters and their ranges

5.2.2 Analysis of the uncontrolled model where $u_1(t) = u_2(t) = 0$.

We first begin by analysing the model in the absence of the controls, $u_1(t)$ and $u_2(t)$.

Positivity and boundedness of solutions

We now show that our model is well posed in the sense that the populations do not become negative and are always bounded.

Denote by \mathbb{R}_+^9 the set of points

$$x_t = (x_1, x_2, x_3, x_4, x_5, x_6, x_7, x_8, x_9) \in \mathbb{R}_+^9$$

with positive coordinates and consider the system with initial values as in **Table 5.1**.

$$x^0 = (x_1^0, x_2^0, x_3^0, x_4^0, x_5^0, x_6^0, x_7^0, x_8^0, x_9^0) \in \mathbb{R}_+^9$$

Lemma 5.2.1 *If $x_i^0 \geq 0$, $i = 1, 2, 3, \dots, 9$, then the solution $x_i(t) \geq 0$, $\forall t > 0$.*

Proof 5.2.2 *The system (5.1) to (5.9) can be written as a system of differential inequalities*

$$\frac{dx_i}{dt} \geq \left(A_i - \sum_{j=1}^9 B_{ij}x_j \right) x_i + \Pi_i \quad (5.10)$$

where $B_{ij} \geq 0$,

$$\Pi = \begin{pmatrix} \Pi_1 & \Pi_2 & \Pi_3 & 0 & 0 & 0 & 0 & 0 & 0 \end{pmatrix}^T \geq \begin{pmatrix} 0 & 0 & 0 & 0 & 0 & 0 & 0 & 0 & 0 \end{pmatrix}^T,$$

$$A = \text{diag}\{-\mu_1, -\mu_2, -\mu_3, -\mu_4, -(\mu_5 + \gamma), -\mu_6, -\mu_7, -\mu_8, -\mu_9\}$$

$$B = \text{diag}\{\beta_1 x_9, \beta_2 x_9, 0, 0, 0, \alpha_6 x_3, \alpha_7 x_3, \alpha_8 x_3, 0\}$$

Suppose the assertion $x_i(t) \geq 0, i = 1, 2, 3, \dots, 9$ is not true. Then there exists a smallest number t_0 , such that

$$x_i(t) > 0 \quad \text{for } 1 \leq i \leq 9, \quad 0 \leq t \leq t_0,$$

$$x_i(t_0) = 0 \quad \text{for at least one } i, \text{ say } i_0.$$

Then, x_{i_0} is a decreasing function and

$$\frac{dx_{i_0}(t_0)}{dt} \leq 0.$$

From the differential inequality (5.10) for $x_{i_0}(t)$, we get

$$\frac{dx_{i_0}(t_0)}{dt} \geq \pi_{i_0} \geq 0$$

which is a contradiction. Hence, if $x_i(0) \geq 0, i = 1, 2, 3, \dots, 9$ then, $x_i(t) \geq 0$ for all $t > 0, i = 1, 2, 3, \dots, 9$.

Lemma 5.2.3 Consider the system (5.1) - (5.9).

If $x_i^0 \geq 0, i = 1, 2, 3, \dots, 9$, then $x_i(t) < \infty, \forall t \geq 0$.

Proof 5.2.4 To establish that every solution of system (5.1) – (5.9) is bounded, it suffices to show that there exists M such that $x_i(t) \leq M$ for all i . Define $i \in \{1, 2, 3, 5, 6, 7, 8\}$ and let

$$y = \sum_i a_i x_i$$

where

$$a_i = \begin{cases} 1 & \text{if } i = 1, 2, 5, 6, 8 \\ \frac{\alpha_6}{r_3} & \text{if } i = 3 \\ \frac{1}{4} & \text{if } i = 8 \end{cases}$$

It can be verified that for all times, t ,

$$\begin{cases} y(t) \leq y(0) + \frac{r_3(\Pi_1 + \Pi_2) + \alpha_6 \Pi_3}{r_3 \hat{\mu}} = M_1, \quad \hat{\mu} = \min\left\{\mu_1, \mu_2, \mu_3, \mu_5, \mu_6, \frac{3}{4}\mu_7, \mu_8\right\} \\ x_4(t) \leq x_4(0) + \frac{r_4}{m\mu_4} = M_2, \\ x_9(t) \leq x_9(0) + \frac{\mu_6 N_9 \left(r_3(\Pi_1 + \Pi_2) + \alpha_6 \Pi_6\right)}{r_3 \hat{\mu} \mu_9} = M_3. \end{cases}$$

We can choose

$$M = \max_{1 \leq k \leq 3} \{M_k\}$$

such that $x_i < M, i = 4, 9$ and $y < M$.

5.2.3 Equilibria and the basic reproduction number, \mathcal{R}_0 .

To determine the equilibria we set the right hand side of (5.1) – (5.9) to zero and solve the resulting equations simultaneously and obtain the following infection free equilibrium, denoted by E_0 .

Infection free equilibrium (IFE), E_0

$$E_0 = \left(x_0^1, x_0^2, x_0^3, x_0^4, x_0^5, x_0^6, x_0^7, x_0^8, x_0^9 \right) = \left(\frac{\Pi_1}{\mu_1}, \frac{\Pi_2}{\mu_2}, \frac{\Pi_3}{\mu_3}, 0, 0, 0, 0, 0, 0 \right)$$

where $x_0^i, i = 1, 2, \dots, 9$ is the i^{th} coordinate of the virus free equilibrium, E_0 .

We calculate the basic reproduction number of our model given by equations (5.1) – (5.9) using the next generation operator method [14]. We define the basic reproduction number as the number of newly infected B cells arising from an HHV-8 infected B cell where the entire population of B cell is totally susceptible to the infection. Our model can be re-written in the form:

$$\begin{aligned} \frac{dX}{dt} &= f(\mathbf{X}, \mathbf{Y}, Z), \\ \frac{dY}{dt} &= g(\mathbf{X}, \mathbf{Y}, Z), \\ \frac{dZ}{dt} &= h(\mathbf{X}, \mathbf{Y}, Z), \end{aligned}$$

where $\mathbf{X} \in \mathbb{R}^4$, denotes the number of susceptibles, recovered and other classes of non-infected individuals, $\mathbf{Y} \in \mathbb{R}^4$ denotes the number of HHV-8 infected cells and $Z \in \mathbb{R}$, represents the number of HHV-8 virions. Note that the equation $g(\mathbf{X}^*, \mathbf{Y}, Z) = \mathbf{0}$ implicitly determines a function $Y = \tilde{g}(\mathbf{X}^*, Z)$. We let $\mathbf{A} = D_Z h(\mathbf{X}^*, \tilde{g}(\mathbf{X}^*, \mathbf{0}), 0)$ and further assume that \mathbf{A} can be decomposed as $\mathbf{A} = \mathbf{M} - \mathbf{D}$, with $\mathbf{M} \geq \mathbf{0}$ (that is $m_{ij} \geq 0$) and $\mathbf{D} \geq \mathbf{0}$, is a diagonal matrix.

The component, Z represent the number of HHV-8 virions. Therefore, we set $\mathbf{X} = (x_1, x_2, x_3, x_4)$, $\mathbf{Y} = (x_5, x_6, x_7, x_8)$, $Z = x_9$ and let $\mathbf{U}_0 = (\mathbf{X}^*, \mathbf{0}, 0)$ denote the infec-

tion free equilibrium, that is

$$f(\mathbf{X}^*, \mathbf{0}, 0) = \mathbf{0}, \quad g(\mathbf{X}^*, \mathbf{0}, 0) = \mathbf{0}, \quad \text{and} \quad \mathbf{h}(\mathbf{X}^*, \mathbf{0}, \mathbf{0}) = \mathbf{0}, \quad \text{with} \quad \mathbf{Y} = \tilde{\mathbf{g}}(\mathbf{X}^*, \mathbf{Z}),$$

where

$$\tilde{\mathbf{g}}(\mathbf{X}^*, Z) = \begin{pmatrix} \tilde{g}_1(\mathbf{X}^*, Z) \\ \tilde{g}_2(\mathbf{X}^*, Z) \\ \tilde{g}_3(\mathbf{X}^*, Z) \\ \tilde{g}_4(\mathbf{X}^*, Z) \end{pmatrix} = \begin{pmatrix} \frac{\rho\beta_1 x_1^0 x_9}{\gamma + \mu_5} \\ \frac{(\mu_5 + \gamma)(1 - \rho)\beta_1 x_1^0 x_9 + \gamma\rho\beta_1 x_1^0 x_9}{(\mu_5 + \gamma)(\mu_6 + \alpha_6 x_3^0)} \\ \frac{\beta_2 x_2^0 x_9}{\mu_7 + \alpha_7 x_3^0} \\ \frac{\mu_7 x_7^0}{\mu_8 + \alpha_8 x_3^0} \end{pmatrix}.$$

We compute $\mathbf{A} = D_Z h(\mathbf{X}^*, \tilde{\mathbf{g}}((\mathbf{X}^*, \mathbf{0}), \mathbf{0}))$ and get

$$\mathbf{M} = \frac{N_9 \mu_3 \mu_6 \beta_1 \Pi_1 (\gamma + \mu_5 (1 - \rho))}{\mu_1 (\mu_5 + \gamma) (\mu_3 \mu_6 + \alpha_6 \Pi_3)} \quad \text{and} \quad \mathbf{D}^{-1} = \frac{1}{\mu_9}$$

The basic reproduction number, \mathcal{R}_0 , is given by the next generation spectral radius $\rho(\mathbf{M}\mathbf{D}^{-1})$ to be

$$\mathcal{R}_0 = \frac{N_9 \mu_3 \mu_6 \beta_1 \Pi_1 (\gamma + \mu_5 (1 - \rho))}{\mu_1 \mu_9 (\mu_5 + \gamma) (\mu_3 \mu_6 + \alpha_6 \Pi_3)},$$

Theorem 5.2.5 *Consider the non-AIDS related KS(NAKS) transmission model (5.1)–(5.9). The infection free equilibrium point, E_0 , of (5.1)–(5.9) is locally asymptotically stable if $\mathcal{R}_0 < 1$, but unstable if $\mathcal{R}_0 > 1$.*

5.2.4 Global stability of the infection free equilibrium (IFE)

point, E_0

In this section, we state the two conditions that, if met, will guarantee the global asymptotic stability of the IFE point. Let the model (5.1) – (5.9) be rewritten as in the appendix A. We can state the global stability of IFE as follows:

Lemma 5.2.6 *In the absence of reactivation of latently infected B cells, ($\gamma = 0$), the infection free equilibrium point, E_0 , is globally asymptotically stable if $\mathcal{R}_0 < 1$.*

Proof 5.2.7 *We observe that*

$$G(X_0, 0) = \mathbf{0} \quad \text{and} \quad (x_1(t), x_2(t), x_3(t), x_4(t)) \rightarrow \left(\frac{\Pi_1}{\mu_1}, \frac{\Pi_2}{\mu_2}, \frac{\Pi_3}{\mu_3}, 0 \right) = X_0 \quad \text{as } t \rightarrow \infty.$$

We therefore conclude that, irrespective of the initial conditions, the solution converges to X_0 . Thus, X_0 is g.a.s. The condition (H1) is satisfied.

We now verify (H2).

$$A = \begin{pmatrix} -(\mu_5 + \gamma) & 0 & 0 & 0 & \beta_1 \rho x_0^1 \\ \gamma & -(\mu_6 + \alpha_6 x_0^3) & 0 & 0 & \beta_1 (1 - \rho) x_0^1 \\ 0 & 0 & -(\mu_7 + \alpha_7 x_0^3) & 0 & \beta_2 x_0^2 \\ 0 & 0 & \mu_7 & -(\mu_8 + \alpha_8 x_0^3) & 0 \\ 0 & \mu_6 N_9 & 0 & 0 & -\mu_9 \end{pmatrix}$$

and

$$\hat{G}(X, Y) = \begin{pmatrix} \beta_1 \rho (x_0^1 - x_1) \\ \alpha_6 x_6 (x_3 - x_0^3) + \beta_1 (1 - \rho) (x_0^1 - x_1) x_9 \\ \alpha_7 x_7 (x_3 - x_0^3) + \beta_2 x_9 (x_0^2 - x_2) \\ \alpha_8 x_8 (x_3 - x_0^3) \\ \frac{\mu_6 N_9}{1 + \theta_4 x_4} x_6 \end{pmatrix}$$

Since $x_0^i \geq x_i$, $i = 1, 2$ and $x_3 \geq x_0^3$, we conclude that $\hat{G}(X, Y) \geq \mathbf{0}$.

5.3 Numerical Simulations and Sensitivity Analysis

To illustrate the results obtained for the system (5.1)–(5.9), we give some simulations using the parameters values in **Table 5.3**. Numerical results are displayed in the following figures.

Figure 5.2 shows the partial rank correlation coefficients (PRCCs) for \mathcal{R}_0 . The sensitivity analysis shows how the model reproduction number is affected by changes in the model parameters. We see that \mathcal{R}_0 is positively and significantly correlated to β_1 and Π_1 . Changes in these two parameters could overestimate the severity of the

infection. Hence, it is important to estimate these two parameters accurately. The reproduction number is negatively correlated to μ_1 but this is not significant.

In Figure 5.3(a) – 5.3(f), we simulate the various populations of the model (5.1) – (5.9) for $\mathcal{R}_0 = 0.9181$. We see that the introduction of HHV-8 fails to establish a persistent infection in the host. Notice that the infected populations eventually decay to low levels while the uninfected B cells decline by only 8%, the uninfected progenitor cells declined by 31.7%.

In Figure 5.4, we simulate the different model populations for $\mathcal{R}_0 = 1.2242$ for the purpose of obtaining the initial steady state values for the model with controls. We investigate how the disease prognosis is altered by introduction of treatment represented by $u_1(t)$ and $u_2(t)$. For this case without treatment, we observe that the growth of the infection is gradual initially but accelerates towards a steady state. Figure 5.4(a), 5.4(b) and 5.4(c) have provided the initial steady state values used in the model with controls $u_1 \neq 0$ and $u_2 \neq 0$, representing drugs that block the infection of B cells and drugs that inhibit lytic activation, respectively.

5.4 Model with Optimal Control

Following techniques outlined in [69], we have formulated the objective (or cost) functional for our problem of the type

$$J(u_1, u_2) = \int_0^{T_f} [A_1 x_5 + A_2 x_6 + \frac{1}{2} B_1 u_1^2 + \frac{1}{2} B_2 u_2^2] dt, \quad (5.11)$$

where the control functions $u_1(t)$ and $u_2(t)$ are bounded, Lebesgue integrable functions. Because of the need to cater for a large section of the population, we have assumed a quadratic cost function where T_f is the final time and the constants A_i, B_i , $i = 1, 2$ differentiate between the types of intervention strategies.

5.4.1 Existence and characterization of optimal control solution

For the system (5.1) – (5.9), we can state the optimal control problem as follows:

Theorem 5.4.1 *Suppose the objective functional*

$$J(u_1, u_2) = \int_0^{T_f} \left[A_1 x_5 + A_2 x_6 + \frac{1}{2} B_1 u_1^2 + \frac{1}{2} B_2 u_2^2 \right] dt,$$

is minimized subject to the controls and state variables given in the model (5.1) – (5.9)

with

$$x_i(0) = x_{i0}, \quad i = 1, 2, 3, \dots, 9$$

as initial conditions. Then, there exists optimal controls $u_1^, u_2^* \in U$ such that*

$$J(u_1^*, u_2^*) = \min \left\{ J(u_1, u_2) \mid u_1, u_2 \in U \right\}$$

where

$$U = \left\{ (u_1, u_2) \text{ such that } u_1, u_2 \text{ are measurable with } 0 \leq u_i \leq 1, \text{ for } t \in [0, T_f] \right\}$$

is the control set. The details of the proof of Theorem 5.4.1 are included in the Appendix. We summarize the steps of the proof as follow:

Proof 5.4.2 *The existence of the solution can be shown using the results obtained in [30] since*

(a) *the class of all initial conditions with controls u_1 and u_2 in the control set U are nonnegative values as stated and proved in Lemma 5.2.1 and non-empty.*

(b) *The integrand, $A_1x_5 + A_2x_6 + \frac{1}{2}B_1u_1^2 + \frac{1}{2}B_2u_2^2$, in the objective functional is convex on $\Omega \subseteq \mathbb{R}_+^4$ as proved in Appendix C)*

(c) *The right hand side of system (5.1) – (5.9) is bounded by a linear function of the state and control variables and the solutions exist as demonstrated in the appendix D.*

(d) *The control set U is convex and closed as demonstrated in appendix E.*

This completes the proof of Theorem 5.4.1.

From the Pontryagin et al [82] Maximum principle, we can convert the systems (5.1) – (5.9) and Eq. (5.11) into a problem of formulating and minimizing point-wise a Hamiltonian H , with respect to u_1 and u_2 . The Hamiltonian function for our

optimal problem is given by:

$$\begin{aligned}
H(\mathbf{x}, \mathbf{u}, \lambda_{\mathbf{x}}, t) = & A_1x_5 + A_2x_6 + \frac{1}{2}B_1u_1^2 + \frac{1}{2}B_2u_2^2 + \lambda_{x_1} \left(\Pi_1 - (1 - u_1)\beta_1x_1x_9 - \mu_1x_1 \right) \\
& + \lambda_{x_2} \left(\Pi_2 - \beta_1x_2x_9 - \mu_2x_2 \right) + \lambda_{x_3} \left(\Pi_3 + r_3x_3x_6 - \mu_3x_3 \right) \\
& + \lambda_{x_4} \left(\frac{r_4x_6}{1 + mx_6} - \mu_4x_4 \right) + \lambda_{x_5} \left((1 - u_1)\rho\beta_1x_1x_9 - (1 - u_2)\gamma x_5 - \mu_5x_5 \right) \\
& + \lambda_{x_6} \left((1 - u_1)(1 - \rho)\beta_1x_1x_9 + (1 - u_2)\gamma x_5 - \alpha_6x_3x_6 - \mu_6x_6 \right) \\
& + \lambda_{x_7} \left(\beta_2x_2x_9 - \alpha_7x_3x_7 - \mu_7x_7 \right) + \lambda_{x_8} \left(\mu_7x_7 - \alpha_8x_3x_8 - \mu_8x_8 \right) \\
& + \lambda_{x_9} \left(\frac{N_9\mu_6x_6}{1 + \theta_4x_4} - \mu_9x_9 \right) \tag{5.12}
\end{aligned}$$

where, $\mathbf{x} = (x_1, x_2, \dots, x_9)$, $\mathbf{u} = (u_1, u_2)$, $\lambda_{\mathbf{x}} = (\lambda_{x_1}, \lambda_{x_2}, \dots, \lambda_{x_9})$ and λ_{x_i} , $i = 1, 2, \dots, 9$ are the adjoint variables corresponding to the state variable $x_i \in \mathbf{x}$.

We can state the minimizing optimal control problem as follows:

Theorem 5.4.3 *Given optimal controls u_1^*, u_2^* that minimize $J(u_1, u_2)$ over U , and the solutions x_1, x_2, \dots, x_9 of the corresponding state system (5.1) – (5.9) and Eq. (5.11), then there exist adjoint variables λ_{x_i} , $i = 1, 2, \dots, 9$ satisfying*

$$\frac{\partial H}{\partial x_i} = -\frac{d\lambda_{x_i}}{dt}$$

and with transversality conditions

$$\lambda_{x_i}(T_f) = 0, \quad i = 1, 2, \dots, 10.$$

and

$$u_i^* = \min \left\{ 1, \max \left(0, \hat{u}_i \right) \right\}, \quad i = 1, 2$$

where \hat{u}_i^* , $i = 1, 2$ are given in appendix (B).

Proof 5.4.4 *The existence of an optimal control solution is proved and given by Fleming and Rishel [30]. The reader is referred to that study for details. For our problem, the differential equations governing the adjoint variables are obtained by differentiating the Hamiltonian in (5.12) with respect to the state variables x_i and evaluated at the optimal control. This gives*

$$\left\{ \begin{array}{l} \frac{d\lambda_{x_1}}{dt} = \lambda_{x_1} \left(\mu_1 + (1 - u_1) \beta_1 x_9 \right) - \lambda_{x_6} \beta_1 (1 - \rho) (1 - u_1) x_9 - \lambda_{x_5} \rho \beta_1 (1 - u_1) x_9, \\ \frac{d\lambda_{x_2}}{dt} = \lambda_{x_2} (\mu_2 + \beta_2 x_9) - \lambda_{x_7} \beta_2 x_9, \\ \frac{d\lambda_{x_3}}{dt} = \lambda_{x_3} (\mu_3 - r_3 x_6) + \lambda_{x_6} \alpha_6 x_6 + \lambda_{x_7} \alpha_7 x_7 + \lambda_{x_8} \alpha_8 x_8, \\ \frac{d\lambda_{x_4}}{dt} = \lambda_{x_4} \mu_4 + \frac{\lambda_{x_9} N_9 \mu_6 \theta_4 x_6}{(1 + \theta_4 x_4)^2}, \\ \frac{d\lambda_{x_5}}{dt} = -A_1 + \lambda_{x_5} \left(\mu_5 + \gamma (1 - u_2) \right) - \lambda_{x_6} \gamma (1 - u_2), \\ \frac{d\lambda_{x_6}}{dt} = -A_2 + \lambda_{x_6} (\mu_6 + \alpha_6 x_3) - \frac{\lambda_{x_4} r_4}{(1 + m x_6)^2} - \lambda_{x_3} r_3 x_3 - \frac{\lambda_{x_9} \mu_6 N_9}{(1 + \theta_4 x_4)}, \\ \frac{d\lambda_{x_7}}{dt} = \lambda_{x_7} (\mu_7 + \alpha_7 x_3) - \lambda_{x_8} \mu_7, \\ \frac{d\lambda_{x_8}}{dt} = \lambda_{x_8} (\mu_8 + \alpha_8 x_3), \\ \frac{d\lambda_{x_9}}{dt} = \lambda_{x_9} \mu_9 + \beta_2 (\lambda_{x_2} - \lambda_{x_7}) x_2 + \beta_1 (1 - u_1) (\lambda_{x_1} - \lambda_{x_6}) x_1 + \beta_1 \rho (1 - u_1) (\lambda_{x_6} - \lambda_{x_5}) x_1 \end{array} \right.$$

Next, we differentiate the Hamiltonian H in (5.12) with respect to $u_i(t)$, $i = 1, 2$ to obtain

$$u_i^* = \min \left\{ 1, \max(0, \hat{u}_i) \right\}, \quad i = 1, 2$$

where u_i^* is obtained from \hat{u}_i in Appendix B. By standard control arguments involving the bounds on the controls, we conclude

$$u_i^* = \begin{cases} \hat{u}_i, & \text{if } 0 < \hat{u}_i < 1; \\ 0, & \text{if } \hat{u}_i \leq 0; \\ 1, & \text{if } \hat{u}_i \geq 1. \end{cases}$$

which can be compactly written as

$$u_i^* = \min \left\{ 1, \max(0, \hat{u}_i) \right\}$$

for $i = 1, 2$.

5.5 Numerical Simulations and Sensitivity Analysis

In Figures 5.5–5.8, we illustrate the effect of drug efficacy on the dynamics of various state variables. The initial values, used to plot the figures, are taken from Figure 5.4 of the uncontrolled system between day 400 and 600 where we observed changes in the state variables from the primary stage to the stable chronic stage. Figure 5.5

shows the impact of control for a scenario $\rho = 0.90$, that is, when 90% of the cells are latently infected and drug efficacies are specified for three different regimens as follows:

- (i) The efficacy of the drug that reduces the infectivity of susceptible B cells and the efficacy of the drug that inhibits the reactivation of latently infected B cells are of high efficacy, assumed in this study to be $u_i \geq 0.8$, $i = 1, 2$.
- (ii) when the efficacies of the drug reducing the infectivity of susceptible B cells and that inhibiting the reactivation of B cells are moderate, assumed to be in the range $0.5 \leq u_i < 0.7$ and
- (iii) when there is no treatment at all, that is, $u_i = 0$, $i = 1, 2$.

From figures 5.5(a) and 5.5(b), we can see that when the efficacies of both drugs are high, the infection does not develop. At the end of the infection period (adaptive stage), 80% of B cells and 90% of progenitor cells are uninfected. The infected B and progenitor cells decline to below detectable levels (Figures 5.5(c)(i), 5.5(d)(i), 5.5(e)(i)), Kaposi's sarcoma cells (Figure 5.5(f)), and the HHV-8 die out (Figure 5.5(g)). For the same parameter values but for drugs of moderate efficacies, the susceptible B cells and progenitor cells decline by 40% for B cells (Figure 5.5(a)(ii)) and 90% for progenitor cells (Figure 5.5(b)(ii)). The infection in this case persists (Figures 5.5(c)(ii), 5.5(d)(ii), 5.5(e)(ii)). We can see from Figure 5.5(f)(ii) that the possibility for Kaposi's sarcoma to develop for drugs of moderate efficacy is as high as that

for no treatment at all.

Figure 5.6 illustrates a scenario for $\rho = 0.10$, that is, when only 10% of the B cells are latently infected. We can see that while the loss of susceptible B cells is 15% (Figure 5.6(a)(i)), the loss of susceptible progenitor cells is very high at 89% (Figure 5.6(b)(i)). For $\rho = 0.10$ the possibility of Kaposi sarcoma developing is equally the same for all drug efficacies (Figure 5.6(f)). The population of HHV-8 in this case is significantly reduced (Figure 5.6(g)(i)) for drugs of high efficacies suggesting that the growth of KS cannot be sustained.

We conclude from the two values of ρ that drugs that reduce the infectivity may be more beneficial than drugs that reduce lytic activation.

Figures 5.7 and 5.8 illustrate scenarios for $\rho = 0.1$ and $\rho = 0.9$, respectively when one of the drugs is of high efficacy and the other of moderate efficacy. From Figure 5.7 ($\rho = 0.1$) we can see that the susceptible progenitor cell population declines significantly when only one drug is of high efficacy. The susceptible B cell population, on the other hand, declines by only 20% when the efficacy of the drug that reduces the infectivity of B cells is of high efficacy. When the drug that reduces infectivity is of moderate efficacy, even if the drug that inhibits lytic activation is of high efficacy, the B cell population declines significantly (by 65% (Figure 5.7(a)(ii))).

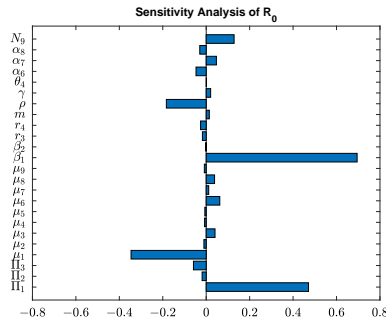
Figure 5.7(f) shows that, for $\rho = 0.1$, regardless of which drug is of high efficacy, the chances of KS developing in the long run remains the same. The conclusion when $\rho = 0.9$ is that the likelihood of KS not developing is the same so long as one of the

drugs is of high efficacy (Figures 5.8(b) and 5.8(f)).

5.6 Summary of Results

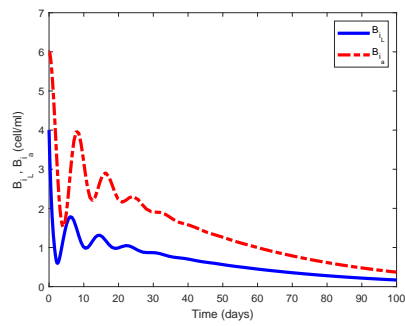
Kaposi's sarcoma (KS) is a malignant disorder of lymphatic endothelial origin that can have two main variants: AIDS-related KS (AKS) and non-AIDS related KS (NAKS) that all share a causal relationship with the human herpesvirus-8 (KSHV or HHV-8). We develop a mathematical model that accounts for B-cells latently and lytically infected with HHV-8 as well as the innate and adaptive arms of the immune system. As a sequel to numerous studies that have investigated the inhibition of HHV-8 endocytosis and reactivation of HHV-8 replication, we employ optimal control strategy to obtain treatment efficacies for these two therapeutic approaches. We have shown that when 90% of the B-cell infections result in latency, administration of high efficacy drugs that inhibit entry and reactivation of latently infected B-cells leads to the clearance of KS as the population of infected cells cannot be sustained. Our results also reveal that at 90% latency of B-cells, the therapy could produce similar results if the drug that targets viral entry is of moderate efficacy but the efficacy of the drug inhibiting reactivation is considerably more than 0.8. Administration of the same drugs but both at moderate efficacy levels leads to the depletion of both uninfected B- and progenitor cells, a scenario which can lead to the growth of KS variants. When 10% of the B-cell infections result in latency, administration with high efficacy drugs reduces the viral entry of HHV-8 but as 90% of the infected B-

cells are productive, this event leads to production of HHV-8 which ultimately results in more progenitor cells getting infected and the growth of KS. Our findings have the potential to offer more effective therapeutic approaches in the treatment of NAKS.

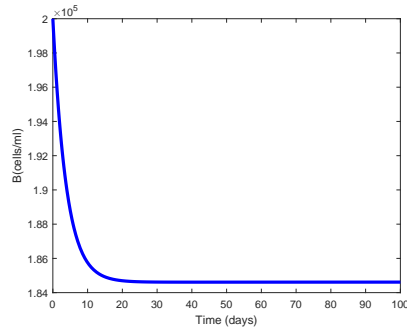


(a) PRCCs for \mathcal{R}_0

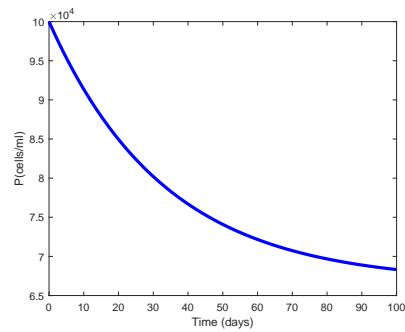
Figure 5.2: \mathcal{R}_0 and PRCCs



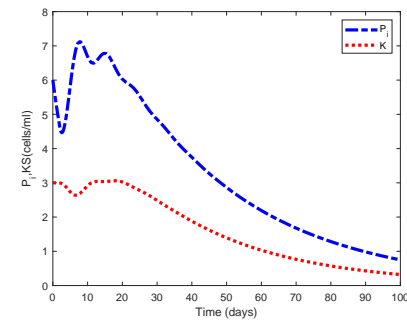
(a) Infected B cell dynamics



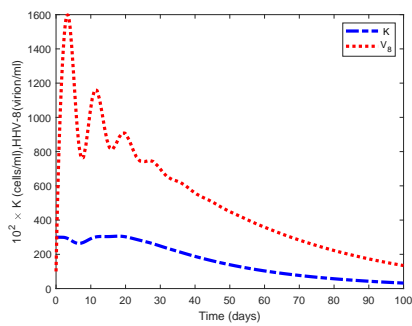
(b) Uninfected B cell dynamics



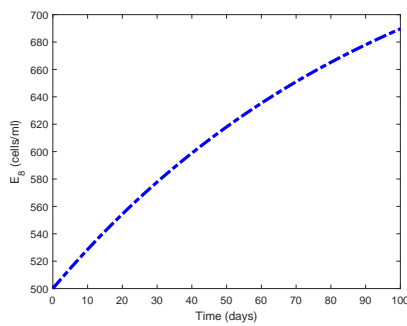
(c) Uninfected progenitor cell dynamics



(d) Infected progenitor and KS cell dynamics

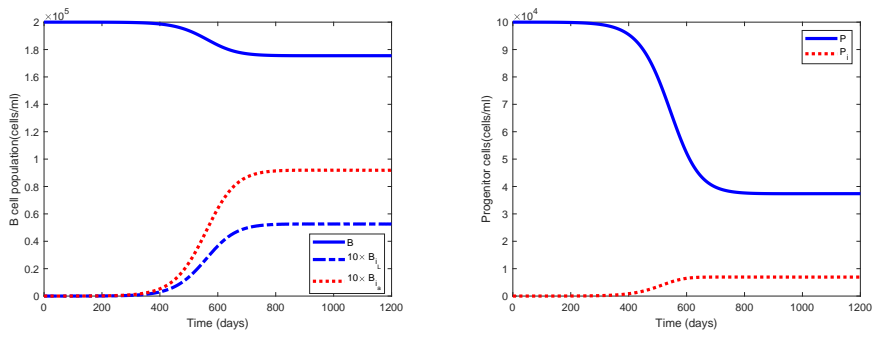


(e) HHV-8 and KS dynamics

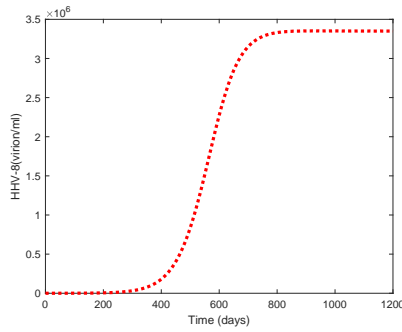


(f) HHV-8 specific effector cell dynamics

Figure 5.3: Population Dynamics with $\mathcal{R}_0 = 0.9181$

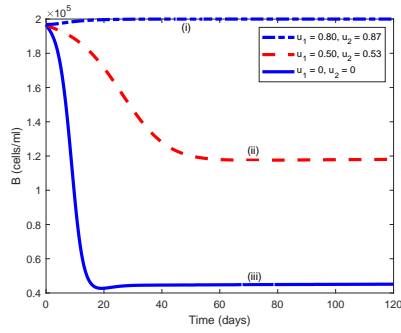


(a) Target B, Latent B and Lytic B cell dynamics (b) Uninfected progenitor and infected progenitor dynamics

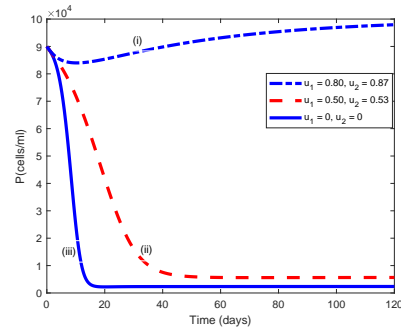


(c) HHV-8

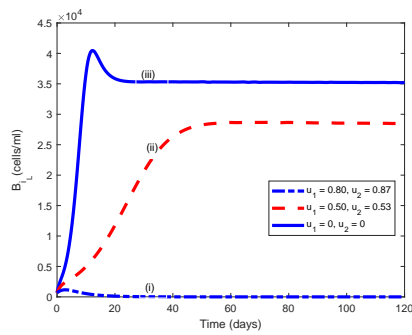
Figure 5.4: Population Dynamics with $\mathcal{R}_0 = 1.2242$



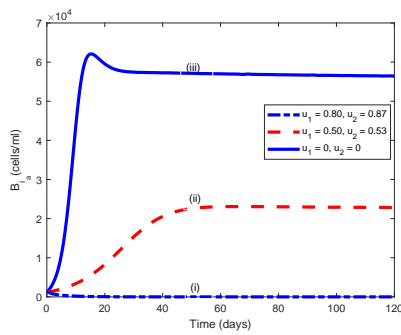
(a) Uninfected B cell dynamics



(b) Uninfected progenitor cell dynamics

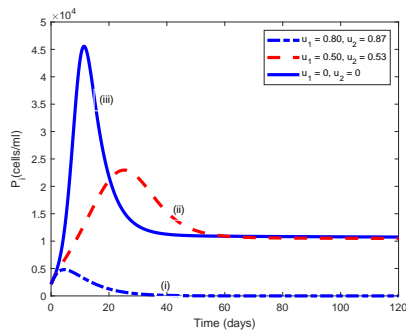


(c) Latently infected B cell dynamics

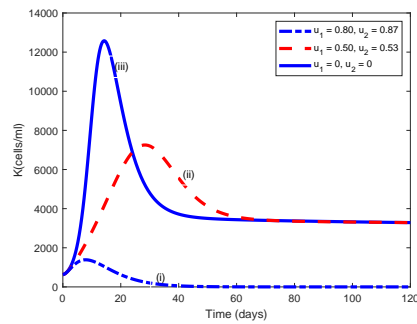


(d) Productively infected B cell dynamics

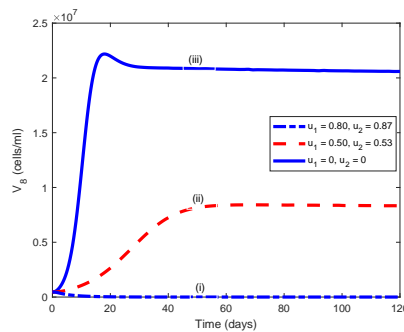
ics



(e) Infected progenitor dynamics

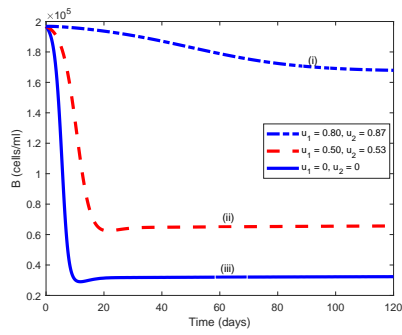


(f) KS cell dynamics

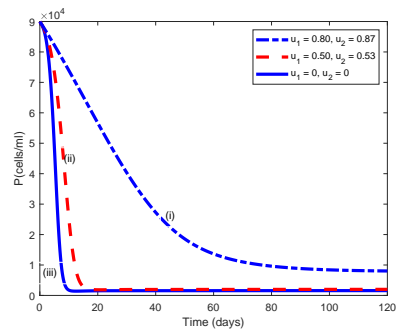


(g) HHV-8 virion dynamics

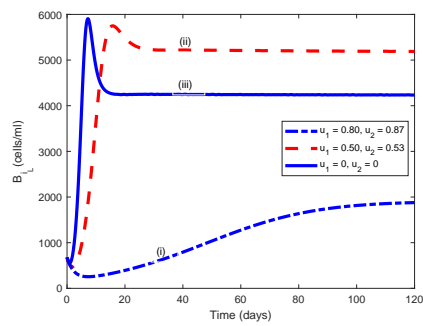
Figure 5.5: Population dynamics for the uncontrolled and controlled systems. In this figure we have used: $\rho = 0.90$. We have set $u_1 = 0, 0.50, 0.80$ and $u_2 = 0, 0.53, 0.87$. The initial values in our simulation are $B(0) = 1.968 \times 10^5$, $P(0) = 8.994 \times 10^4$, $B_{i_L}(0) = 678.9$, $B_{i_a}(0) = 1418$, $P_i(0) = 2144$, $V_8(0) = 4.483 \times 10^5$, $E_8 = 759.3$, $K(0) = 629.9$. The rest of the parameters are as indicated in Table 3.



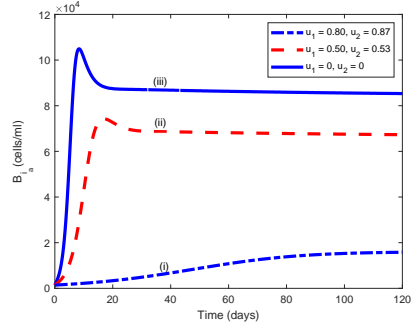
(a) Uninfected B cell dynamics



(b) Uninfected progenitor cell dynamics

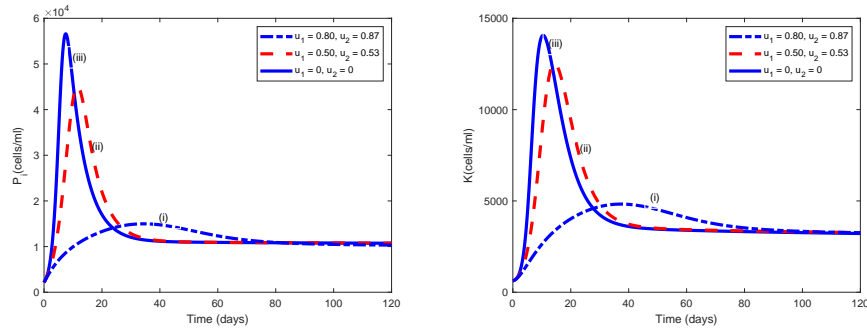


(c) Latently infected B cell dynamics



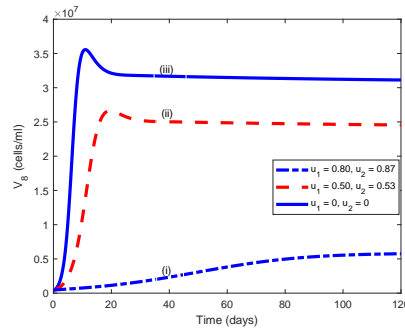
(d) Productively infected B cell dynamics

ics



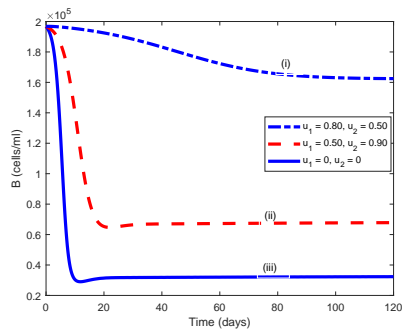
(e) Infected progenitor dynamics

(f) KS cell dynamics

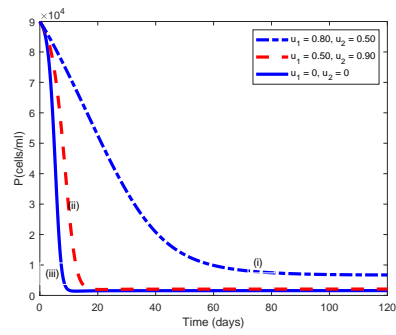


(g) HHV-8 virion dynamics

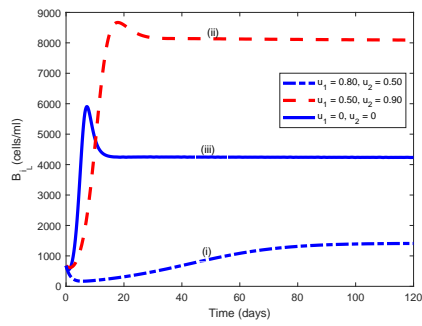
Figure 5.6: Population Dynamics for the uncontrolled and controlled systems. In this figure we have used: $\rho = 0.10$. We have set $u_1 = 0, 0.50, 0.80$ and $u_2 = 0, 0.53, 0.87$. The initial values in our simulation are $B(0) = 1.968 \times 10^5$, $P(0) = 8.994 \times 10^4$, $B_{i_L}(0) = 678.9$, $B_{i_a}(0) = 1418$, $P_i(0) = 2144$, $V_8(0) = 4.483 \times 10^5$, $E_8 = 759.3$, $K(0) = 629.9$. The rest of the parameters are as indicated in Table 3.



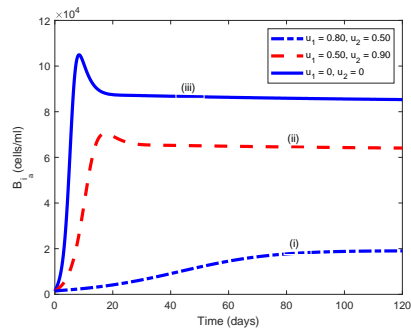
(a) Uninfected B cell dynamics



(b) Uninfected progenitor cell dynamics

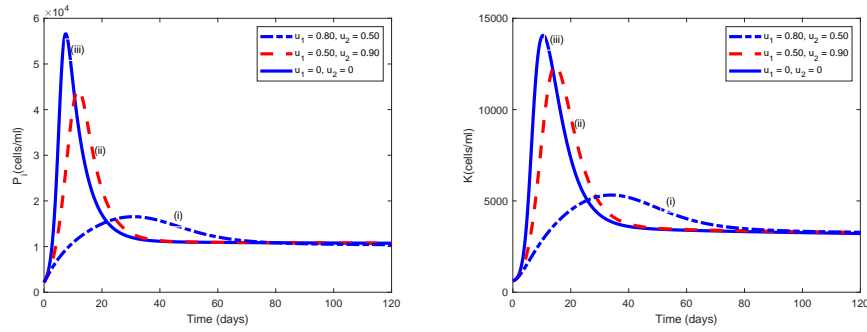


(c) Latently infected B cell dynamics



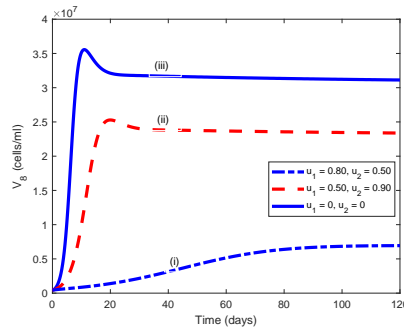
(d) Productively infected B cell dynamics

ics



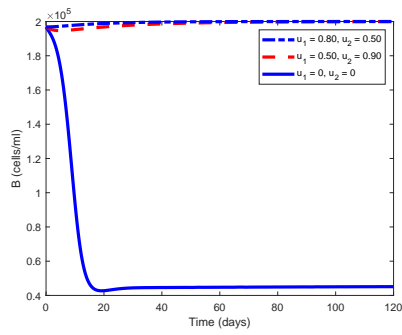
(e) Infected progenitor dynamics

(f) KS cell dynamics

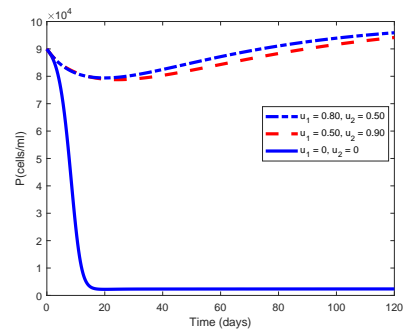


(g) HHV-8 virion dynamics

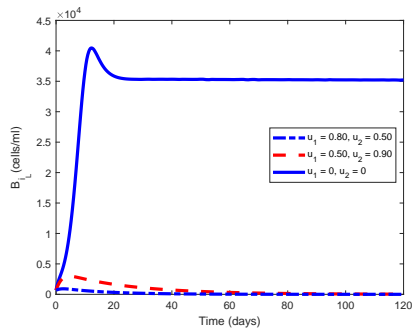
Figure 5.7: Population Dynamics for the uncontrolled and controlled systems. In this figure we have used: $\rho = 0.10$. We have set $u_1 = 0, 0.50, 0.80$ and $u_2 = 0, 0.50, 0.90$. The initial values in our simulation are $B(0) = 1.968 \times 10^5$, $P(0) = 8.994 \times 10^4$, $B_{i_L}(0) = 678.9$, $B_{i_a}(0) = 1418$, $P_i(0) = 2144$, $V_8(0) = 4.483 \times 10^5$, $E_8 = 759.3$, $K(0) = 629.9$. The rest of the parameters are as indicated in Table 3.



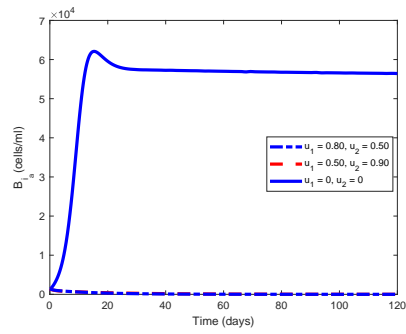
(a) Uninfected B cell dynamics



(b) Uninfected progenitor cell dynamics

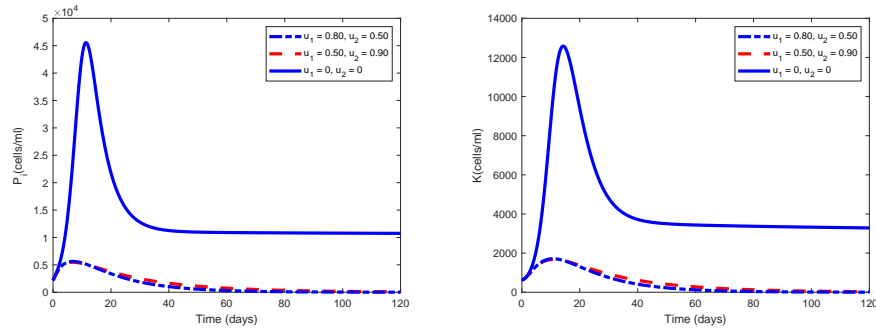


(c) Latently infected B cell dynamics



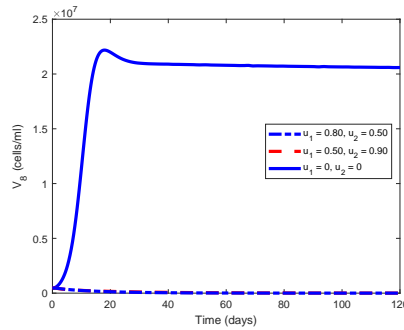
(d) Productively infected B cell dynamics

ics



(e) Infected progenitor dynamics

(f) KS cell dynamics



(g) HHV-8 virion dynamics

Figure 5.8: Population Dynamics for the uncontrolled and controlled systems. In this figure we have used: $\rho = 0.90$. We have set $u_1 = 0, 0.50, 0.80$ and $u_2 = 0, 0.50, 0.90$. The initial values in our simulation are $B(0) = 1.968 \times 10^5$, $P(0) = 8.994 \times 10^4$, $B_{i_L}(0) = 678.9$, $B_{i_a}(0) = 1418$, $P_i(0) = 2144$, $V_8(0) = 4.483 \times 10^5$, $E_8 = 759.3$, $K(0) = 629.9$. The rest of the parameters are as indicated in Table 3.

Chapter 6

Discussion, Future Work and Recommendation

6.1 Discussion

In this chapter, we present main conclusions, interpretations and significance of our results. Understanding and controlling the HIV-1 and HHV-8 infections is critical to resolving a huge burden on health and social care settings and systems especially in developing countries. The models developed in this thesis would have been theoretical and speculative a few years back but now we know there are efforts towards finding a cure for non-AIDS related KS. Our models can be used to find optimal efficacy levels of treatment.

Currently, there is no treatment available to eradicate HHV-8 infection of B cells and

the erroneously infected progenitor cells. The purpose of our work was to give insight into the efficacy of the anti-KS therapies required to slow down disease progression and hopefully KS development, the most common neoplasm associated with AIDS. It is not surprising that most therapies at the moment emphasize the effective administration of HAART in AIDS-KS patients. This may be due, in part, to the fact that AIDS affects most countries globally whereas KS affects mostly the poor nations.

The two models presented in this thesis have presented how viral infections develop during the two stages of the immune response, the innate and adaptive stages. This approach is aimed at finding early therapies to stop the infection from developing during the innate phase. We have also presented detailed analysis and explored how immune response can be supported and at what levels of drug efficacy during the adaptive phase.

Some evidence suggests that immune activation is a requisite for development of Classic KS [29, 65]. Hence, we included the effect of the immune response in the model with innate mechanism and showed that *in silico* treatment of Classic KS can significantly reduce HHV-8 infection. We determined a critical value of the efficacy threshold for the innate immune response below which KS burden is diminished even if $\mathcal{R}_0 > 1$. This is completely novel to the best of our knowledge and has important implications, since therapies involving cytokines such as IL-2 [92] may have adverse side effects. Because it is not known how long the innate response for HIV-1 and

HHV-8 co-infection lasts, this study is not able to suggest the dosage and frequency of treatment regimen. It is hoped a clinical study can explore the potential suggested by this study.

About 30% of Classic KS patients develop a second malignancy like non-Hodgkin lymphoma [26], hence, an early diagnosis that may prevent second malignancies is essential. The model with innate mechanism demonstrated the potential for controlling HHV-8 infection and consequently, also HIV-1 and HHV-8 co-infection. Currently, there are early HIV-1 tests capable of revealing that an individual has been in contact with someone infected with HIV-1 [42].

The strategy described in this study can be used to prevent HIV-1 infections before they develop for example in rape victims who are treated with antiretroviral drugs for 28 days immediately after the crime [78].

In the absence of any treatment the long term prognosis of AIDS-KS is poor. This is shown by Figures 4.6 – 4.7 of the model with adaptive mechanism. However, if cART (e.g. HAART plus KS therapy) is administered at optimal levels, both HIV-1 and HHV-8 infection can decline to undetectable levels (Figures 4.10 – 4.11). The simulations indicate that HAART at suboptimal levels cannot eradicate the viral load, a scenario which can possibly lead to the emergence of drug-resistant mutations [4]. For cART, when the efficacy of a potential fusion inhibitor or reverse transcriptase

inhibitor is kept at optimal level, a very low level efficacy for KS therapy is sufficient to control the HHV-8 infection. This result has important implications for patients with more than one underlying conditions as it helps them to take fewer drugs, a strategy which can protect their kidneys [39].

The implications of our study are two-fold. First, early intervention in the form of KS-therapy can control HHV-8 infection from developing into KS and possibly also slow HIV-1 infection to develop into AIDS. Second, optimal control of HIV-1 infection using HAART is an integral part of a successful AIDS-KS therapy and should be used in combination with low-level KS therapy. These recommendations have the potential to impact the therapeutic goal in KS, by focusing on short term control and thus, aiding long term remission.

The innate immune response model has revealed that externally administered cytokine drugs can reduce the chances of Kaposi Sarcoma developing. This is supported in part by a study by [93, 99] involving IL-2 and IL-12 which showed that administration of cytokines can prevent or delay the development of infection. However, to the best of our knowledge there are no clinical studies that have determined the safe levels of these cytokine drugs that can be taken.

The model system (4.30) – (4.39) shows that treatment with sub-optimal drugs can lead to endemic infections and possibly to drug resistance. By including dual therapy

such as chemotherapy with cytokine based drugs together with HAART treatment, the adaptive phase has revealed that treatment at optimal and super-optimal levels can clear the KS infection. Based on this result, we recommend HAART treatment for KS infection to be enhanced with chemotherapy treatment.

In our future works we intend to address the problem of incomplete eradication of HIV-1 in patients currently accessing HAART [56]. It is a well known fact that, in spite of having the viremia brought down below the level of detection, a complete eradication of HIV-1 is still not possible. This phenomenon is attributed to the presence of certain reservoirs in which the HIV-1 virus can remain in latency, and it is known that latently infected $CD4^+$ T cells are never affected by HAART due to non expression of viral proteins [91]. Can innovators develop a device that can detect latently infected $CD4^+$ T and B cells?

Currently there is no definite cure for non-AIDS related KS and the purpose of anti-viral therapies is aimed at slowing down KS progression without targeting the virus as an etiological agent. Unlike traditional therapeutic approaches that may have adverse side effects, novel anti-viral therapies are now being studied and already they are showing promise with regard to relative drug safety. The therapies include, but are not limited to, the use of chemical inhibitors that block virus endocytosis and lytic reactivation of HHV-8 [16, 33].

6.2 Future Work

In all our models we have assumed that proliferation of different effector cell populations continues indefinitely and that these cells remain potent for all future time. This may not be realistic in the case of HIV-1 infection. The continual antigen stimulation as a result of the infection should lead to effector cell dysfunctionality [28]. As an extension of the AIDS-KS model with adaptive immune response we intend to explore the role of CD8⁺ T cell dysfunctionality and how this phenomenon worsens the prognosis of KS.

The cellular-mediated immune response is regarded as the most powerful weapon of fighting any viral infection. As a future assignment we intend to explore the potency of adoptive cellular immunotherapy in the fight against both non-AIDS-related KS (NAKS) and AIDS-related KS (AKS).

6.3 Recommendation

We recommend the exploration of the role of reactivation of lytic replication in the case of AKS and determination of efficacy levels for drugs that can block the entry of HHV-8 into the susceptible B and progenitor cells and reactivation of lytic replication of HHV-8.

Chapter 7

Appendix

AIDS-KS MODEL

Lemma 7.0.1 *The lemma is based on the work of Castillo-Chavez et al [14]. Consider the system*

$$\begin{aligned}\frac{d\mathbf{X}}{dt} &= F((\mathbf{X}, \mathbf{I})), \\ \frac{d\mathbf{I}}{dt} &= G((\mathbf{X}, \mathbf{I})), G(\mathbf{X}, \mathbf{0}) = 0,\end{aligned}\tag{7.1}$$

where $\mathbf{X} \in \mathbb{R}^m$ denotes the components of the uninfected states, $\mathbf{I} \in \mathbb{R}^n$ denotes the components of the infected states and $\mathbf{U}_0 = (\mathbf{X}^*, \mathbf{0})$ denotes the disease-free equilibrium of (7.1). Assume the conditions (H1) and (H2) below are satisfied

(H1) For $\frac{d\mathbf{X}}{dt} = F(\mathbf{X}, \mathbf{0})$, \mathbf{X}^* is globally asymptotically stable (g.a.s) ,

(H2) $G(\mathbf{X}, \mathbf{I}) = \mathbf{A}\mathbf{I} - \hat{G}(\mathbf{X}, \mathbf{I})$, $\hat{G}(\mathbf{X}, \mathbf{I}) \geq \mathbf{0}$ for $(\mathbf{X}, \mathbf{I}) \in \Omega$,

where $\mathbf{A} = \mathbf{D}_1 \mathbf{G}(\mathbf{X}^*, \mathbf{0})$ is an M -matrix (the off diagonal elements of A are nonnegative) and Ω is the region where the model makes biological sense. Then \mathbf{U}_0 is globally asymptotically stable.

Proof 7.0.2 (Lemma 4.3.1(b)) Let $y_1(t) = x_1(t) + x_5(t)$ and $y_2(t) = x_2(t) + x_6(t)$ denote the total sub - populations of the $CD4^+$ T cells and B cells at time t , respectively, where $x_i(t) \geq 0$ by Lemma 1(a).

Adding equations (4.15) and (4.19), and then (4.16) and (4.20) we get.

$$\begin{aligned} \frac{dy_j(t)}{dt} &\leq \Pi_j \left(1 + 2\alpha_5 \frac{x_9}{x_9 + S_9} + 2\alpha_6 \frac{x_{10}}{x_{10} + S_{10}} \right) - \mu_j x_j - \mu_{j+4} x_{j+4}, \quad j = 1, 2. \\ &\leq \underbrace{\Pi_j (1 + 2(\alpha_5 + \alpha_6))}_{M_j} - \hat{\mu}_j y_j(t), \quad \text{where } \hat{\mu}_j = \min\{\mu_j, \mu_{j+4}\} \end{aligned}$$

It is easy to show that as $t \rightarrow \infty$, $y_j(t) \leq \frac{M_j}{\hat{\mu}_j}$, $j = 1, 2$. Equations (4.23) and (4.24)

can be represented by

$$\frac{dx_j(t)}{dt} = N_j \mu_{j-4} x_{j-4} - \mu_j x_j \leq N_j \mu_{j-4} \frac{M_{j-8}}{\hat{\mu}_{j-8}} - \mu_j x_j \quad j = 9, 10.$$

It is easy to show that

$$\limsup_{t \rightarrow \infty} x_j(t) \leq \frac{N_j \mu_{j-4} M_{j-8}}{\mu_j \hat{\mu}_{j-8}}, j = 9, 10,$$

$$\limsup_{t \rightarrow \infty} Z(t) \leq \frac{\Pi_3(1 + c_{10}) + \Pi_4(1 + c_9)}{\xi}, \text{ where } \xi = \min\{\mu_3, \mu_4\} \text{ and } Z(t) = x_3(t) + x_4(t), \}$$

$$\limsup_{t \rightarrow \infty} x_7(t) \leq \frac{\mu_6 r_7 N_{10} M_2}{\hat{\mu}_2 \mu_7 \mu_{10}} \left(1 - \frac{\mu_6 N_{10} M_2}{\hat{\mu}_2 \mu_{10} x_{10_{max}}} \right)$$

$$\limsup_{t \rightarrow \infty} x_8(t) \leq \frac{\mu_6 \mu_7 r_7 N_{10} M_2}{\hat{\mu}_2 \mu_8 \mu_9 \mu_{10}} \left(1 - \frac{\mu_6 N_{10} M_2}{\hat{\mu}_2 \mu_{10} x_{10_{max}}} \right)$$

Non-infected States:

$$\dot{x}_1 = \Pi_1 \left(1 + \frac{\alpha_5 x_9}{x_9 + S_9} + \frac{\alpha_6 x_{10}}{x_{10} + S_{10}} \right) - \mu_1 x_1 - \beta_1 x_1 x_9, \quad (7.2)$$

$$\dot{x}_2 = \Pi_2 \left(1 + \frac{\alpha_5 x_9}{x_9 + S_9} + \frac{\alpha_6 x_{10}}{x_{10} + S_{10}} \right) - \mu_2 x_2 - \beta_2 x_2 x_{10}, \quad (7.3)$$

$$\dot{x}_3 = \Pi_3 + \frac{c_{10} \Pi_3 x_{10}}{x_{10} + f_{10}} - \mu_3 x_3, \quad (7.4)$$

$$\dot{x}_4 = \Pi_4 + \frac{c_9 \Pi_4 x_9}{x_9 + f_9} - \mu_4 x_4, \quad (7.5)$$

Infected States:

$$\dot{x}_5 = \Pi_1 \left(\frac{\alpha_5 x_9}{x_9 + S_9} + \frac{\alpha_6 x_{10}}{x_{10} + S_{10}} \right) + \beta_1 x_1 x_9 - m_4 x_4 x_5 - \mu_5 x_5, \quad (7.6)$$

$$\dot{x}_6 = \Pi_2 \left(\frac{\alpha_5 x_9}{x_9 + S_9} + \frac{\alpha_6 x_{10}}{x_{10} + S_{10}} \right) + \beta_2 x_2 x_{10} - m_3 x_3 x_6 - \mu_6 x_6, \quad (7.7)$$

$$\dot{x}_7 = r_7 x_{10} \left(1 - \frac{x_{10}}{x_{10max}} \right) - \mu_7 x_7 - d_3 x_3 x_7, \quad (7.8)$$

$$\dot{x}_8 = \mu_7 x_7 - \mu_8 x_8, \quad (7.9)$$

$$\dot{x}_9 = N_9 \mu_5 x_5 - \mu_9 x_9, \quad (7.10)$$

$$\dot{x}_{10} = N_{10} \mu_6 x_6 - \mu_{10} x_{10}, \quad (7.11)$$

$$\mathcal{R}_{V_1} = \frac{N_9 \Pi_1 (\alpha_5 \mu_1 + \beta_1 S_9)}{\mu_1 \mu_9 S_9} \cdot \frac{\mu_4 \mu_5}{(\mu_4 \mu_5 + m_4 \Pi_4)} < \frac{N_9 \Pi_1 (\alpha_5 \mu_1 + \beta_1 S_9)}{\mu_1 \mu_9 S_9} = \mathcal{R}_1. \quad (7.12)$$

$$\mathcal{R}_{V_8} = \frac{N_{10} \Pi_2 (\alpha_6 \mu_2 + \beta_2 S_{10})}{\mu_2 \mu_{10} S_{10}} \cdot \frac{\mu_3 \mu_6}{(\mu_3 \mu_6 + m_3 \Pi_3)} < \frac{N_{10} \Pi_2 (\alpha_6 \mu_2 + \beta_2 S_{10})}{\mu_2 \mu_{10} S_{10}} = \mathcal{R}_8. \quad (7.13)$$

From (7.13) we can deduce that

- \mathcal{R}_{V_i} , $i = 1, 8$ are the reproduction numbers when virus i specific effector cells are active but their effect varies from being weak to perfect as m_j , $j = 3, 4$, increases.

- \mathcal{R}_i , $i = 1, 8$ are the reproduction numbers when virus i specific effector cells are dysfunctional.

1. Let $x = (x_5, x_6, x_7, x_8, x_9, x_{10})^T$, $y = (x_1, x_2, x_3, x_4)^T$. The system (4.15) – (4.24) can be written as

$$\begin{aligned}\frac{dx}{dt} &= \mathcal{F}(x, y) - \mathcal{V}(x, y), \\ \frac{dy}{dt} &= g_j(x, y)\end{aligned}$$

The matrices for new infections and other class transition, respectively given by F

and V , are

$$\begin{aligned}
 F &= \begin{pmatrix} 0 & 0 & 0 & 0 & \frac{\Pi_1 K_1}{\mu_1 S_9} & \frac{\alpha_6 \Pi_1}{S_{10}} \\ 0 & 0 & 0 & 0 & \frac{\alpha_5 \Pi_2}{S_9} & \frac{\Pi_2 K_2}{\mu_2 S_{10}} \\ 0 & 0 & 0 & 0 & 0 & r_7 \\ 0 & 0 & \mu_7 & 0 & 0 & 0 \\ 0 & 0 & 0 & 0 & 0 & 0 \\ 0 & 0 & 0 & 0 & 0 & 0 \end{pmatrix}, \quad V = \begin{pmatrix} \frac{a_{11}}{\mu_4} & 0 & 0 & 0 & 0 & 0 \\ 0 & \frac{a_{22}}{\mu_3} & 0 & 0 & 0 & 0 \\ 0 & 0 & \frac{a_{33}}{\mu_3} & 0 & 0 & 0 \\ 0 & 0 & 0 & \mu_8 & 0 & 0 \\ -N_9 \mu_5 & 0 & 0 & 0 & \mu_9 & 0 \\ 0 & -N_{10} \mu_6 & 0 & 0 & 0 & \mu_{10} \end{pmatrix} \\
 FV^{-1} &= \begin{pmatrix} \frac{\mu_4 \mu_5 N_9 \Pi_1 K_1}{\mu_1 \mu_9 a_{11} S_9} & \frac{\mu_3 \mu_6 \alpha_6 N_{10} \Pi_1}{\mu_{10} a_{22} S_{10}} & 0 & 0 & \frac{\Pi_1 K_1}{\mu_1 \mu_9 S_9} & \frac{\alpha_6 \Pi_1}{\mu_{10} S_{10}} \\ \frac{\mu_4 \mu_5 \alpha_5 N_9 \Pi_2}{\mu_9 a_{11} S_9} & \frac{\mu_3 \mu_6 N_{10} \Pi_2 K_2}{\mu_2 \mu_{10} a_{22} S_{10}} & 0 & 0 & \frac{\alpha_5 \Pi_2}{\mu_9 S_9} & \frac{\Pi_2 K_2}{\mu_2 \mu_{10} S_{10}} \\ 0 & \frac{\mu_3 \mu_6 r_7 N_{10}}{\mu_{10} a_{22}} & 0 & 0 & 0 & \frac{r_7}{\mu_{10}} \\ 0 & 0 & \frac{\mu_3 \mu_7}{a_{33}} & 0 & 0 & 0 \\ 0 & 0 & 0 & 0 & 0 & 0 \\ 0 & 0 & 0 & 0 & 0 & 0 \end{pmatrix} \\
 K_1 &= \alpha_5 \mu_1 + \beta_1 S_9, \quad K_2 = \alpha_6 \mu_2 + \beta_2 S_{10}, \quad a_{11} = \mu_4 \mu_5 + m_4 \Pi_4, \quad a_{22} = \mu_3 \mu_6 + m_3 \Pi_3, \\
 a_{33} &= \mu_3 \mu_7 + d_3 \Pi_3
 \end{aligned}$$

(7.14)

Variable	Initial value	Source
$x_1(0)$	$10^5 \text{ cell ml}^{-1}$	[80]
$x_2(0)$	$10^4 \text{ cell ml}^{-1}$	Estimated
$x_3(0)$	50 cell ml^{-1}	Estimated
$x_4(0)$	$10^4 \text{ cell ml}^{-1}$	Estimated
$x_5(0)$	300 cell ml^{-1}	Estimated
$x_6(0)$	20 cell ml^{-1}	Estimated
$x_7(0)$	50 cell ml^{-1}	
$x_8(0)$	18 cell ml^{-1}	
$x_9(0)$	$100 \text{ virion ml}^{-1}$	
$x_{10}(0)$	$40 \text{ virion ml}^{-1}$	

Parameter	Value	Source
α_5	0.013	Estimated
α_6	0.045	Estimated
β_1	$2.4 \times 10^{-8} \text{ ml virion}^{-1} \text{ day}^{-1}$	[95]
β_2	$1.5 \times 10^{-7} \text{ ml virion}^{-1} \text{ day}^{-1}$	[95]
Π_1	$10^4 \text{ cell ml}^{-1} \text{ day}^{-1}$	[95]

Π_2	$48000 \text{ cell ml}^{-1} \text{ day}^{-1}$	[95]
Π_3	$5 \times 10^3 \text{ cell ml}^{-1} \text{ day}^{-1}$	Estimated
Π_4	$2 \times 10^4 \text{ cell ml}^{-1} \text{ day}^{-1}$	
S_9	$3 \times 10^5 \text{ virions ml}^{-1}$	Estimated
S_{10}	$2 \times 10^5 \text{ virions ml}^{-1}$	Estimated
μ_1	0.01 day^{-1}	[95]
μ_2	0.24 day^{-1}	[95]
μ_3	0.1 day^{-1}	[95]
μ_4	0.1 day^{-1}	[95]
μ_5	0.24 day^{-1}	[95]
μ_6	0.33 day^{-1}	[95]
μ_7	0.1 day^{-1}	[95]
μ_8	0.21 day^{-1}	[95]
μ_9	3 day^{-1}	[95]
μ_{10}	0.57 day^{-1}	[95]
N_9	$1000 \text{ virions cell}^{-1}$	[95]
N_{10}	$700 \text{ virions cell}^{-1}$	[95]

m_3	1.08×10^{-4} ml cell ⁻¹ day ⁻¹	Estimated
m_4	2×10^{-7} ml cell ⁻¹ day ⁻¹	Estimated
c_9	0.03	[95]
c_{10}	0.047	[95]
d_3	5×10^{-4} ml cell ⁻¹ day ⁻¹	Estimated
r_7	0.33 cells virion ⁻¹ day ⁻¹	[95]
f_9	3×10^5 virions ml ⁻¹	Estimated
f_{10}	2×10^5 virions ml ⁻¹	Estimated
$x_{10_{max}}$	8×10^9	Estimated

Table 7.4: Estimation of parameters.

Non-AIDS KS MODEL

(A)

$$\begin{cases} \frac{dX}{dt} = F(X, Y), \\ \frac{dY}{dt} = G(X, Y), \quad G(X, 0) = \mathbf{0}. \end{cases} \quad (7.15)$$

where $X \in \mathbb{R}^m$ denotes the number of uninfected individuals and \mathbb{R}^n denotes the number of infected individuals or components including latent, infectious

etc. In our case, the two new classes for the model system are represented as follows:

$$\begin{cases} X = (x_1, x_2, x_3, x_4), \\ Y = (x_5, x_6, x_7, x_8, x_9). \end{cases} \quad (7.16)$$

The conditions (H1) and (H2) below must be met for our model to be globally asymptotically stable (g.a.s).

$$\begin{cases} (H1) \text{ For } \frac{dX}{dt} = F(X, 0), \quad X^* \text{ is g.a.s.} \\ (H2) \quad G(X, Z) = AY - \hat{G}(X, Y), \quad \hat{G}(X, Y) \geq 0 \quad \forall (X, Y) \in \Omega, \end{cases} \quad (7.17)$$

where $A = D_Y G(X, 0)$ is an M- matrix (that is, the off diagonal elements of A are nonnegative) and Ω is the region where the model makes biological sense.

(B) Next, we differentiate the Hamiltonian, H , with respect to u_i , $i = 1, 2$ and set the result to zero. Solving the resulting equations yields

$$\hat{u}_1 = \frac{\beta_1 \left(-\lambda_{x_1} + \lambda_{x_5} \rho + \lambda_{x_6} (1 - \rho) \right) x_1 x_9}{B_1}, \quad (7.18)$$

$$\hat{u}_2 = \frac{\gamma (\lambda_{x_6} - \lambda_{x_5}) x_5}{B_2}. \quad (7.19)$$

(C) Recalling that a function f is convex on a set D_f if for all $X, Y \in D_f$, we have

$$f(\alpha X + (1 - \alpha)Y) \leq \alpha f(X) + (1 - \alpha)f(Y) \text{ with } \alpha \in [0, 1].$$

Let

$$\begin{aligned} X &= (x_5, x_6, u_1, u_2) \text{ and } Y = (x_5^{(1)}, x_6^{(1)}, u_1^{(1)}, u_2^{(1)}) \text{ and} \\ L(X) &= A_1 x_5 + A_2 x_6 + \frac{1}{2} B_1 u_1^2 + \frac{1}{2} B_2 u_2^2, \end{aligned} \quad (7.20)$$

Then,

$$\begin{aligned}\alpha X + (1 - \alpha)Y &= \left(\alpha x_5 + (1 - \alpha)x_5^{(1)}, \alpha x_6 + (1 - \alpha)x_6^{(1)}, \alpha u_1 \right. \\ &\quad \left. + (1 - \alpha)u_1^{(1)}, \alpha u_2 + (1 - \alpha)u_2^{(1)} \right),\end{aligned}$$

Hence, Eqn (7.20) gives

$$\begin{aligned}L(\alpha X + (1 - \alpha)Y) &= A_1(\alpha x_5 + (1 - \alpha)x_5^{(1)}) + A_2(\alpha x_6 + (1 - \alpha)x_6^{(1)}) \\ &\quad + \frac{1}{2}B_1(\alpha u_1 + (1 - \alpha)u_1^{(1)}) \\ &\quad + \frac{1}{2}B_2(\alpha u_2 + (1 - \alpha)u_2^{(1)}) \\ &\leq \alpha \left(A_1 x_5 + A_2 x_6 + \frac{1}{2}B_1 u_1 + \frac{1}{2}B_2 u_2 \right) + (1 - \alpha) \left(A_1 x_5^{(1)} + A_2 x_6^{(1)} \right. \\ &\quad \left. + \frac{1}{2}B_1 u_1^{(1)} + \frac{1}{2}B_2 u_2^{(1)} \right) \\ &= \alpha L(X) + (1 - \alpha)L(Y)\end{aligned}\tag{7.21}$$

(D) By definition, each f_i , $i = 1, 2, 3, \dots, 9$ of system (5.1) – (5.9) is continuous where f_i is the i^{th} function representing the right hand side of the system. f_i can be rewritten as a linear function of $u = (u_1, u_2)$ with coefficients depending on time and state. Moreover, all the state and control variables, x_i , $i = 1, 2, 3, \dots, 9$ and u_j , $j = 1, 2$ are bounded on $[0, T_f]$. In particular, the control system (5.1) – (5.9) with initial conditions x_{i0} , of the respective variables can be written in the form:

$$\dot{X} = AX + F(X),\tag{7.22}$$

$$F(X) = \begin{pmatrix} \Pi_1 - (1 - u_1(t))\beta_1 x_1 x_9 \\ \Pi_2 - \beta_2 x_2 x_9 \\ \Pi_3 + r_3 x_3 x_6 \\ \frac{r_4 x_6}{1 + m x_6} \\ (1 - u_1(t))\rho\beta_1 x_1 x_9 \\ (1 - \rho)(1 - u_1(t))\beta_1 x_1 x_9 - \alpha_6 x_3 x_6 \\ \beta_2 x_2 x_9 - \alpha_7 x_3 x_7 \\ -\alpha_8 x_3 x_8 \\ \frac{N_9 \mu_6 x_6}{1 + \theta_4 x_4} \end{pmatrix} \quad (7.25)$$

The system (7.22) is a non-linear system with a bounded coefficient.

Let

$$B(X) = A(X) + F(X), \quad (7.26)$$

Following a similar technique in [69], it follows that the function $B(X)$ is uniformly Lipschitz continuous.

From the definition of the controls u_1 and u_2 and the restrictions on the non-negativeness of the state variables, then the solutions of the system (7.22) exists.

(E) To show that the set U is convex, let $u_i, u_j \in U$ with $u_i = (u_i^{(1)}, u_i^{(2)})$ and

$u_j = (u_j^{(1)}, u_j^{(2)})$. Suppose $\alpha \in [0, 1]$. Then,

$$\begin{aligned} \alpha u_i + (1 - \alpha)u_j &= \alpha(u_i^{(1)}, u_i^{(2)}) + (1 - \alpha)(u_j^{(1)}, u_j^{(2)}) \\ &= (\alpha u_i^{(1)} + (1 - \alpha)u_j^{(1)}, \alpha u_i^{(2)} + (1 - \alpha)u_j^{(2)}) \in U. \end{aligned}$$

Hence, U is convex.

To establish that U is closed, it suffices to show that U contains any convex combination

$$y = \sum_{i=1}^n \alpha_i u_i \tag{7.27}$$

of vectors $u_i \in U$. We establish the result via mathematical induction on n . For $n = 1$, it is evident. The only one term convex combinations are of the form $1 \cdot u_1 = u_1 \in U$.

We suppose any convex combination of $n - 1$ vectors for $n \geq 2$, taken from U is an element of U , we proceed to verify that the statement holds for any convex combinations of n vectors in U . Let Eqn. (7.27) be such a combination. We suppose that $1 > \alpha_n$, otherwise there is nothing to prove (note that when $\alpha_n = 1$, then the other α_i 's should vanish, because each α is nonnegative and their sum is unit, and we thus have $y = y_n \in U$).

Assuming $\alpha_n < 1$, we can write

$$y = (1 - \alpha_n) \left\{ \sum_{i=1}^{n-1} \frac{\alpha_i}{1 - \alpha_n} y_i \right\} + \alpha_n y_n,$$

the sum in the parenthesis is clearly a convex combination of $n - 1$ points from U and thus, by the inductive assumption, there is a point, let it be called z ,

from U , we have

$$y = (1 - \alpha_n)z + \alpha_n y_n,$$

(7.28)

with z and $y_n \in U$, and $y \in U$ by the definition of a convex set U .

Parameter	Range	Units
K_1	0.11 – 0.39	day ⁻¹
K_2	0.0154 – 0.0193	day ⁻¹
K_3	0.013 – 0.054	day ⁻¹
θ_{x_3}	100 – 500	cell mm ⁻³
θ_{x_5}	0.002 – 0.069	
x_{3max}	200 – 650	cell mm ⁻³
x_{4max}	$10^4 – 5.1 \times 10^5$	virions mm ⁻³
μ_{x_1}	0.1 – 0.3	day ⁻¹
μ_{x_2}	0.001 – 0.067	ml day ⁻¹
μ_{x_3}	0.2 – 0.5	day ⁻¹
μ_{x_4}	0.45 – 0.65	day ⁻¹
N_{x_4}	100 – 1000	virions cell ⁻¹

Table 7.1: Range of parameters for sensitivity analysis for the innate model.

Parameter	Range	Units
N_9	100 – 1000	virions cell ⁻¹
N_{10}	100 – 1000	virions cell ⁻¹
Π_1	$10^3 - 10^4$	cell ml ⁻¹ day ⁻¹
Π_2	$70 \times 10^3 - 4.275 \times 10^5$	cell ml ⁻¹ day ⁻¹
Π_3	$10^2 - 10^3$	cell ml ⁻¹ day ⁻¹
Π_4	$10^4 - 3 \times 10^4$	cell ml ⁻¹ day ⁻¹
r_7	0.045 – 0.055	cells virion ⁻¹ day ⁻¹
d_3	$5.47 \times 10^{-5} - 1.09 \times 10^{-4}$	ml cell ⁻¹ day ⁻¹
m_3	$5.47 \times 10^{-5} - 1.09 \times 10^{-4}$	ml cell ⁻¹ day ⁻¹
m_4	$10^{-7} - 10^{-5}$	ml cell ⁻¹ day ⁻¹
α_5	$10^{-2} - 1.5 \times 10^{-4}$	
α_6	$1.4 \times 10^{-2} - 5.5 \times 10^{-2}$	
S_9	$2 \times 10^5 - 5 \times 10^5$	virions ml ⁻¹
S_{10}	$10^5 - 3 \times 10^5$	virions ml ⁻¹
β_1	$2.4 \times 10^{-8} - 2.5 \times 10^{-7}$	ml virion ⁻¹ day ⁻¹
β_2	$4.75 \times 10^{-9} - 4.75 \times 10^{-7}$	ml virion ⁻¹ day ⁻¹
μ_9	2 – 5	day ⁻¹
μ_{10}	0.45 – 0.65	day ⁻¹

Table 7.2: Range of parameters for sensitivity analysis for the adaptive model.

Bibliography

- [1] S.S.Ahrabi and A. Momenzadeh. Metaheuristics and Pontryagins minimum principle for optimal therapeutic protocols in cancer immunotherapy: a case study and methods comparison. *Journal of Mathematical Biology*, **81**(2):691-723,2020.
- [2] K.K. Anaje and Y. Yuan. Reactivation and Lytic Replication of Kaposi's sarcoma-Associated Herpesvirus: An Update. *Front. Macrobiol*, **8**:613,2017.
- [3] K. Antman, Y. Chang. Kaposi's sarcoma. *N Engl J Med*, **342**:1027-1038,2000.
- [4] M. Arnedo-Valero, F. García, C. Gil, T. Guila, E. Fumero, P. Castro, J. L. Blanco, J. M. Miró, T. Pumarola, J. M. Gatell. Risk of Selecting De Novo Drug-Resistance Mutations during Structured Treatment Interruptions in Patients with Chronic HIV Infection. *Clinical Infectious Diseases*, **41**(6):883-890,2005.
- [5] G. Balaji. Recapitulation of acquired immuno deficiency syndrome associated Kaposi's sarcoma. *Indian J Sex Transm Dis AIDS*, **37**(2):115-122,2016. doi: 10.4103/2589-0557.192120.
- [6] S.Baral, R. Antia and N.M.Dixit. A dynamical motif comprising the interactions

- between antigens and CD8 T cells may underlie the outcomes of viral infections. *Proceedings of the National Academy of Sciences*, **116**(35):17393-17398,2019.
- [7] G. Beauclair, E. Naimo, T. Dubich, J. R'uckert, S. Koch, A. Dhingra, D. Wirth, T. F. Schulz. Targeting Kaposi's Sarcoma-Associated Herpesvirus ORF21 Tyrosine Kinase and Viral Lytic Reactivation by Tyrosine Kinase Inhibitors Approved for Clinical Use. *Journal of Virology*, **94**: e01791-19,2020.
- [8] A.P. Bhatt and B. Damania . AKTivation of PI3K/AKT/mTOR signaling pathway by KSHV. *Front. Immunol*, **4**:401,2013. doi: 10.3389/fimmu.2012.00401
- [9] F. Bihl, A Mosam, L.N. Henry, J.V. Chisholm, S. Dollard, D.T. Scadden, C. Brander. Kaposi's sarcoma-associated herpesvirus-specific immune reconstruction and antiviral effect of combined HAART/chemotherapy in HIV clade C-infected individuals with Kaposi's sarcoma. *AIDS*, **21**(10):1245-1252,2007.
- [10] C. Boshoff, R. Weiss. AIDS-related malignancies. *Nature Reviews Cancer*, **2**:373-382,2002.
- [11] J.J. Brooks. Kaposi's sarcoma: A reversible hyperplasia. *Lancet*, **2**:1309-1311,1986.
- [12] L.M.Butler, D.H. Osmond,A.G. Jones, et al. Use of saliva as a lubricant in anal sexual practices among homosexual men. *J Acquir Immune Defic Syndr*, **50**:162167,2009. [PubMed: 19131893]

- [13] J.W.Cain and A.M.Reynolds. Ordinary and Partial Differential Equations. An Introduction to Dynamical Systems, Creative Commons. Virginia Commonwealth University, Richmond, 2010.
- [14] C. Castillo-Chavez, et al. On the computation of \mathcal{R}_0 and its role on global stability, in Mathematical approaches for emerging and reemerging infectious diseases: an introduction (Minneapolis, MN, 1999). *Math. Appl., Springer, New York*, **125**: 229-250,2002.
- [15] Y. Chang, E. Cesarman, MS Pessin, F. Lee, J. Culpepper, DM. Knowles, PS Moore. Identification of herpesvirus-like DNA sequences in AIDS-associated Kaposi's sarcoma. *Science*, **266**(5192): 1865-1869,1994.
- [16] J. Chen, et al. Celecoxib Inhibits the Lytic Activation of Kaposi's Sarcoma-Associated Herpesvirus through Down-Regulation of RTA Expression by Inhibiting the Activation of p38 MAPK. *Viruses*, **7**:2268-2287,2015. doi: 10.3390/v7052268.
- [17] M. Dedicoat and R. Newton. Review of the distribution of Kaposi's sarcoma-associated herpesvirus (KSHV) in Africa in relation to the incidence of Kaposi's sarcoma. *British journal of cancer*, **88**(1):1-3,2003.
- [18] O. Diekmann, J.A.P. Heesterbeek, J.A.J. Metz. On the definition and the computation of the basic reproduction ratio \mathcal{R}_0 in models for infectious diseases in heterogeneous populations. *J. Math. Biol.*, **28**:365-382,1990.

- [19] J.J. Dliveira and F.O. Torres. Kaposi's sarcoma in the Bantu of Mozambique. *Cancer*, **30**: 553-561, 1972.
- [20] J.L. Douglas, J.K. Gustin, A.V. Moses, B.J. Dezube, L. Pantanowitz, Kaposi sarcoma Pathogenesis: A triad of Viral Infection, Oncogenesis and Chronic Inflammation, *Translational Biomedicine*, **1**(2), 2010.
- [21] N.H. Dukers, N.Renwick,M. Prins, et al. Risk factors for human herpesvirus 8 seropositivity and seroconversion in a cohort of homosexual men. *Am J Epidemiol*, **151**:213224,2000. [PubMed: 10670545]
- [22] D.C. Edelman: Human herpesvirus-8-a novel human pathogen. *Virology journal* 2005, **2**(1):1-32,2005.
- [23] E.A. Engels, M.D. Sinclair, R.J. Biggar, D. Whitby, P. Ebbesen, J.J. Goedert, J.L. gastwirth. Latent class analysis of human herpesvirus 8 assay performance and infection prevalence in sub-Saharan Africa and Malta. *Int J Cancer*, **88**(6):1003-1008,2000.
- [24] E.A. Engels, R.M. Pfeiffer, J.J. Goedert, et al. Trends in cancer risk among people with AIDS in the United States 1980-2002. *AIDS*, **20**:16451654,2006.
- [25] E.A. Engels, R.J. Biggar,H.I. Hall, et al. Cancer risk in people infected with human immunodeficiency virus in the United States. *Int J Cancer*, **123**:187194,2008.

- [26] M.P.Escalon and F.B.Hagemeister. AIDS-related malignancies. Kantarjian HM, Wolff Ra, and Koller CA. MD Anderson Manual of Medical Oncology, McGraw-Hill, pp.903-910,2006.
- [27] L.Feller, C. Anagnostopoulos, N.H. Wood, M. Bouckaert, E.J. Raubenheimer and J. Lemmer. Human Immunodeficiency VirusAssociated Kaposi Sarcoma as an Immune Reconstitution Inflammatory Syndrome: A Literature Review and Case Report. *Journal of periodontology*, **79**(2): 362-368,2008.
- [28] C.Fenwick, V. Joo, P.Jacquier, A. Noto, R. Banga, M. Perreau and G.Pantaleo. T- cell exhaustion in HIV infection. *Immunological Reviews*, **292**(1):149-163,2019.
- [29] V. Fiorelli, R. Gendelman, M. C. Sirianni MC, et al. Gamma-Interferon produced by CD8+ T cells infiltrating Kaposi's sarcoma induces spindle cells with angiogenic phenotype and synergy with human immunodeficiency virus-1 Tat protein: an immune response to human herpesvirus-8 infection? *Blood*, **91**(3):956-67,1998.
- [30] W.H. Fleming, R.W. Rishel. Deterministic and Stochastic Optimal Control, Springer Verlag, New York, 1975.
- [31] K. E. Foreman, J. Friberg Jr., W.P. Kong et al., "Propagation of a human herpesvirus from AIDS-associated Kaposi sarcoma", *New England Journal of Medicine*, **336**(3):163-171, 1997.

- [32] K.E. Foreman. Kaposi's sarcoma: the role of HHV8 and HIV1 in pathogenesis. *Expert Reviews in Molecular Medicine*, **3**(9):1-17,2001.
- [33] R. Giovanna, R.R. Charles et al. Human herpesvirus infects and replicates in primary cultures of activated B lymphocytes through DC-SIGN. *J Virol.*, **82**(10):47934806,2008.doi: 10.1128/JVI.01587-07.
- [34] Global Cancer Observatory, International Agency for Research on Cancer. Population fact sheets. <http://gco.iarc.fr/today/fact-sheetspopulations> (accessed May 23, 2019).
- [35] J.J.Goedert: The epidemiology of acquired immunodeficiency syndrome malignancies. *Semin Oncol*, **27**(4):390-401,2000.
- [36] G.J. Gottlieb et al. A preliminary communication on extensively disseminated Kaposi's sarcoma in young homosexual men. *Am. J. Dermatopathol*, **3**: 111-114,1981.
- [37] L. Gradoville, J. Gerlach, E. Grogan, D. Shedd, S. Nikiforow, C. Metroka, et al. Kaposi sarcoma-associated herpesvirus open reading frame 50/Rta protein activates the entire lytic cycle in the HH-B2 primary effusion lymphoma cell line. *J. Virol*, **74**:62076212,2000. doi: 10.1128/JVI.74.13.6207-6212.2000
- [38] A.E. Grulich,M.T. van Leeuwen, M.O. Falster, et al. Incidence of cancers in people with HIV/AIDS compared with immunosuppressed transplant recipients: a meta-analysis. *Lancet*, **370**:5967,2007.

- [39] S.K.Gupta, J.A. Eustace, J.A. Winston, I.I. Boydston, T.S. Ahuja, R.A. Rodriguez, K.T. Tashima, M. Roland, N. Franceschini, F.J. Palella and J.L.Lennox. Guidelines for the management of chronic kidney disease in HIV-infected patients: recommendations of the HIV Medicine Association of the Infectious Diseases Society of America. *Clinical Infectious Diseases*, **40**(11):1559-1585,2005.
- [40] G.S. Hayward, Initiation of angiogenic Kaposi's sarcoma lesions. *Cancer Cell*, **3**(1),1-3,2003.
- [41] R.U.Hernandez-Ramirez, M.S. Shiels, R. Dubrow and E.A. Engels. Cancer risk in HIV-infected people in the USA from 1996 to 2012: a population-based, registry-linkage study. *The lancet HIV*, **4**(11)e495-e504,2017.
- [42] <http://hivinsite.ucsf.edu/inSite?page=basics-01-01>.
- [43] <http://i-base.info/guides/testing/what-is-the-window-period>.
- [44] H.L. Ioachim et al. Kaposi's sarcoma of internal organs. A multiparameter study of 86 cases. *Cancer*, **75**:1376-1885,1995. PubMed ID: 95188120.
- [45] R.G. Jenner. et al. Kaposi sarcoma-associated herpesvirus latent and lytic gene expression as revealed by DNA arrays. *J Virol*, **75**:891-902,2001. PubMed ID: 20578224.
- [46] A. Judd, R. Zangerle, G. Touloumi, et al. Comparison of Kaposi sarcoma risk

- in human immunodeficiency virus-positive adults across 5 continents: a multiregional multicohort study. *Clinical infectious diseases*, **65**(8): 13161326,2017.
- [47] J.C. Kamgang, G. Sallet. Computation of threshold conditions for epidemiological models and global stability of the disease-free equilibrium(DFE). *Mathematical Biosciences*, **213**:1-12,2008.
- [48] M. Kaposi. Idiopatisches multiples pigmentsarkom der haut [German]. *Arch. Dermatol.Syph*, **4**:265-273,1872.
- [49] L.Kestens,M. Melbye, R.J. Biggar, W.J.Stevens, P.Piot, et al. Endemic African Kaposi sarcoma isnot associated with immunodeficiency. *Int J Cancer*, **36**(1):4954,1985. [PubMed: 4018905].
- [50] L. Kestens, M. Melbye, R.J. Biggar, W.J. Stevens, P. Piot, et al. Endemic African Kaposi's sarcoma is not associated with immunodeficiency. *Int J Cancer*, **36**(1):29-34,1985.
- [51] M.E. Kim Nader, L.M. Casey, R.C. Liane, N.P. Kazembe. Pediatric Kaposi sarcoma in context of the HIV epidemic in sub-Saharan Africa: Current perspectives. *Pediatric Health, Medicine and Therapeutics*, **9**: 3546,2018.
- [52] C. Klatt Edward , et al. Pathology of HIV/AIDS. *Mercer University of Medicine Savannah*, pp.650,2017.

- [53] D.M. Knipe, P.M. Howley. *Fields Virology*, Lippincott Williams & Wilkins, Philadelphia, 2001.
- [54] E.R. Knowlton, L.M. Lepone, J. Li, G. Rappocciolo, F.J. Jenkins and C.R. Rinaldo. Professional antigen presenting cells in human herpesvirus 8 infection. *Frontiers in immunology*, **3**:427, 2013.
- [55] D.M. Koelle, M.L. Huang, B. Chandran, et al. Frequent detection of Kaposi's sarcoma-associated herpesvirus (human herpesvirus 8) DNA in saliva of human immunodeficiency virus-infected men: clinical and immunologic correlates. *J Infect Dis*, **176**:941-947, 1997. [PubMed: 9207354].
- [56] S.E. Krown. Highly Active Antiretroviral Therapy in AIDS Associated Kaposi's Sarcoma: Implications for the Design of Therapeutic Trials in Patients with Advanced, Symptomatic Kaposi's Sarcoma. *J. Clin. Oncol*, **22**(3), 399-402, 2004.
- [57] J.Y. Lee, I. Dhakal, C. Casper, et al. Risk of cancer among commercially insured HIV-infected adults on antiretroviral therapy. *J Cancer Epidemiol.*, **2016**:2138259, 2016.
- [58] L. Liu, H. Liu, J. Jiao, A. Bergeron, J.F. Dong, J. Zhang. Changes in Circulating Human Endothelial Progenitor Cells after Brain Injury. *J. of Neurotrauma*, **24**(6):936-943, 2007.
- [59] H. Longwe, S. Gordon, R. Malamba, N. French. Characterising B cell numbers

- and memory B cells in HIV infected and uninfected Malawian adults. *BMC Infectious Diseases* , **10**: 280,2010.
- [60] E. Lungu, T.J. Massaro, E. Ndelwa, N. Ainea, S. Chibaya and N.J. Malunguza,2013. Mathematical modeling of the HIV/Kaposi sarcoma coinfection dynamics in areas of high HIV prevalence. *Computational and Mathematical Methods in Medicine*, 2013. %bibitemNader
- [61] J.N. Martin,D.E. Ganem , D.H.Osmond, K.A. Page-Shafer,D. Macrae , et al. Sexual transmission and thenatural history of human herpesvirus 8 infection. *N Engl J Med*, **338**(14):94854,1998. [PubMed:9521982].
- [62] J. N. Martin, D.E. Ganem, D.H. Osmond, K.A. Page - Shafer, D. Macrae, et al. Sexual transmission and the natural history of human herpesvirus 8 infection. *N Engl J Med.*, **338**(14):948-54,1998.
- [63] E.A. Mesri, E. Cesarman and C. Boshoff. Kaposi sarcoma herpesvirus/Human herpesvirus-8 (KSHV/HHV8), and the oncogenesis of Kaposi sarcoma. Nature reviews. *Cancer*, **10**(10):707,2010.
- [64] G. Miller,L. Heston, E. Grogan, L. Gradoville, M. Rigsby, R. Sun et al. Selective switch between latency and lytic replication of Kaposi sarcoma herpesvirus and EpsteinBarr virus in dually infected body cavity lymphoma cells. *J. Virol*, **71**: 314324,1997.
- [65] P. Monini , S. Colombini, M. Sturzl et al. Reactivation and persistence of human

- herpesvirus-8 infection in B cells and monocytes by Th-1 cytokines increased in Kaposi's sarcoma. *Blood*, **93**(12):4044-58,1999.
- [66] D.M. Muema, N.A. Akilimali, O.C. Ndumnego, S.S. Rasehlo, R. Durgiah, D.B. Ojwach, N. Ismail, M. Dong, A. Moodley, K.L. Dong and Z.M.Ndhlovu. Association between the cytokine storm, immune cell dynamics, and viral replicative capacity in hyperacute HIV infection. *BMC medicine*, **18**(1):1-17,2020.
- [67] J.Müller and C. Kuttler. Methods and models in mathematical biology. Deterministic and Stochastic Approaches, *Springer-Verlag Berlin Heidelberg*,2015.
- [68] Myoung J, Ganem D. Active lytic infection of human primary tonsillar B cells by KSHV and its noncytolytic control by activated CD4+ T cells. *J Clin Invest*, **121**: 1130-1140,2011.
- [69] H. Namawejje, L.S. Luboobi, D. Kuznetsov, E. Wobudeya. Modeling Optimal Control of Rotavirus with different Control Strategies. *J. Math. Comput. Sci.*, **4**(5):892-914,2014.
- [70] S.M. Blower , H. Dowlatabadi , Sensitivity and uncertainty analysis of complex models of disease transmission: an HIV model, as an example, *Int. Stat. Rev.* **62** (1994) 229-243.
- [71] A. Hoare , D.G. Regan , D.P. Wilson , Sampling and statistical analyses tools (SaSAT) for computational modelling, *Math. Biosci.* **5** (2008) doi.10.1186/174246854.

- [72] F. Nani, M. Jin. Dynamics of HIV-1 Associated Kaposi sarcoma during HAART Therapy. *Math and Computer Science Working Papers*, pp.20, 2011.
- [73] F.Nani and M.Jin. Analysis of Dynamics of HIV-1 Associated Kaposi Sarcoma during HAART and ACI. *Journal of Advances in Mathematics and Computer Science*, pp.1-22,2016.
- [74] C. Natacha, D. Sophie, S. Robert, and G. Andrei. KSHV Targeted Therapy: An Update on Inhibitors of Viral Lytic Replication. *Viruses*, **6**(11):4731-4759,2014.
[https:// doi. org/10.3390/v6114731](https://doi.org/10.3390/v6114731).
- [75] http://www.natap.org/2020/CROI/croi_134.
- [76] P.Patel ,D.L Hanson, P.S.Sullivan , et al. Incidence of types of cancer among HIV-infected persons compared with the general population in the United States, 1992-2003. *Ann Intern Med*, **148**:728736,2008.
- [77] J. Pauk , M.L.Huang, S.J.Brodie, et al. Mucosal shedding of human herpesvirus 8 in men. *N Engl J Med.*, **343**:13691377,2000. [PubMed: 11070101].
- [78] Post-Exposure Prophylaxis. Department of Health and Human Services. USA.<https://www.hiv.gov/hiv-basics/hiv-prevention/using-hiv-medication-to-reduce-risk/post-exposure-prophylaxis>.
- [79] P.E. Pellett, D.J. Wright, E.A. Engels, D.V. Ablashi, S.C. Dollard, B. Forghani, S.A. Glynn, J.J. Goedert, F.J. Jenkins, T.H. Lee, et al: Multicenter comparison

- of serologic assays and estimation of human herpesvirus 8 seroprevalence among US blood donors. *Transfusion*, **43**(9): 1260-1268,2003.
- [80] A.S. Perelson, D.E. Kirschner. Dynamics of HIV infection of CD4 T cells. *Math. Biosciences*, **114**:81-125,1993.
- [81] B. Peter Bloland. Drug resistance in malaria. World Health Organisation, 2001. WHO/CDS/CSR/DRS/2001.4.
- [82] L.S Pontryagin, V.G. Boltyanskii, R.V. Gamkrelidze, E.F Mishchenko. The Mathematical Theory of Optimal Processes, Wiley, New York, 1962.
- [83] A. Potthoff, N. H. Brockmeyer. HIV-associated Kaposi sarcoma: pathogenesis and therapy. *J Dtsch Dermatol Ges*, **5**:1091-1094,2007.
- [84] P.Purushothaman, T. Uppal and S.C Verma. Molecular biology of KSHV lytic reactivation. *Viruses*, **7**(1):116-153,2015.
- [85] R. Renne, M. Lagunoff, W. Zhong, and D. Ganem. The size and conformation of Kaposi sarcoma-associated herpesvirus (human herpesvirus8) DNA in infected cells and virions. *J. Virol*, **70**:81518154,1996.
- [86] R.C. Robey, S. Mletzko and F.M. Gotch. The T-Cell immune response against Kaposi sarcoma-associated herpesvirus. *Adv. Virol.*, **2010**:19,2010. doi: 10.1155/2010/340356.

- [87] E.Rohner,N. Wyss,Z. Heg , et al. HIV and human herpesvirus 8 co-infection across the globe: Systematic review and meta-analysis. *Int J Cancer*, **138**:4554,2016. [PubMed: 26175054] ** This systematic review describes studies reporting the prevalence of KSHV in HIV positive and negative patients in several countries. HIV positive patients are more likely to be KSHV positive than HIV negative patients and this association is strongest in men who have sex with men, children and hemophiliacs.
- [88] R. Sarid. et al. Transcription mapping of the Kaposi sarcoma-associated herpesvirus (human herpesvirus 8) genome in a body cavity-based lymphoma cell line (BC-1). *J Virol*, **72**:1005-1012,1998. PubMed ID: 98105738.
- [89] T.F.Schulz. Kaposi sarcoma-associated herpesvirus (human herpesvirus-8). *J Gen Virol*, **79**:1573-1591,1998. PubMed ID: 98343713
- [90] A.S. Semeere, N. Busakhala, J.N. Martin. Impact of antiretroviral therapy on the incidence of Kaposi sarcoma in resource-rich and resource-limited settings. *Current opinion in oncology*, **24**(5):522-530,2012.
- [91] L.Shan, K. Deng, N.S. Shroff, C.M. Durand, S.A. Rabi, H.C. Yang, H. Zhang, J.B. Margolick, J.N. Blankson and R.F.Siliciano. Stimulation of HIV-1-specific cytolytic T lymphocytes facilitates elimination of latent viral reservoir after virus reactivation. *Immunity*, **36**(3):491-501,2012.

- [92] R. Shibagaki, S. Kishimoto, H. Takenaka. Recombinant Interleukin 2 Monotherapy for Classic Kaposi Sarcoma. *Arch Dermatol.*, **134**(10):1193-1196,1998.
- [93] K.A. Smith. Cornell Research Foundation Inc. Stimulation of immune response with low doses of cytokines. *U.S. Patent*, **6**(509):313,2003.
- [94] L.M.Sompayrac. How the immune system works, John Wiley & Sons, UK, 2019.
- [95] B. Szomolay, E.M. Lungu. A Mathematical model for the treatment of AIDS-related Kaposi's sarcoma. *Journal of Biological Systems*, **22**(3):495-522,2014.
- [96] van den Driessche, P., and Watmough, J., Reproduction numbers and sub-threshold endemic equilibria for compartmental models of disease transmission, *Math. Biosci.*180: 29 - 48 (2002).
- [97] M. V. Veetil, C. Bandyopadhyay, D. Dutta, B. Chandran. Interaction of KSHV with Host Cell Surface Receptors and Cell Entry. *Viruses*,**6**:4024-4046,2014.
- [98] <https://www.who.int/gho/hiv/en/>
- [99] R. Yarchoan, et al. Treatment of AIDS-Related Kaposi's Sarcoma with Interleukin-12: Rationale and Preliminary Evidence of Clinical Activity. HIV and AIDS Malignancy Branch. R.Yarchoan, J.M. Pluda, K.M. Wyvill, K. Aleman, I.R. Rodriguez-Chavez, G. Tosato, A.T. Catanzaro, S.M. Steinberg and R.F.Little. Treatment of AIDS-related Kaposi's sarcoma with interleukin-

- 12: rationale and preliminary evidence of clinical activity. *Critical reviews in immunology*, **27**(5):401,2007.
- [100] W. Zhang, F. Zhou, W. Greene, S. Gao. Rhesus Rhadinovirus Infection of Rhesus Fibroblasts Occurs through Clathrin-Mediated Endocytosis. *Journal of virology*, **84** : 11709-11717,2010.